

General Disclaimer

One or more of the Following Statements may affect this Document

- This document has been reproduced from the best copy furnished by the organizational source. It is being released in the interest of making available as much information as possible.
- This document may contain data, which exceeds the sheet parameters. It was furnished in this condition by the organizational source and is the best copy available.
- This document may contain tone-on-tone or color graphs, charts and/or pictures, which have been reproduced in black and white.
- This document is paginated as submitted by the original source.
- Portions of this document are not fully legible due to the historical nature of some of the material. However, it is the best reproduction available from the original submission.

CONTRACT # NAS-9-14151

AIL PROJECT NO. C011

NASA CR.

144443

LOW COST TRACKING
NAVAIDS ERROR MODEL VERIFICATION

A. CHARYCH
A. TATZ
J. LOVELL
R. FREDERICK

MAY 1975

FINAL REPORT

PREPARED FOR
NATIONAL AERONAUTICS AND SPACE ADMINISTRATION
HOUSTON, TEXAS

(NASA-CR-144443) LOW COST TRACKING NAVAIDS
ERROR MODEL VERIFICATION Final Report
(Airborne Instruments Lab.) 125 p HC \$5.25

CSCL 17G

G3/17

Unclas

35066

AIL a division of
CUTLER-HAMMER



DEER PARK, LONG ISLAND, NEW YORK 11729

TABLE OF CONTENTS

	<u>PAGE</u>
I. ABSTRACT	1
II. SUMMARY	3
III. BVE CONCEPT	4
IV. MSBLS BVE REQUIREMENTS	7
A. GROUND STATION PARAMETERS	9
B. MSBLS TRAJECTORY	18
C. SIGNAL PERTURBATIONS DUE TO PROPAGATION EFFECTS	40
V. RADAR ALTIMETER BVE REQUIREMENTS	50
A. RADAR ALTIMETER TRAJECTORY	50
B. RADAR ALTIMETER ERROR FUNCTIONS	53
VI. TACAN BVE REQUIREMENTS	59
A. TACAN BVE TRAJECTORY	59
B. BVE TACAN ERROR MODEL	63
VII. ONE WAY DOPPLER BVE REQUIREMENTS	66
VIII. RENDEZVOUS RADAR BVE REQUIREMENTS	77
A. ERROR SOURCES	77
B. BVE CONCEPT FORMULATION	80
C. BVE HARDWARE DESCRIPTION	84
IX. SELECTION OF NAVAIDS FOR BVE SIMULATION	89
X. SYSTEM DESCRIPTION OF ERROR VERIFICATION TECHNIQUE	90
A. GENERATION OF PSEUDORANDOM NUMBER SEQUENCES	90

TABLE OF CONTENTS (Cont'd.)

	<u>PAGE</u>
B. MSBLS SIMULATION	94
C. RADAR ALTIMETER SIMULATION	105
XI. VERIFICATION OF NAVAID ERROR MODEL	110
A. MSBLS	110
B. RADAR ALTIMETER	117
XII. REFERENCES	120

I. ABSTRACT

The Space Shuttle Orbiter vehicle will draw position data from five different tracking nav aids and, will use this information in on-board computers to come up with a best estimate of the Orbiter state vector. Since by design the coverage regions of some of these nav aids overlap to give more than one source of position data at most points in the maneuver, accurate information as to the error present in the received data must be derived for each nav aid, throughout its region of coverage. Using these data, the guidance and navigation computer will weigh incoming data to optimize the position and velocity vector estimate. While it is understood that no true "handoff" (in the sense of a sharply defined switchover from one nav aid to another) is intended, it is well to note that regions must be defined for a smooth transfer from one source of data to another. Correct definition of these transfer regions, based on good nav aid error information, will do much to increase the safety and reliability of the mission.

The ideal way to derive such information is by flying the nav aids in the shuttle maneuver, while making extremely careful measurements to determine how well they perform. In practice, such flight tests are always compromised

by economic and technical considerations and so generate imperfect data usually at great cost. Realizing this fact, it is reasonable to decide, to approach the navaid error estimation task from another route, that of analysis and simulation to verify the analysis.

II. SUMMARY

Features and characteristics of the tracking Nav aids (Microwave Scanning Beam Landing System, Radar Altimeter, Tacan, rendezvous radar and one way doppler extractor) were investigated. From the investigation, a set of specifications were developed for building equipment to verify the error model of the tracking Nav aids. Breadboard verification equipment (BVE) was built for the Microwave Scanning Beam Landing System and the Radar Altimeter.

The Breadboard Verification Equipment generates signals to the Tracking Nav aids which simulate the Space Shuttles trajectory in the terminal area.

The BVE simulates sources of nav aids error by generating pseudorandom perturbations on the nav aids signals.

Differences between the trajectory value and the nav aid derived values are taped and form the basis for the nav aids error model.

III. BVE CONCEPT

The concept of the breadboard verification equipment (BVE) is to present to the candidate tracking navaid a signal which resembles as closely as possible a real signal encountered during the shuttles operation.

The BVE is a real time computer controlled simulation procedure. A typical shuttle trajectory is recreated in order to present a signal to the navaid which is in dynamic motion. The signal is corrupted by pseudorandom noise of a magnitude and spectral density judged to be typical of errors in ground based equipment and due to energy propagation. Capability exists to alter the noise variables (magnitude and spectral density) so that system behaviors can be studied and evaluated under a wide range of field conditions.

Differences between instantaneous trajectory values and navaid derived values are taped and form the basis of the navaid error model.

A block diagram of the BVE test set up looks something like Figure 1. A signal generator under control of the processor drives the candidate navaid with a signal which resembles a system in dynamic motion. The signal generator outputs a "perfect" signal. One we would like the navaid to see, but one which is seldom attained in less than perfect environment. This "perfect" signal is, therefore, corrupted by noise in order to more closely

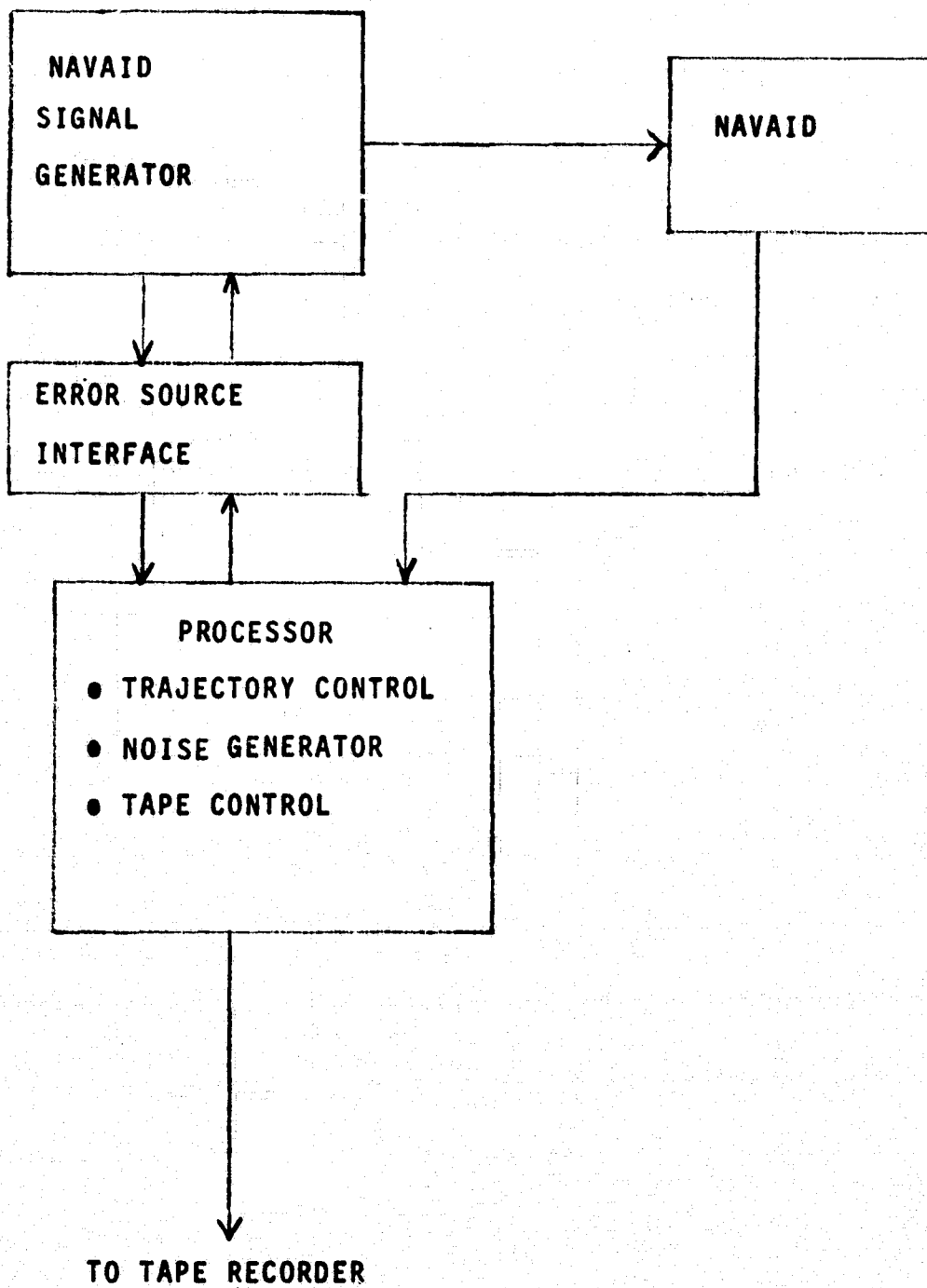


FIGURE 1. BVE CONCEPT

resemble a signal encountered during operation. The processor generates this noise by utilizing pseudorandom number generation techniques. The noise is in digital form and must be transformed to perturbations in the output signal. These perturbations may take the form of random AM or FM modulation, fluctuation in signal strength, etc. The error source interface provides this digital to signal perturbation conversion.

It must be pointed out that no attempt is made to simulate errors due to airborne equipment (navaid). The idea here is to evaluate navaid accuracy in a field environment. Signal to the navaid is to contain simulated perturbations due to error sources external to the navaid. Errors due to the navaid itself will show up within the system error model taped during the simulation.

The following sections summarize the investigations and the resulting BVE requirements for each of the tracking nav aids.

IV. MSBLS BVE REQUIREMENTS

A simulation procedure which accurately verifies the analytic error model of the MSBLS navigation set must take into account all parameters which have a bearing on the data derived from the MSBLS nav set.

These parameters can be broken down into three broad categories:

- a) MSBLS ground station parameters
- b) Space shuttles trajectory in the terminal area
- c) Signal perturbations due to propagation effects

BVE setup for MSBLS (see block diagram of figure 2) is envisioned as a modified MSBLS test set being driven by a processor which generates the shuttles reference trajectory, simulates expected error sources and tapes the difference between programmed and Nav Set measured parameters.

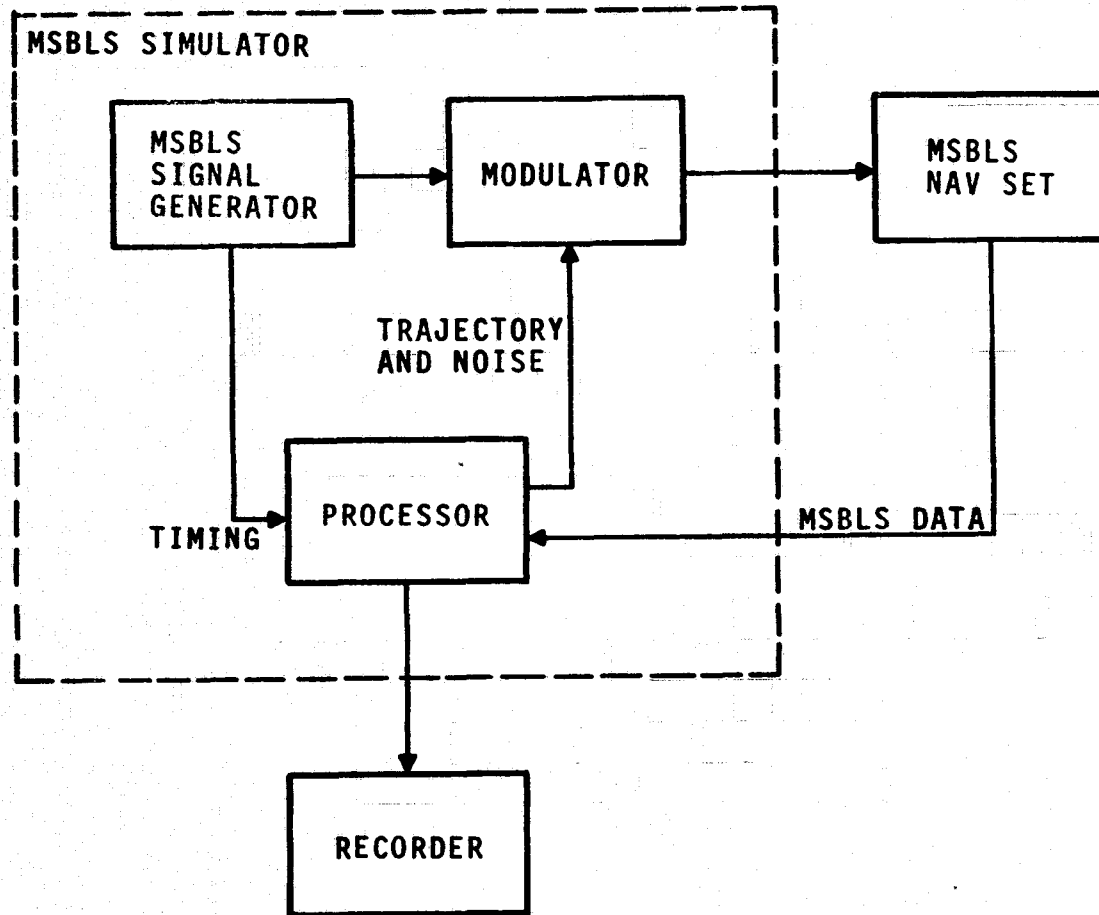


FIGURE 2 MSBLS SIMULATION, BLOCK DIAGRAM

A. GROUND STATION PARAMETERS

Analysis of BVE requirements is based on system parameters currently being designed into the MSBLS ground stations.

Azimuth

Antenna Beamwidth (azimuth)	2°
Scan motion (2 way scan)	2.5 HZ
Scan Amplitude	44°
Scan coverage	<u>+20°</u>
Peak transmitter power	2.2 KW
Angle pickoff resolution	1/8°
Code scale factor	2 usec/deg

Elevation

Antenna Beamwidth	1.3°
Scan Rate (2 way scan)	2.5 HZ
Scan Amplitude	22°
Mechanical Antenna Offset	15°
Peak transmitter power	2.2 KW
Angle Pickoff resolution	1/8°
Code Scale factor	2 usec/deg

DME

Antenna beamwidth shaped in elevation plane to achieve +23db gain at 16° elevation.

PRF 600 pps

DME interval 35 msec

1. SCAN RATE FOR BVE SIMULATION

Antenna angular scan rate (in degrees per second) is one of the factors which determine the number of pulses which will be averaged during the dwell time of the angle beams.

Since the azimuth and elevation antennas are in an oscillatory motion, maximum angular rate occurs at the center of mechanical scan. Peak angular rate for the azimuth antenna is 691 degrees per second at zero degrees azimuth and drops off the 649 degrees per second at 20 degrees off azimuth centerline.

Scan rate at a given point in the antenna scan cycle contributes to the error with which the pulsed angle beam can be resolved in the air (beam pulse resolution error).

If 691 deg/sec instead of 649 deg/sec is used at 20 degrees off azimuth centerline, the expected resolution error becomes .0141 degrees instead of .0132 degrees. The difference in expected error (.0009 degrees) is small enough to justify the use of a fixed scan rate in the BVE Simulation. The fixed scan rate is much easier to generate compared to sinusoidal scan.

In the case of elevation, angular rate varies from 345 deg/sec at 15° elevation, to 333 deg/sec at 0 degrees. If a fixed scan rate of 345 deg/sec is used, expected error due to beam pulse resolution is .0063 deg instead of .0061 deg. Use of a fixed scan rate for elevation is therefore also justified.

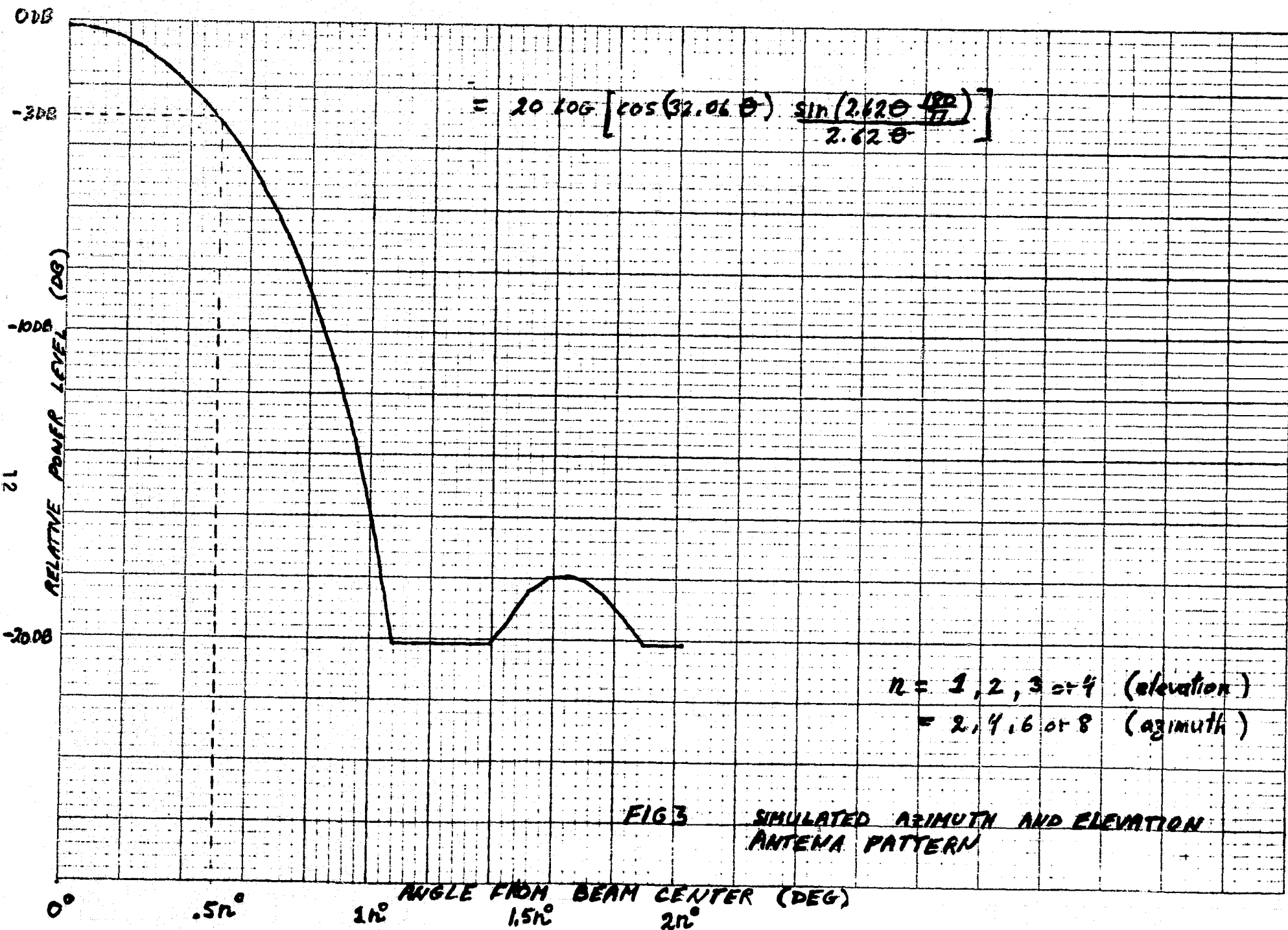
2. AZIMUTH AND ELEVATION ANTENNA PATTERN

Beamwidth of the azimuth and elevation antennas contributes to the total number of pulses averaged by the MSBLS Navigation Set and plays a large role in the systems ability to reject multipath transmissions.

Table 2 (page 114) shows that multipath from antenna sidelobes (item 8) is the overriding source of noise error in the system. Equation 4-16 (page 41) gives the analytic derivation of system error as a function of multipath signal level. From the derivation, it can be seen that system susceptibility to multipath depends on the slope of the antenna pattern at the receivers threshold level.

The antenna pattern must therefore be accurately reconstructed for the BVE simulation. A $\sin x/x$ type pattern is an accurate prediction of the actual antenna beam.

Figure 3 shows a pattern to be used for the BVE simulation. The pattern is adjusted for a 3db beamwidth of 2° Azimuth and 1° elevation. The actual beamwidth



can be set by moving this pattern at a faster or slower angular rate. A $.5^\circ$, 1° , 1.5° and 2° elevation beamwidths are possible, and a 1° , 2° and 3° azimuth beamwidths are possible. The 1.5° elevation beamwidth is close enough to the actual 1.3° beamwidth to warrant its use in the simulation.

The pattern is clipped at the 20db point so as not to impose unnecessary dynamic range requirements on the Ku band modulator.

The cosine function appearing in expression in Figure 3 is used to decrease the sidelobe level to a value of 18db below the peak of the beam.

3. ANGLE PICKOFF RESOLUTION AND CODE SCALE FACTOR

Instantaneous position of the MSBLS-GS scanning antenna is digitized to a resolution of $1/8$ degree. A scale factor of 2 usec/deg is used to generate the angle code. i.e. a $1/8$ degree step in the antenna pointing angle constitutes a .25 usec change in the angle code spacing.

The BVE simulation will utilize the same resolution and code scale factor.

Digitizing the position of the scanning antenna introduces a random noise error of approximately .001 degree. This error source (angle pickoff increment) is inherent in the MSBLS system and therefore no special procedure is required to simulate it.

4. INSTALLATION BIAS ERRORS

ANGLE BIAS

Errors in alignment of station in roll, pitch and yaw axis cause an error in azimuth and elevation guidance which is a function of azimuth and elevation angle.

On azimuth centerline, elevation bias due to pitch is the only alignment bias of significance. Errors due to roll and yaw being 5 orders of magnitude lower.

Azimuth bias error on azimuth centerline is primarily due to yaw with some dependence on pitch. If a 1σ deviation of .01 degrees is assumed for each of the 3 axes, azimuth bias due to yaw would be .01 degrees, while bias error due to pitch and roll would be .0026 degrees at the maximum elevation angle going to zero as the angle is lowered. The RSS summation of these errors yields .01 degrees 1σ at the lower elevation angles and .0107 degrees at the maximum elevation angle.

We conclude that a fixed bias error for azimuth incorporated into the BVE is sufficient. Bias magnitudes will be selected from a gaussian distributed function prior to each simulation run and held constant through that run.

Bias error will be simulated by delaying (or advancing) the angle data pickoff waveform from a reference waveform.

Alignment of the angle pickoff device constitutes an additional source of system bias. Alignment of the pickoff device can generally be held to better than .02 degrees. If .01 degrees is allowed for the accuracy of station alignment, an RSS summation of .022 degrees results. A standard deviation of .022 degrees should, therefore, be used for the gaussian distributed bias function.

DME BIAS

DME bias is primarily due to an offset in the 80 usec turnaround delay from reception of an interrogation to transmission of a reply.

The offset is due to imperfections in the automatic calibrate loop.

It is not feasible to include an automatic calibrate loop into the BVE simulation of range because of the extensive modifications this would require of the basic MSBLS signal generator.

Since it is expected that error in the turnaround time will be different for each reentry of the shuttle, the best procedure is to synthetically simulate this error.

To do this, the total DME system must first be calibrated at a given range, say 200 feet. Once the system is calibrated, the bias is added by selecting a gaussian distributed offset prior to each simulation run. A standard deviation of 10 feet for the gaussian distributed function would be "typical" of the error in turnaround time.

5. ENCODER OSCILLATOR BIAS

Bias in the ground oscillator is expected to be within .003% (1 sigma).

A 30 ppm error in oscillator frequency will result in a decoded angle error on the order of .001 degrees, and a contribution to range error of 1.2 feet.

Since oscillator bias would be difficult and expensive to simulate and since the expected error from this source is more than an order of magnitude lower than boresighting errors, this source will not be incorporated

6. ANGLE PICKOFF JITTER

A .025 degree jitter on the waveform from the angle pickoff device contributed .0001 degrees of system error. While it would not be difficult to simulate this source, the small error contribution does not warrant it.

7. PULSE TRANSMISSION JITTER

An expected transmitted pulse jitter of 10nsec contributes .0003 degrees to the angle error and 5 feet to the distance error. Since the RF pulse from the test set will have a certain amount of jitter associated with it, no additional effort should be made to simulate this source.

8. ANGLE PICKOFF HISTERISIS

Histerisis of the waveform from the angle pickoff device is primarily due to the bidirectional motion of the scanning antenna. Histerisis is associated with gear lash.

Since the MSBLS-GS equipment has the angle pickoff device directly mounted to the scanning antenna (gears are not used), there is no need to simulate this source.

B. MSBLS TRAJECTORY

1. AZ/EL AND DME SIMULATION

Shuttles trajectory for MSBLS simulation is based on latest information of a typical trajectory which provides a good exercise for the BVE simulation. The trajectory in the xz plane (figure 4) starts off at an altitude of 16,000 feet and exponentially captures a 24 degree glideslope towards an aiming point 4,000 feet in front of runway threshold. Transition to shallow 3 degree glide (pull up) is initiated at 1,910 feet altitude. Shuttles velocity starts decreasing from 290 knots to 170 knots at touchdown. Final flare starts over runway threshold so as to decrease the sink rate to 2 fps at touchdown.

Trajectory in the xy plane starts on a 20,000 feet radius circle centered at $x = 45,950$ feet. MSBLS simulation starts at a point at which the vehicles yaw angle (tangent to the circle) is 50 degrees with respect to runway centerline.

In order to simplify the trajectory defining equations, shuttles ground speed, x , is assumed a constant 290 knots (489 fps) before pull-up (altitude $z > 1910$ feet and $x > 23,290$ feet). In this region;

$$x = -489t + 23,290$$

where time, t , is defined as zero at start of pullup and negative before pullup.

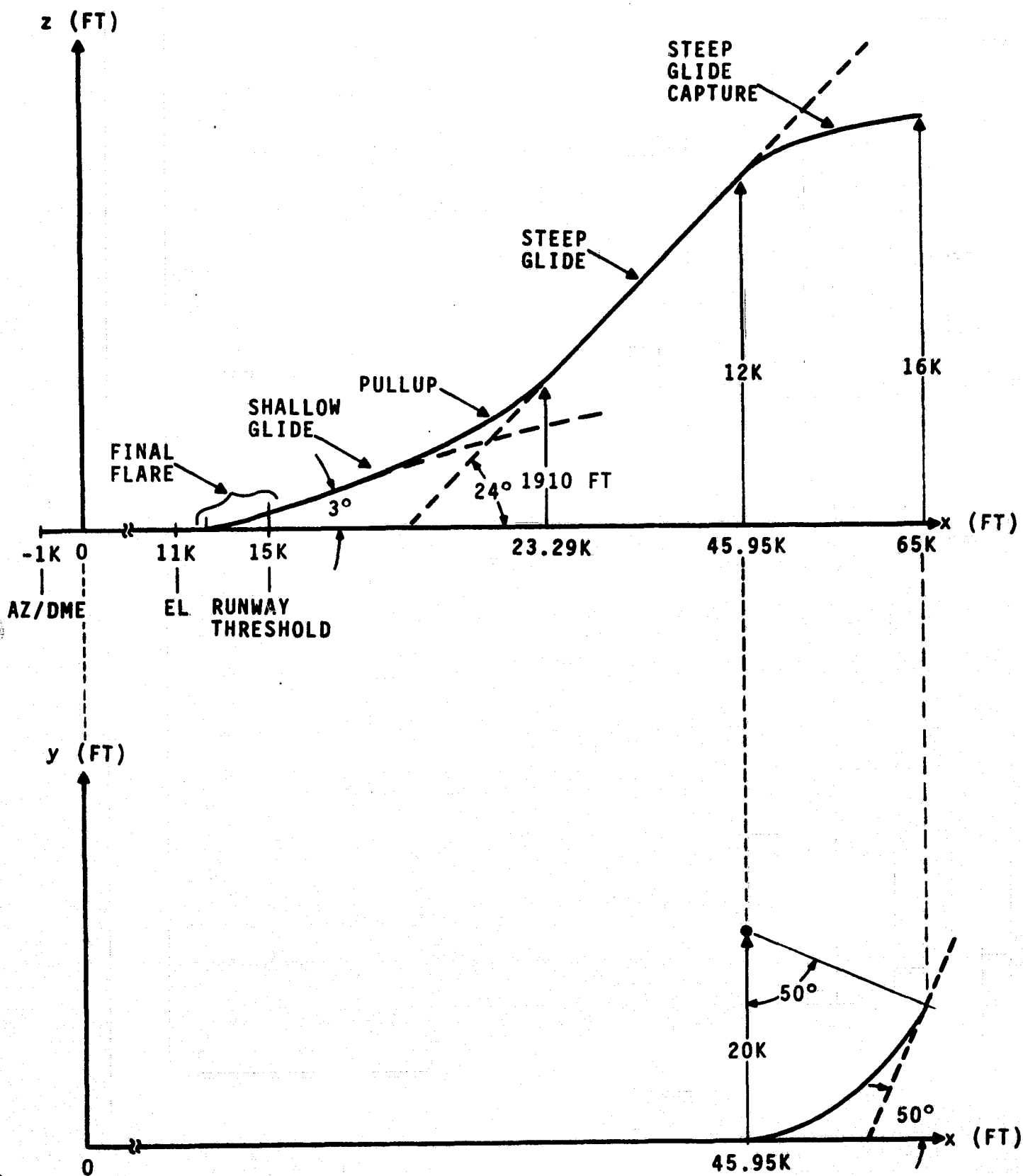


FIGURE 4. MSBLS TRAJECTORY

After pullup, a constant deceleration \ddot{x} is assumed. If the vehicles ground speed is constrained to zero at about 1 mile from the stop end of the runway, then for $x < 23,290$ feet.

$$(4-1) \quad x = \frac{7.197t^2}{2} - 489t + 23,290$$

The trajectory is divided into five regions

- | | |
|--------------------------------|-----------------------|
| 1. Capture of steep glideslope | $x > 45,950$ feet |
| 2. Steep glideslope | $45,950 > x > 23,290$ |
| 3. Transition to shallow glide | $23,290 > x > 16,600$ |
| 4. Shallow glide | $16,600 > x > 15,000$ |
| 5. Final flare | $15,000 > x$ |

Assuming an exponential capture of the steep glide with a constraint that the merger occurs at $z = 12,000$ feet altitude and that sink rate, \dot{z} , matches that of the steep glide, relation for altitude becomes

$$(4-2) \quad z = -1635.07 \exp [(t+77.675)/25.318] + 17,636$$

In the xy plane, equation around the TAEM circle becomes

$$(4-3) \quad y = 20,000 (1 - \cos[\sin^{-1}[\frac{x-45,950}{20,000}]])$$

figure 5 shows the trajectory in the xy.

Transforming the x, y, z coordinates to elevation angle ϕ and azimuth angle θ ,

FIGURE 5

TRAJECTORY AROUND THEM CIRCLE

$$y = 20(1 - \cos[\sin^{-1}(\frac{x - 45.95}{20})]) \text{ K FT}$$

y coordinate (FT)

GROUND RANGE FROM STOP END OF RUNWAY (FT)

40K

50K

60K

65K

21

$$\begin{aligned}
 (4-4) \quad \phi_o &= \tan^{-1} \left[\frac{z}{\sqrt{(x-11,000)^2 + y^2}} \right] \\
 (4-5) \quad \theta_o &= \tan^{-1} \frac{y}{x}
 \end{aligned}
 \left. \vphantom{\begin{aligned} (4-4) \quad \phi_o &= \tan^{-1} \left[\frac{z}{\sqrt{(x-11,000)^2 + y^2}} \right] \\ (4-5) \quad \theta_o &= \tan^{-1} \frac{y}{x} \end{aligned}} \right\} x > 45,950$$

Azimuth angle around the TAEM circle as a function of time is shown in figure 6. Merger with azimuth centerline occurs at $t = -46$ sec. Azimuth trajectory stays on azimuth centerline for the remainder of the simulation run.

Trajectory on the steep 24 degree ($45,950 > x > 23,290$) glide is a geometric relation of the variables;

$$(4-6) \quad z = (x - 19,000) \tan 24^\circ$$

$$(4-7) \quad \phi_I = \tan^{-1} \left[\frac{\tan 24^\circ (x-19,000)}{(x-11,000)} \right]$$

Figure 7 shows a graph trajectory in xz plane including steep glide capture and steep glide.

Transition to the shallow 3 degree glide (pullup) is based on a parabolic curve in the xz plane. A parabolic curve is approximated by a constant elevation angle rate.

If γ is defined as the elevation angle from the aiming point of the shallow glide (1,500 feet in back of threshold) and the slope, $\frac{dz}{dx}$ is constrained to match the shallow 3 degree glide, then γ can be chosen as

FIGURE 6 AZIMUTH ANGLE AROUND THEM CIRCLE
DVE PROGRAM

AZIMUTH ANGLE (DEG)

23

TIME FROM PULLUP (SEC)

-70

-50

-60

-70

-80

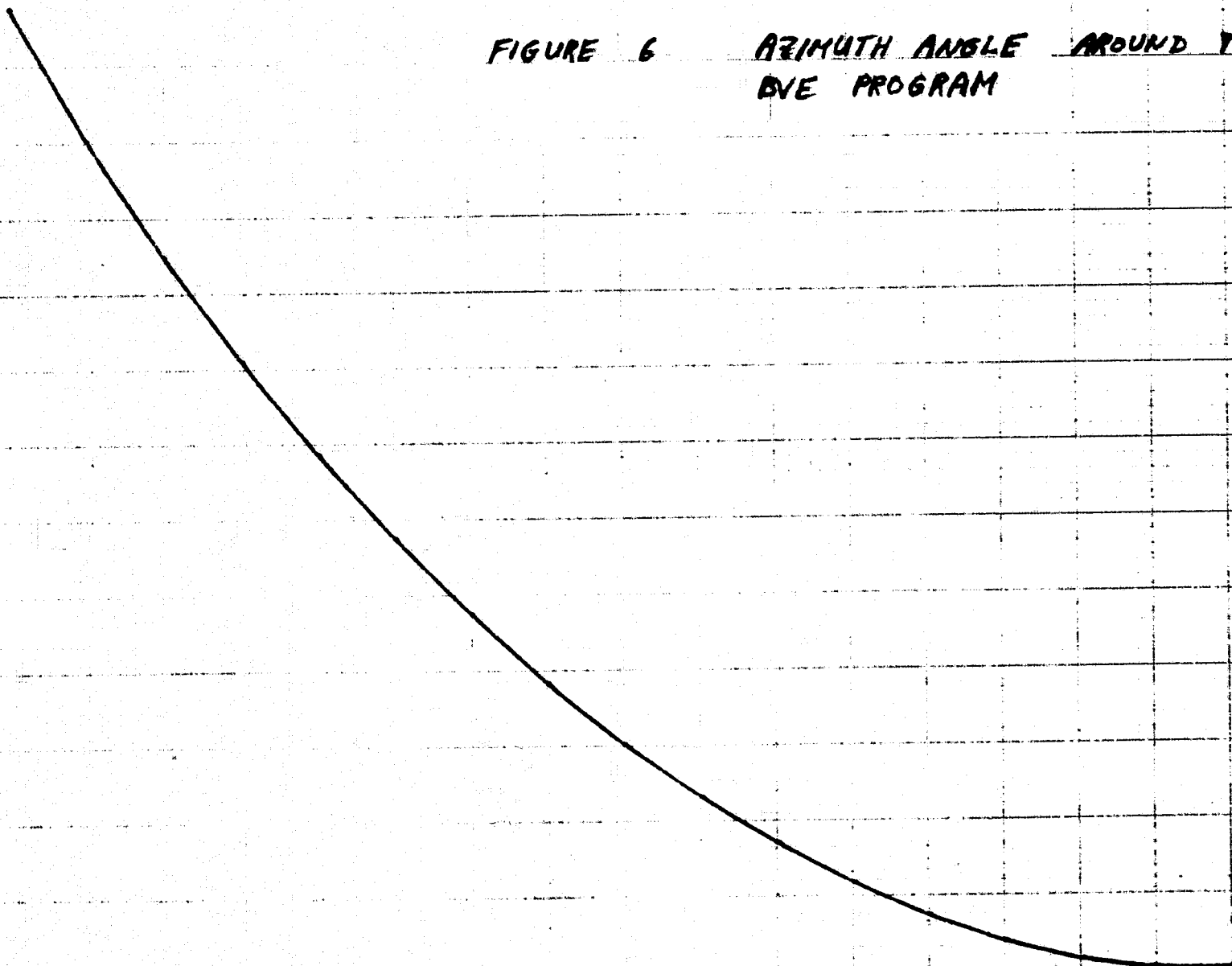


FIGURE 7 SHUTTLE TRAJECTORY
FOR MSBLS BVE EXERCISE

HEIGHT (FT)

24

10K

20K

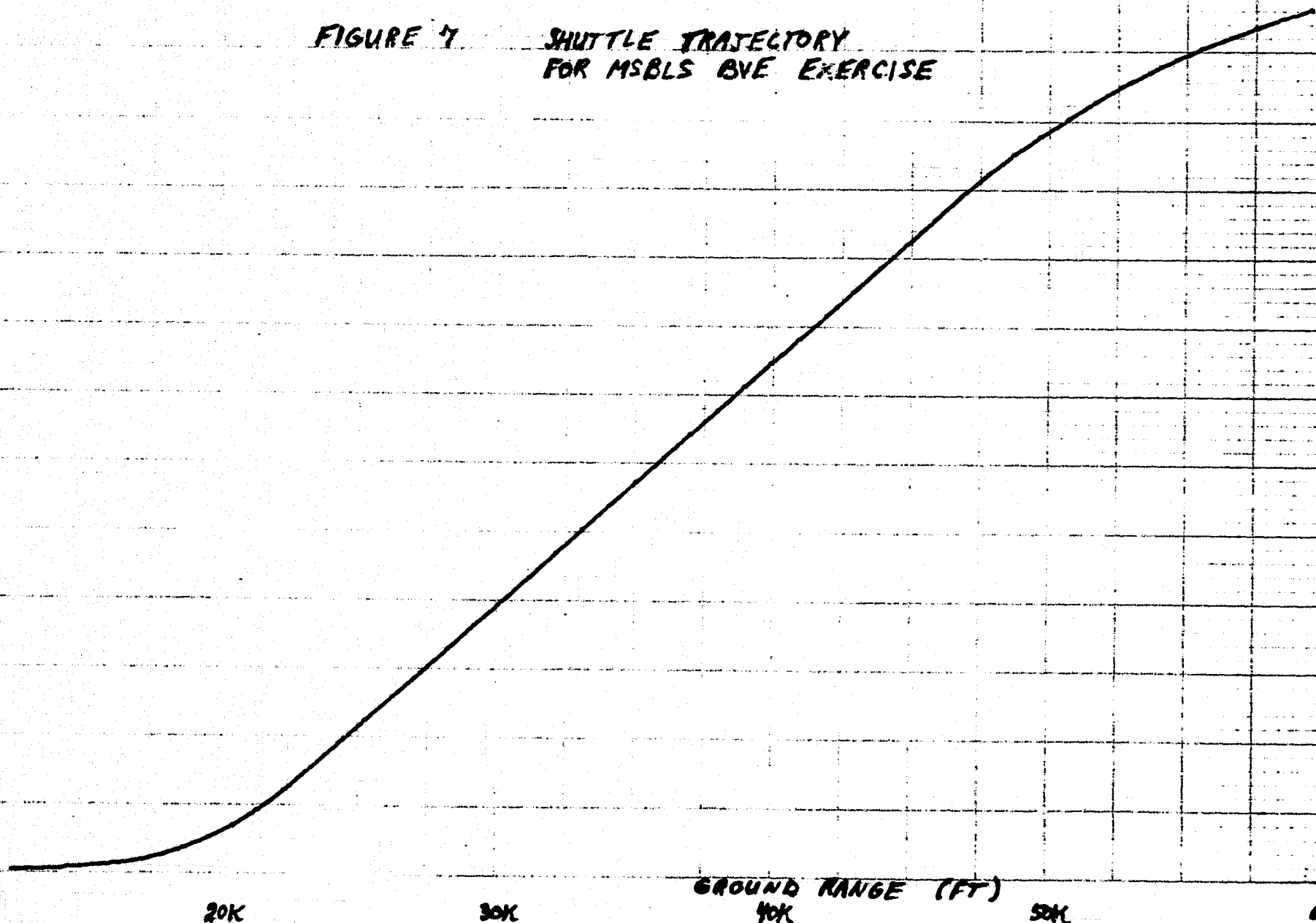
30K

GROUND RANGE (FT)

40K

50K

60K



$$(4-8) \quad \gamma = 3^\circ + (x-16,600)^{(1.3)} (8.5535 \times 10^{-5}) \text{ deg}$$

$$(4-9) \quad z = (x-13,500) \tan \gamma$$

Transforming this to the elevation angle from the glideslope transmitter (4,000 feet in back of threshold)

$$(4-10) \quad \phi_{II} = \tan^{-1} \left[\frac{\tan \gamma (x-13,500)}{(x-11,000)} \right]$$

The transition region as a function of x is shown in figure 8.

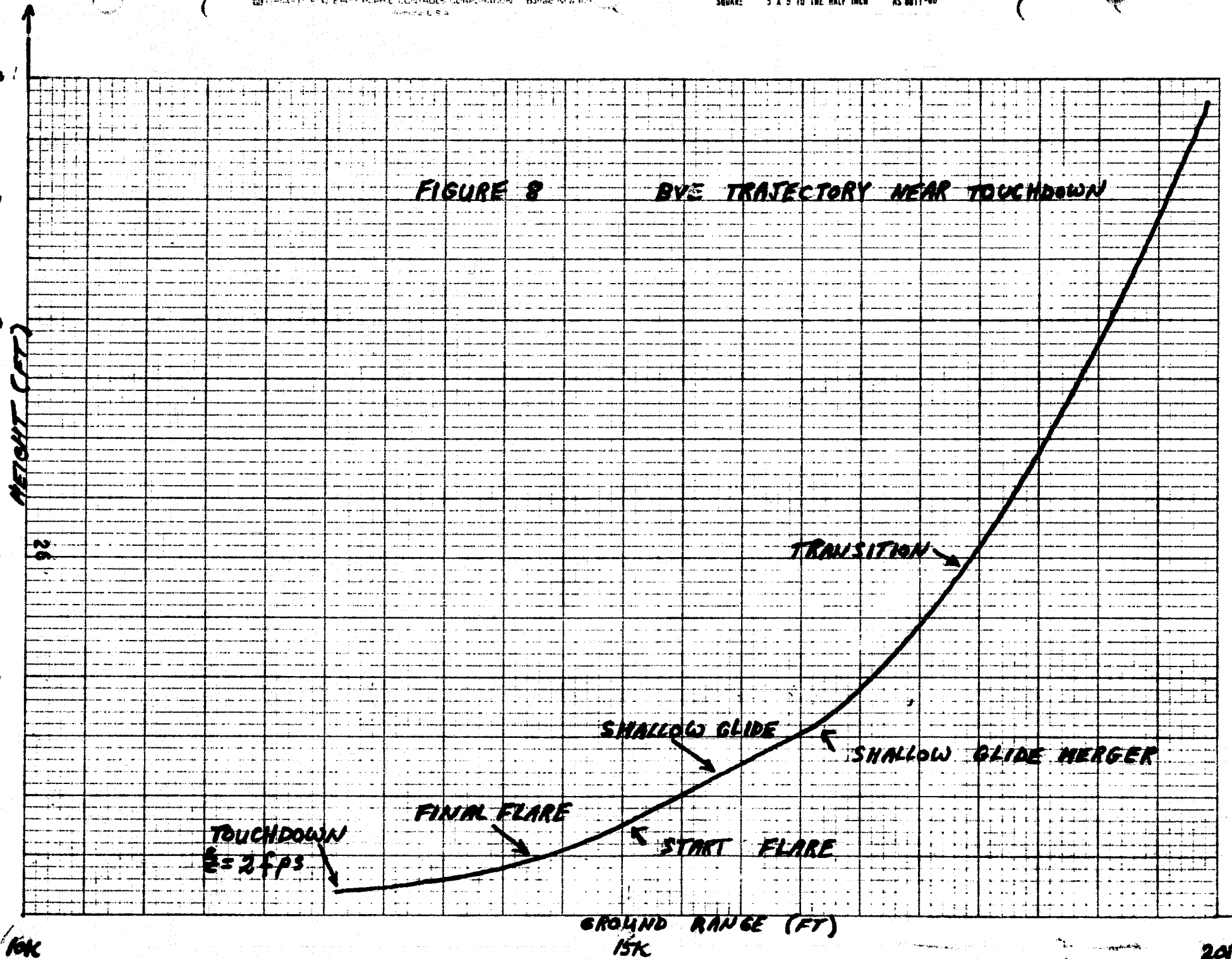
The shallow 3 degree glide ($16,600 > x > 15,000$) is just the equation for ϕ_{II} with γ set equal to 3 degrees.

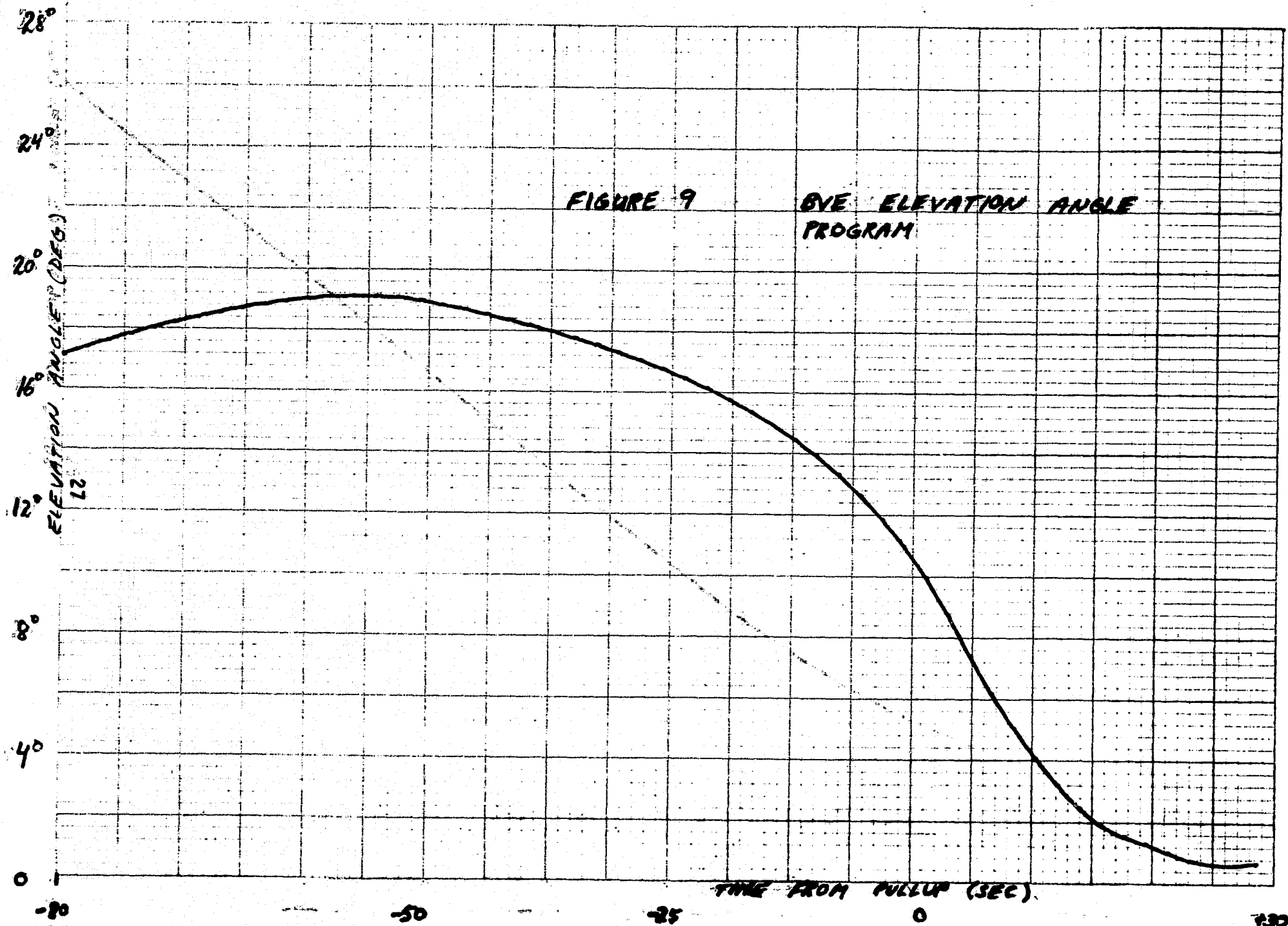
Final flare ($15,000 > x$) is an exponential decay of height. Slopes are constrained to match at start of final flare and sink rate is constrained to 2 f.p.s. at touchdown. Airborne antenna height at touchdown is assumed as 18.6 feet

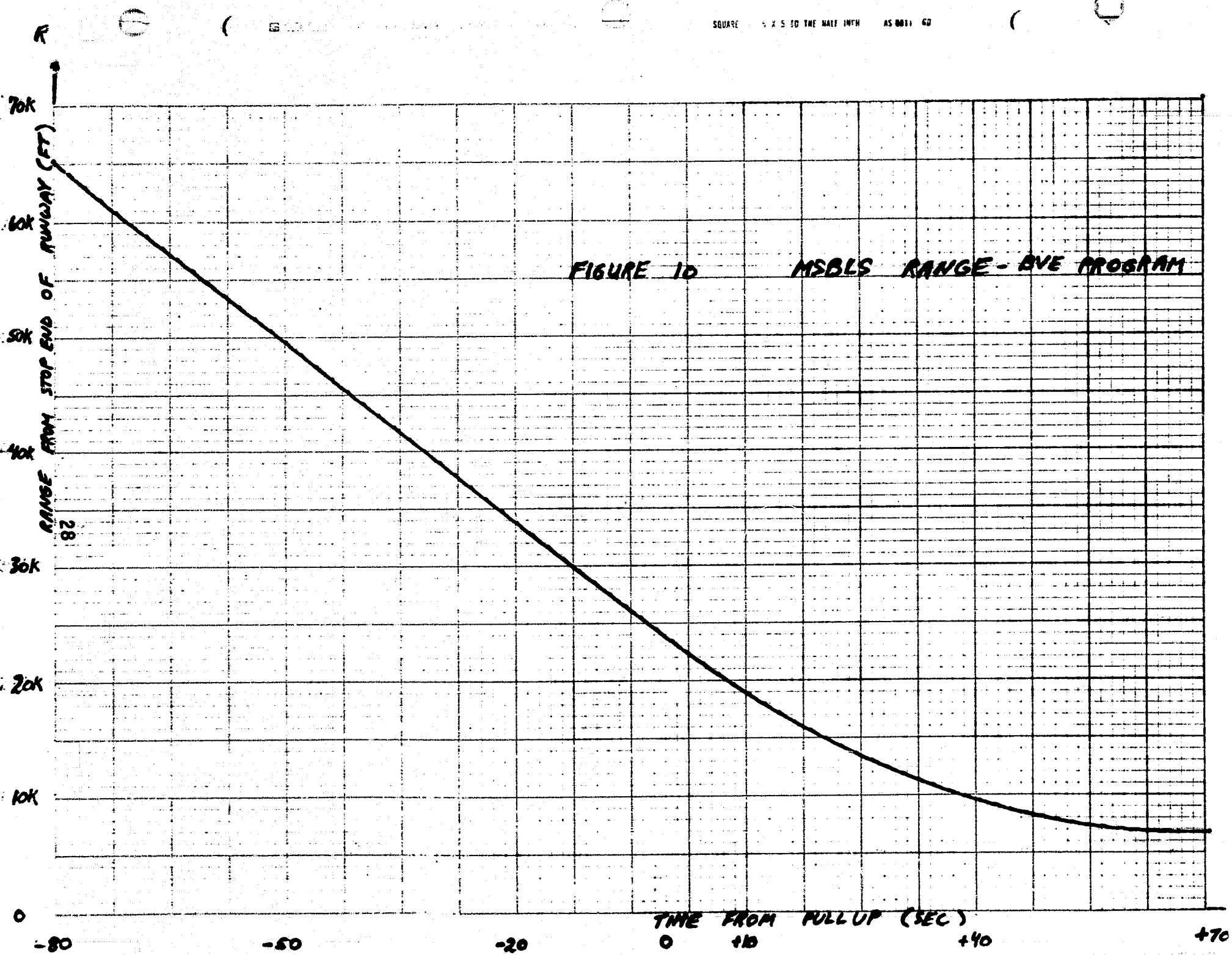
$$(4-11) \quad z = 67.435 \exp [(-t + 19.853)/3.718] + 11.175$$

$$(4-12) \quad \phi_{IV} = \tan^{-1} z/(x-11,000)$$

Figure 9 shows the composite elevation angle program to be simulated by the BVE. Range program is shown in Figure 10.







The BVE will step the MSBLS Nav Set through these programs as a function of time.

Resolution of the programmed angle functions should be such so as to make the trajectory "seem" smooth to the MSBLS Nav Set. i.e. a resolution higher than system error should be chosen. Resolution of 1/128th degree for the azimuth and elevation function should be sufficient.

The DME function requires a different approach. Because the MSBLS Nav Set integrates DME replies over a 35 msec interval, the measured distance reported at the end of the DME interval is not the instantaneous value, but contains a time lag of approximately 1/2 that interval.

Simulation of range must take into account the fact that the vehicle is in motion during the DME interval. i.e. the range between adjacent interrogations is changing. Otherwise, bias of derived range due to velocity and occasional errors due to loss of a reply would not show up in the data derived from the MSBLS Nav Set.

Range simulation can be done using a precision, high resolution delay generator. Rather than programming range directly, range rate can be programmed. Range delay is then decremented in 1 nsec (1/2 radar foot) steps at a preprogrammed rate.

2. UPLINK SIGNAL STRENGTH SIMULATION

Signal strength at the receivers terminals determines the thermal noise content of the video beam envelope. Thermal noise contributes on the order of .01 degree error at 10 nmi range, decreasing to a negligible value as the ground transmitters are neared.

Aside from this error contribution, rate of change of signal strength is important in exercising the Nav Sets AGC loop.

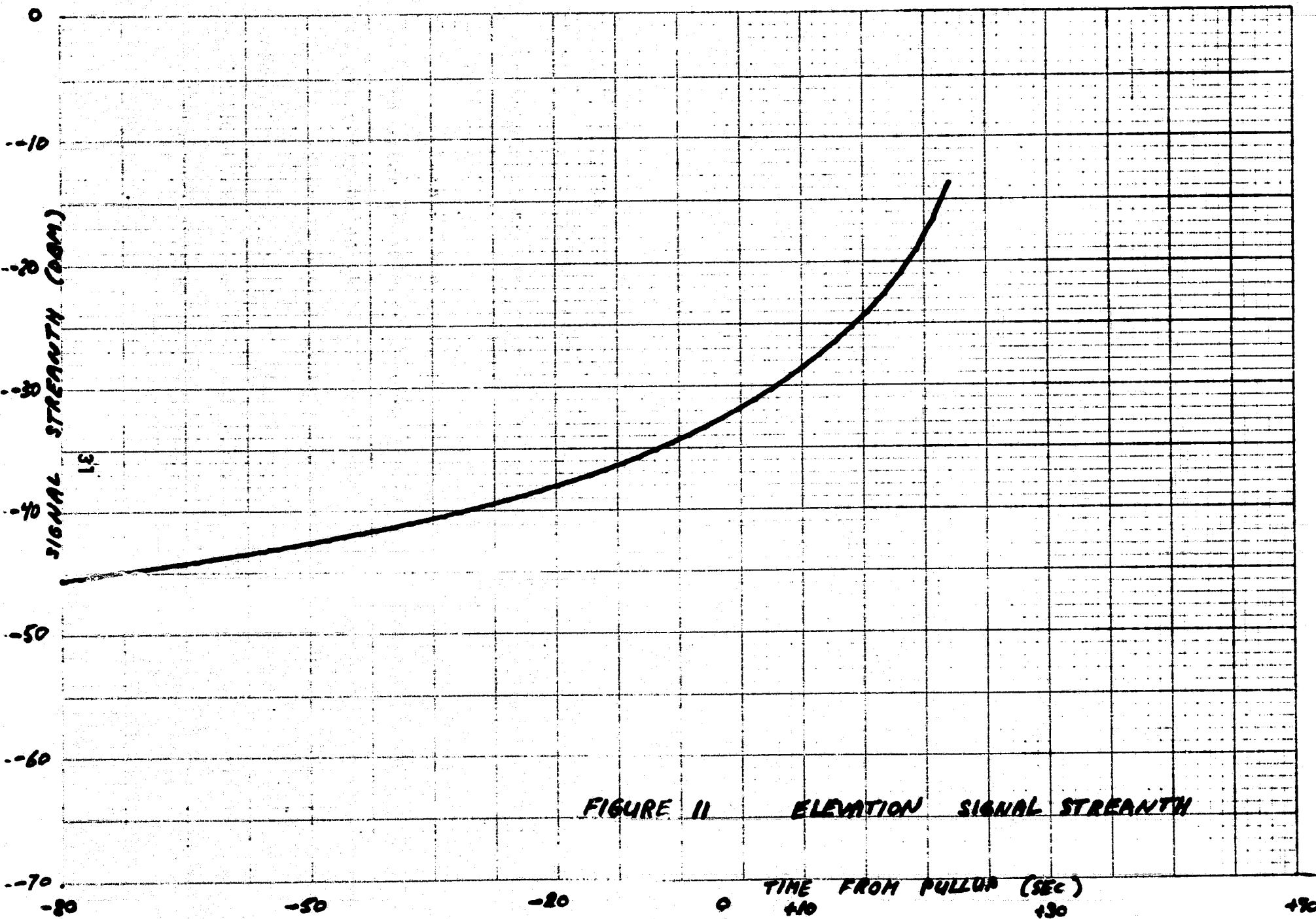
The MSBLS is a sampled data system. Signal for the azimuth function, for example, appears at the receivers terminals for 3 msec out of 200 msec. The Nav Set receiver must keep track of the AGC level of each of the functions (AZ, EL & DME). Each will have a different AGC level.

If signal strength for one of the angle functions is changing too rapidly, the receiver would track too high or too low on the beam envelope. Both of these conditions introduce additional uncertainty in derived data.

The BVE should therefore simulate a realistic signal strength and rate of signal strength.

The received power level is defined as

$$(4-13) \quad P_R = P_T + G_G + G_A - \alpha$$



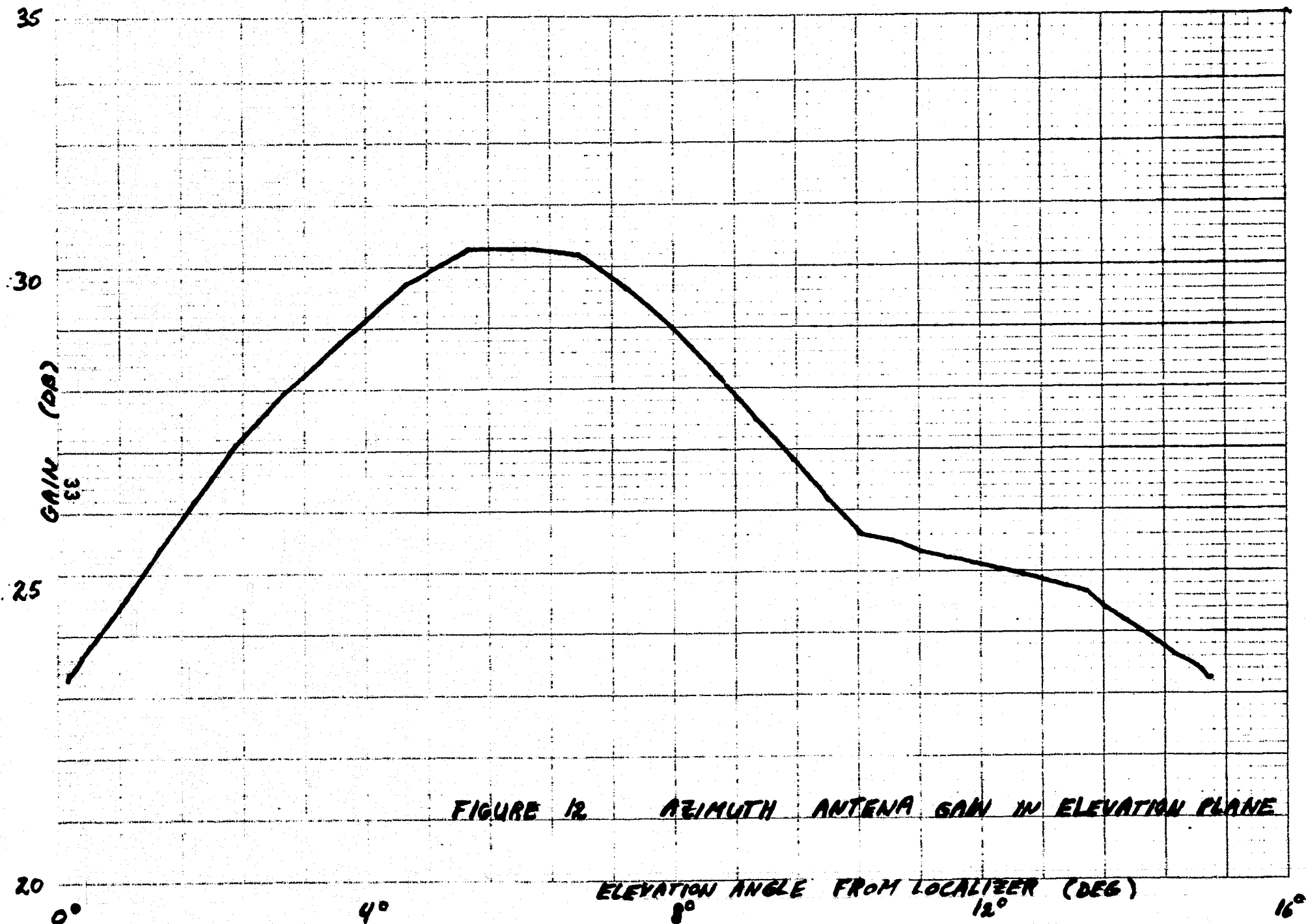
where P_R = received power level (dbm)
 P_T = transmitted power level (+63 dbm)
 G_G = ground antenna gain
 a. Elevation, +27 db
 b. Azimuth, function of elevation angle
 c. DME, function of elevation angle
 G_A = airborne antenna gain minus line losses, + 5 db
 α = path attenuation
 $= 36.6 + 20 \log f + 20 \log \left(\frac{R}{5280} \right)$
 where f = frequency in MHZ
 R = range in feet

Elevation power level calculation is based on a fixed ground antenna gain of 27 db. Figure 11 shows a plot of elevation signal strength as a function of time.

Azimuth and DME signal strength calculations must take into account the ground antenna gain as a function of elevation.

Gain of the azimuth antenna in the elevation plane is modeled after an azimuth antenna from the TILS program which is presently being outfitted for the MSBLS-GS stations.

Modeled gain pattern in the elevation plane of this antenna is shown in Figure 12. The pattern is aligned such that the 8 db point is placed on the horizon. This will be typical of the MSBLS-GS stations.



30

GAIN (DB)

20

34

10

0°

4°

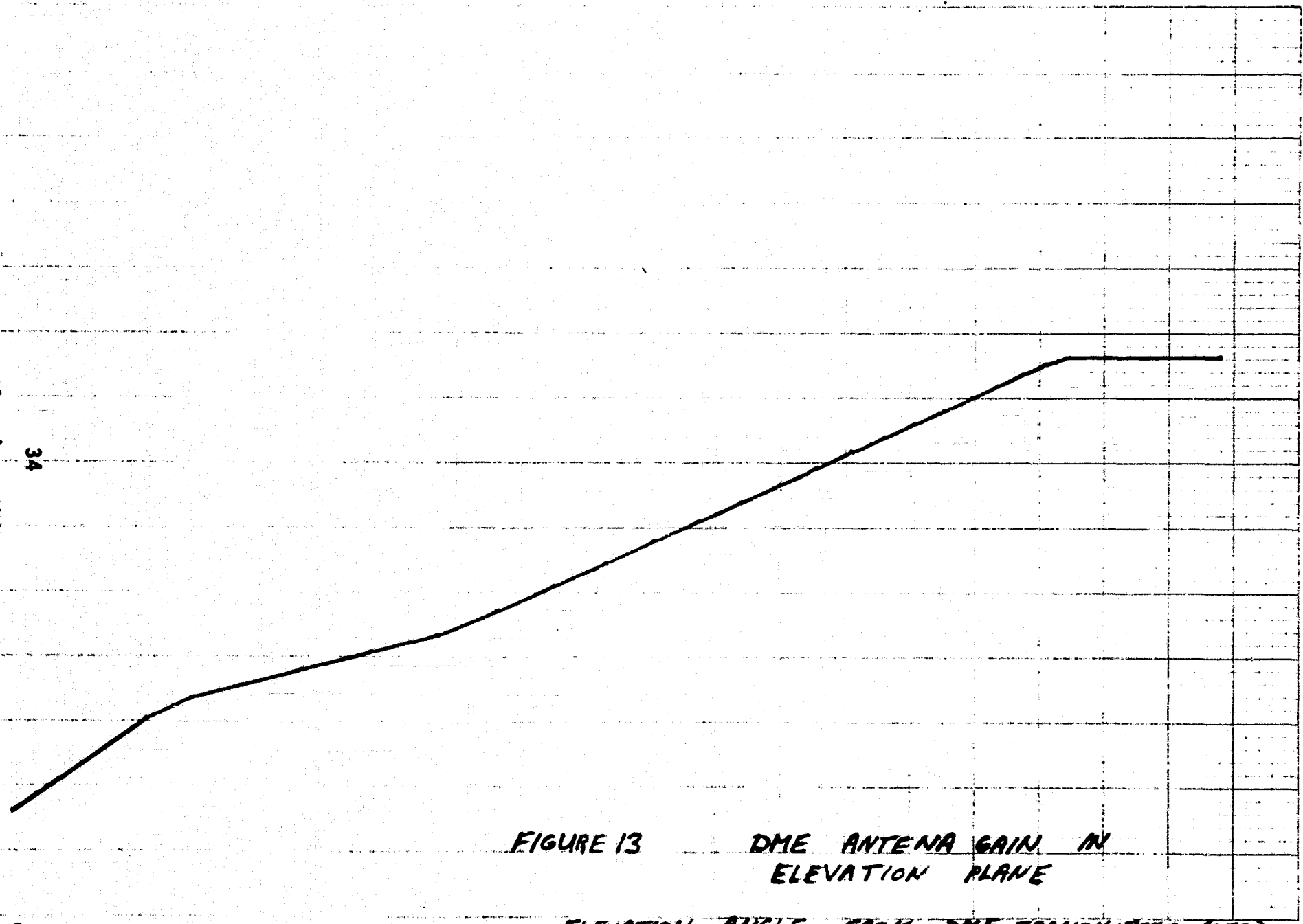
FIGURE 13

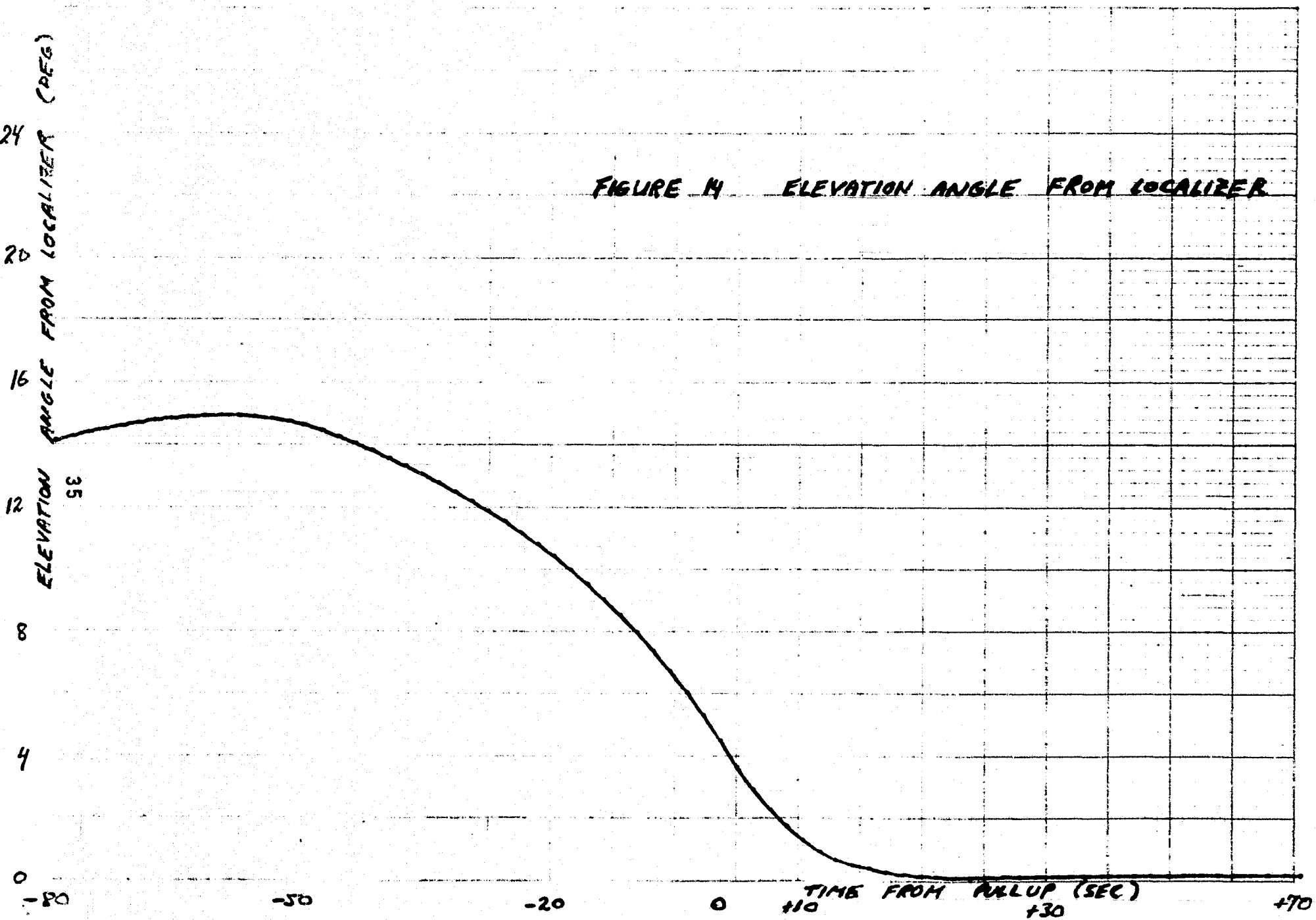
DME ANTENNA GAIN IN
ELEVATION PLANE

ELEVATION ANGLE FROM DME TRANSMITTER (DEG)

12°

16°





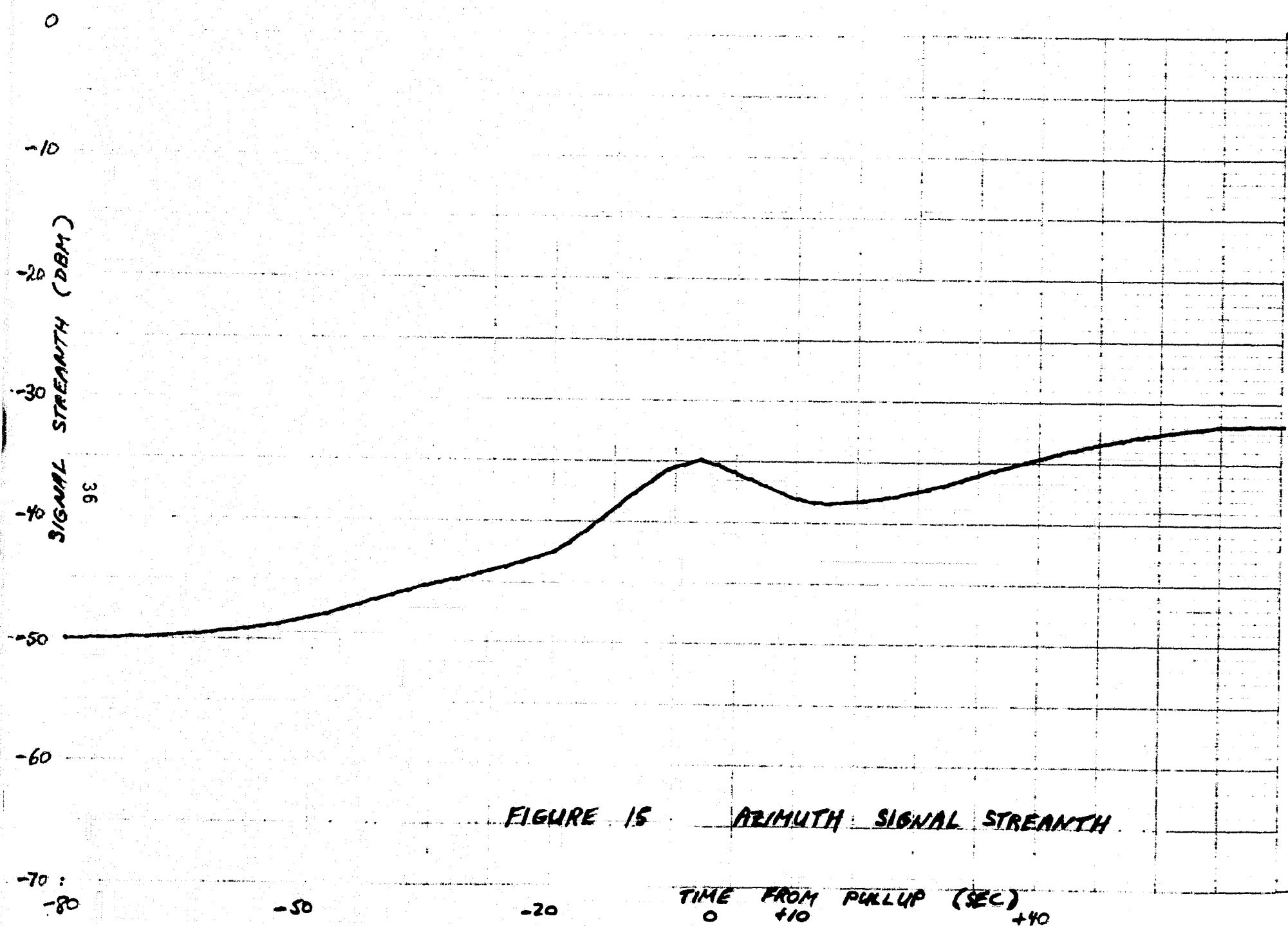
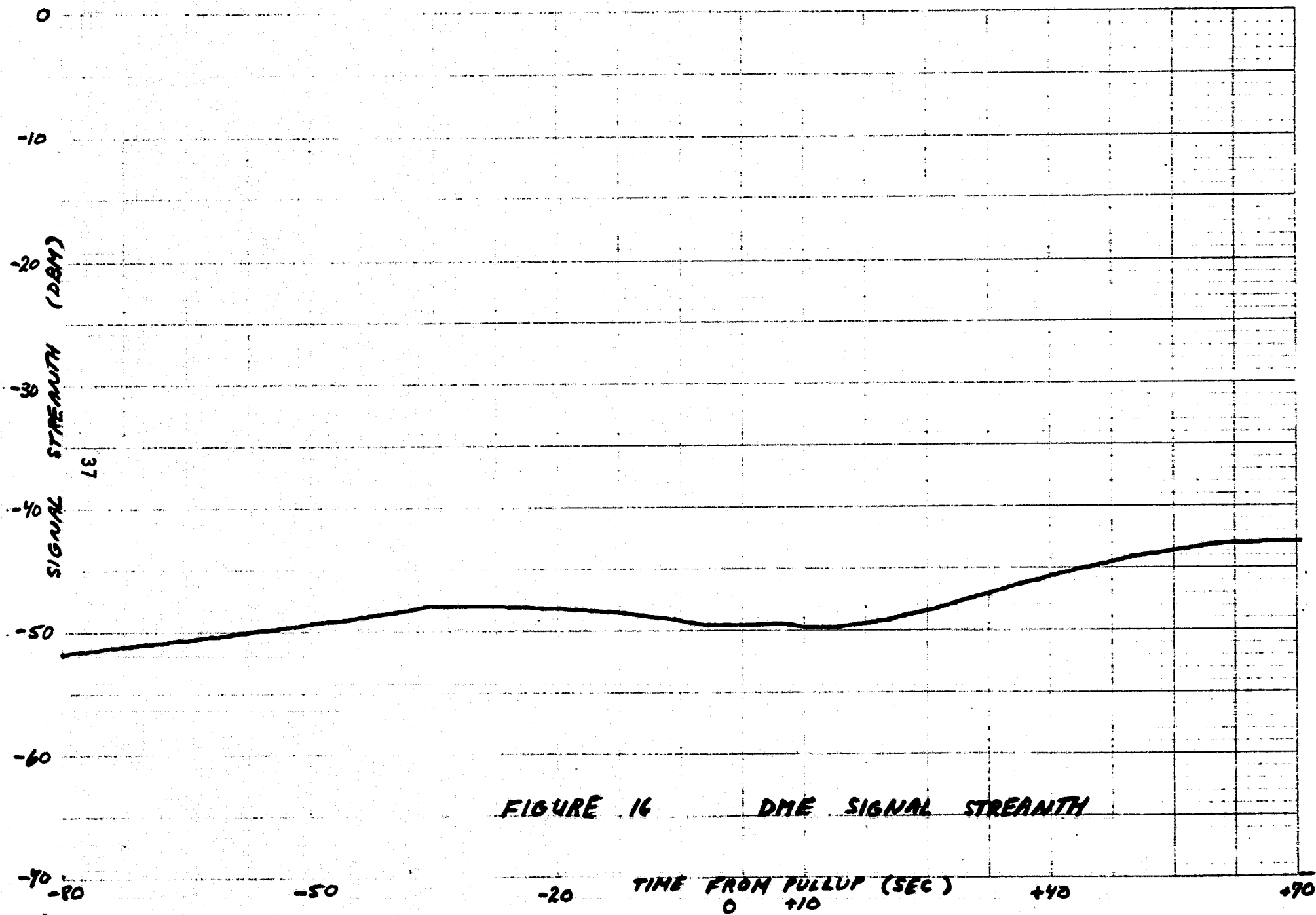


FIGURE 15 AZIMUTH SIGNAL STRENGTH



The DME pattern (Figure 13) is modeled after an antenna from the TLS program. The TLS antenna pattern was placed upside down to allow more energy at the top section (above 16 degrees) of the trajectory. The gain of the TLS pattern was increased somewhat to compensate for the smaller volumetric coverage of the MSBLS system.

Calculation of received power level for Azimuth and DME is done by superimposing the gain of these antennas on the trajectory of the elevation angle from the localizer site (Figure 14).

Resultant signal strength as a function of time plots to be used in the BVE stimulation for the azimuth and DME function are shown in Figures 15 and 16.

3. DOWN LINK SIGNAL STRENGTH SIMULATION

Signal power level on the DME interrogation link determines the thermal noise content of the received interrogation signal and generates a bias (Ground pulse level shift) in the decoded DME data.

Error due to thermal noise is small (less than .4 feet) and can be ignored for all practical purposes.

The bias, however, is quite large. It can reach a value of 20 feet. It is due to using a fixed gain (wide open) receiver on the ground.

Airborne interrogations are detected by the fixed gain receiver. Video threshold level on the pulse risetime is, therefore, a function of signal strength, generating a bias error which is a function of distance.

Using a signal strength program for the downlink function would require a heterodyne receiver within the MSBLS simulator. It would also require over 100 db of attenuation. All this would tend to be expensive. Problems with RF leakage would probably be encountered.

Another way to simulate ground pulse level shift is to leave the detection of interrogations as it is now, using a crystal video receiver. The bias can be precalculated as a function of signal strength and added to the simulation of range delay.

C. SIGNAL PERTURBATIONS DUE TO PROPAGATION EFFECTS

1. MULTIPATH FROM ANTENNA SIDELOBES

Table 2 (page 114) shows that multipath from antenna sidelobes is the overriding source of noise error for the MSBLS angle functions.

Multipath beam distortion generates a thresholding error. The thresholding error transforms to an angle error according to the slope of the beam envelope which in turn is a function of antenna beamwidth.

Expected error due to multipath can be estimated by assuming that an amplitude disturbance δA due to multipath alters the time at which the beam envelope crosses the threshold used for decoding.

The amplitude disturbance is translated to a time disturbance δt according to the slope of the time envelope at the threshold. For small disturbances, this is essentially equal to the slope of the undisturbed envelope. Calling this m , and the angular rate of scan α , the one edge angle error is:

$$(4-14) \quad \Delta\theta = \frac{1}{2} \alpha \delta t = \frac{1}{2} \alpha \delta A / m$$

Assuming the time envelope $E = A_0 [\sin(t/\tau)/(t/\tau)]$

$$(4-15) \quad m = \left. \frac{dE}{dt} \right|_{t=t_1} = \frac{A_0}{t_1} \left\{ \cos(t_1/\tau) - \left[\sin(t_1/\tau)/t_1/\tau \right] \right\}$$

where $2t_1$ = beam dwell time.

In terms of 3-dB beam width B , $\uparrow = B/(2.78)$. Therefore,

$$(4-16) \quad \Delta\theta = \frac{0.5 \alpha t_1 (\delta A/A_0)}{[\cos (2.78 \alpha t_1/B) - [\sin (2.78 \alpha t_1/B)]/(2.78 \alpha t_1/B)]}$$

Since the multipath effects change with beam pointing angle, the two threshold effects may be considered independent; hence, the expected resultant angle error might be increased by $\sqrt{2}$. However, the assumed amplitude disturbance due to multipath, δA , is a sinusoidal function of relative phase and has an rms value $1/\sqrt{2}$ of its peak value. Therefore,

$\Delta\theta$ is the statistical (1 sigma) expectation if δA is the multipath magnitude.

Scanning speed, α , is 691 degrees per second for the azimuth antenna and 345 degrees per second for the elevation antenna.

The relative multipath level ($\delta A/A_0$) is based on the sidelobe levels of the scanning antennas.

A survey of elevation antennas which will be utilized for the MSBLS-GS shows a typical sidelobe level of 20 db below the peak of the beam. Assuming a 3 db loss due to reflection, a multipath level of 23 db below the peak of the beam results.

Azimuth antenna sidelobes are lower down. Typical multipath level for azimuth is 28 db below the peak of the beam.

Simulation of multipath can be realized by superimposing

a noise function on the beam envelope whose rms amplitude corresponds to a given multipath level.

In order to achieve a δA amplitude change at the nav sets video output, a change in RF attenuation of

$$(4-17) \quad \Delta A_{tt} = 20 \log \left(1 - \frac{\delta A}{A_0} \right) \text{ db}$$

is required.

But since multipath adds vectorially to the main beam at RF, the disturbance δA is a function of relative phase and has an RMS value of $1/\sqrt{2}$ of its peak. The amplitude perturbations then become

$$(4-18) \quad \Delta A_{tt} (1 \text{ sigma}) = 20 \log \left(1 - \frac{\delta A}{\sqrt{2} A_0} \right)$$

In terms of the "db below the peak of the beam"

$$(4-19) \quad \Delta A_{tt} (1 \text{ sigma}) = 20 \log \left(1 - \frac{10^{(M_u/20)}}{\sqrt{2}} \right)$$

where M_u = multipath level in db below the peak of the beam.

The noise function should therefore have an rms amplitude of ΔA_{tt} .

A Rayleigh distributed noise variable is a good approximation of the video amplitude fluctuations due to two RF signals combining in a random phase relationship.

2. SIGNAL STRENGTH FLUCTUATIONS

Signal strength fluctuations at the MSBLS navsets input are expected to arise due to scalloping of the airborne antenna pattern. Because the MSBLS antennas are looking through the skin of the spacecraft, the airborne antenna pattern is expected to contain peaks and valleys not usually encountered in other applications of the scanning beam system.

During flight, the craft pitches, rolls and yaws as the control surfaces servo the vehicle along its reference trajectory. The movement of the airborne antenna looking angle will generate fluctuations in received signal strength.

Signal strength fluctuations have a secondary effect on angular error, but they could play havoc with the receivers AGC if their amplitude and/or periodicity is too high.

Although the airborne antenna pattern may be precisely known, the fluctuations constitute a random phenomenon because they are a function of the error in estimation of the vehicles state vector, wind gusts, etc.

One thing that can be said about the fluctuations is that they don't change very rapidly. The sheer mass of the craft restricts rapid movement of the antenna looking angle.

Until more is known about these parameters, we have tentatively chosen the RMS noise amplitude as 1 db and the time constant as 1 second. Provision is made within the BVE to reprogram these parameters to other values, should they prove to be more appropriate.

Description of the signal strength fluctuations suggest the use of a time correlated pseudorandom process. We have used the Gauss Markoff sequence to generate the slowly changing random waveform. The standard deviation (noise amplitude) of the random sequence is determined as a function of the difference between the peaks and valleys of the antenna pattern. The time constant (noise beamwidth) is determined from the periodicity of the shuttles movements.

3. ERRORS DUE TO ATMOSPHERIC EFFECTS

The most common atmospheric effect on Kuband signals is attenuation due to rain. Attenuation (in db per nautical mile) varies according to rain rate (in millimeters per hour). Attenuation tables can be found in reference books, Reference Data for Radio Engineer for-one.

The MSBLS system is being designed for a 10 nmi range at a 10 mm/hr precipitation rate, so that attenuation due to rain does not quite fit into the MSBLS error model (except for reduced signal to noise ratio at a given point in the trajectory).

There is no problem with bending of radio waves (refraction) due to the precipitation itself since the rain drops are much smaller than the wavelength of the radiation. Backscatter is also not a problem since signal echos are not involved.

Areas of precipitation can, however, form regions within the MSBLS coverage which are at a higher relative humidity (partial pressure of water vapor). Relative humidity is one of the factors which determines the index of refraction of the atmosphere, so a random component is introduced into the calculation of bias due to refraction. In order to determine the magnitude of this component, refraction due to an ideal atmosphere must first be considered.

Mean error due to refraction effects the elevation and DME functions of the MSBLS system. The signal travels a

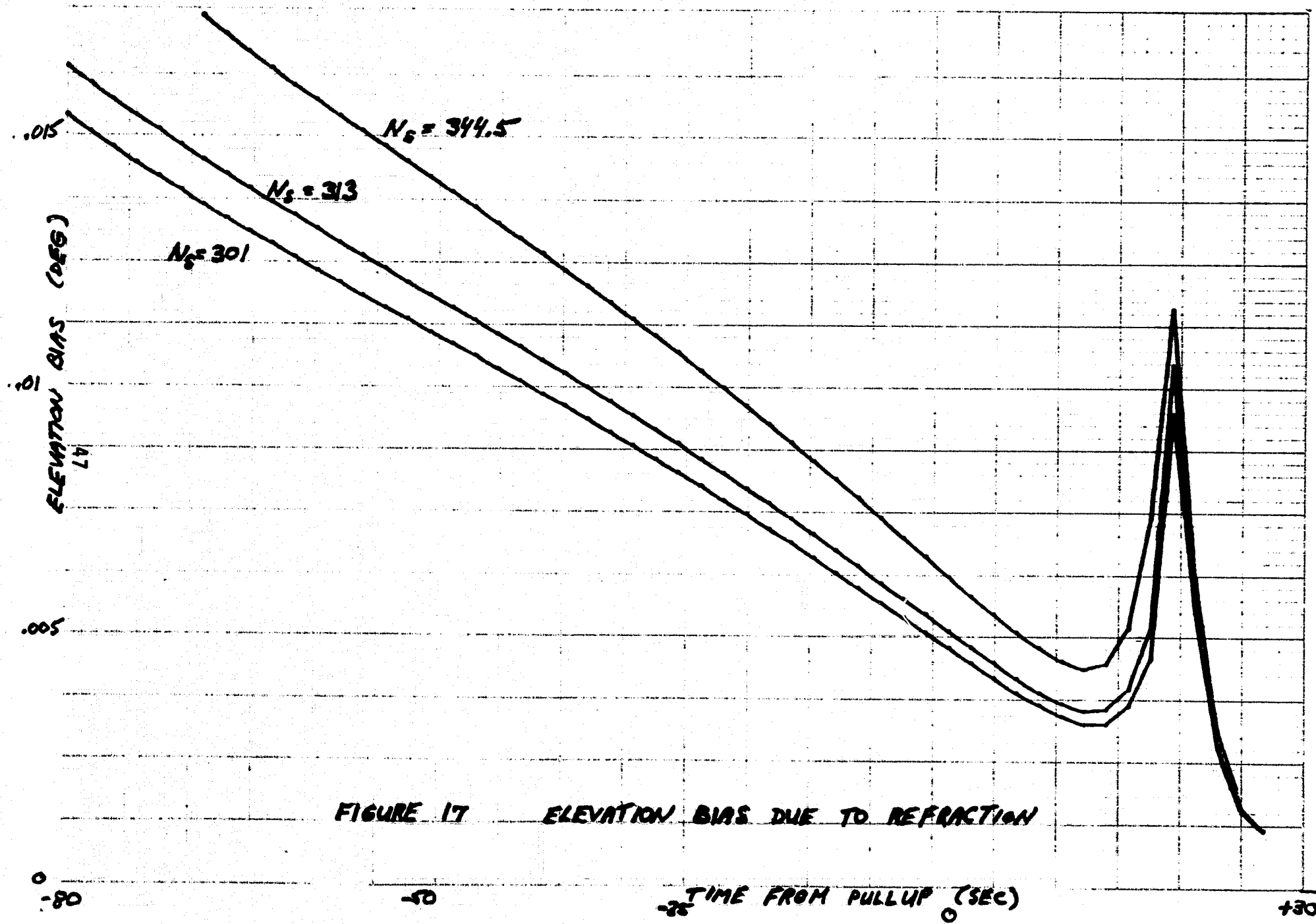
curved path so that range and elevation angle appears larger than it actually is.

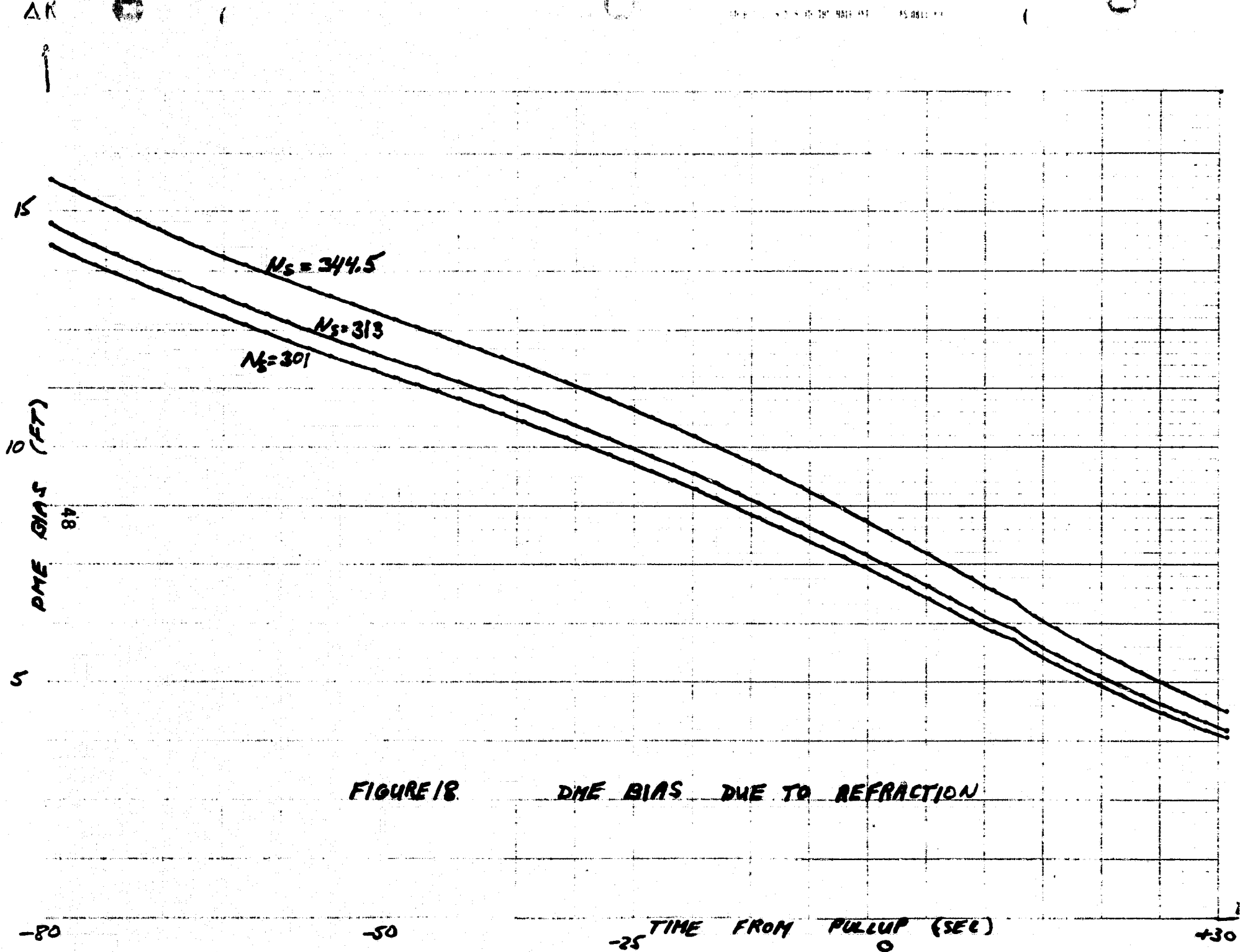
Refraction bias is a function of the surface index of refraction. This parameter depends on atmospheric pressure, temperature and relative humidity. Given an accurate measurement of these variables, the index of refraction can be calculated to an accuracy of better than 1 percent. A scaled up version of the index of refraction called refractivity is commonly in use. A mean value of refractivity at sea level is taken as 313 N-units with typical values in the order of 300 to 350 N-units. Bias due to refraction is calculated by assuming an exponentially decreasing refractivity as a function of height. Figures 17 and 18 show the Elevation and DME refraction bias for the MSBLS trajectory for a number of refractivity values.

Elevation error is seen as .015 degrees at the start of MSBLS trajectory and decreases to approximately .003 degrees. DME error starts at about 10 feet and decreases to approximately 6 feet.

If the shuttle navigation subsystem corrects MSBLS Data for refraction, then only a residual error due to atmospheric perturbations (such as regions of humidity variations) and the uncertainty of calculation of surface refractivity results.

The residual error is given in reference 1 as about 5 percent of the refraction correction, or a maximum 1 sigma





error of .0075 degrees for elevation and .5 feet for DME. The residual error is seen to have a negligible effect on MSBLS data.

If MSBLS Data is not corrected for refraction, then the refraction bias ought to be included in the BVE simulation. Since refractivity at the surface is a random variable, it would appear that one curve from the family of curves of figures 17 and 18 should be chosen at random for each simulation run. But reference 2 gives the standard deviation of refractivity variations as 10 N units so that 1 sigma deviation of refraction bias from the mean curve (N=313) is less than .001 degrees for elevation and less than 1 foot for DME through the MSBLS trajectory.

Random selection of a refraction bias is seen as not worth the effort. The BVE simulation will introduce a fixed bias curve for refraction (N=313) with the ability to override this function should the MSBLS data be subsequently corrected for refraction.

V. RADAR ALTIMETER BVE REQUIREMENTS

Simulation of radar altimeter functions should be done to provide a realistic exercise to the radar altimeter navaid.

Included in the simulation are 1) space shuttle trajectory and 2) radar altimeter error sources.

Simulation of height can be done by synthetically triggering the radar altimeter timing circuits without transmitting the RF pulse. At the end of the elapsed height delay, the radar altimeters transmitter can be externally triggered. Figure 19 shows the block diagram of this simulation. The RF energy is passed through attenuators and fed back into the receiving port. The altimeter takes the delay from start of its timing cycle to reception of the RF pulse as the height.

A. RADAR ALTIMETER TRAJECTORY

The radar altimeter will be exercised by a time delay generator so as to progress from wheel height 200 feet to wheel height zero.

The trajectory of this program has two parts. In the first part, from 200 feet to 60 feet wheel height over threshold, the path has a 3 degree constant slope; in order to come out at 60 feet over threshold with an aiming point of 1500 feet inside threshold.

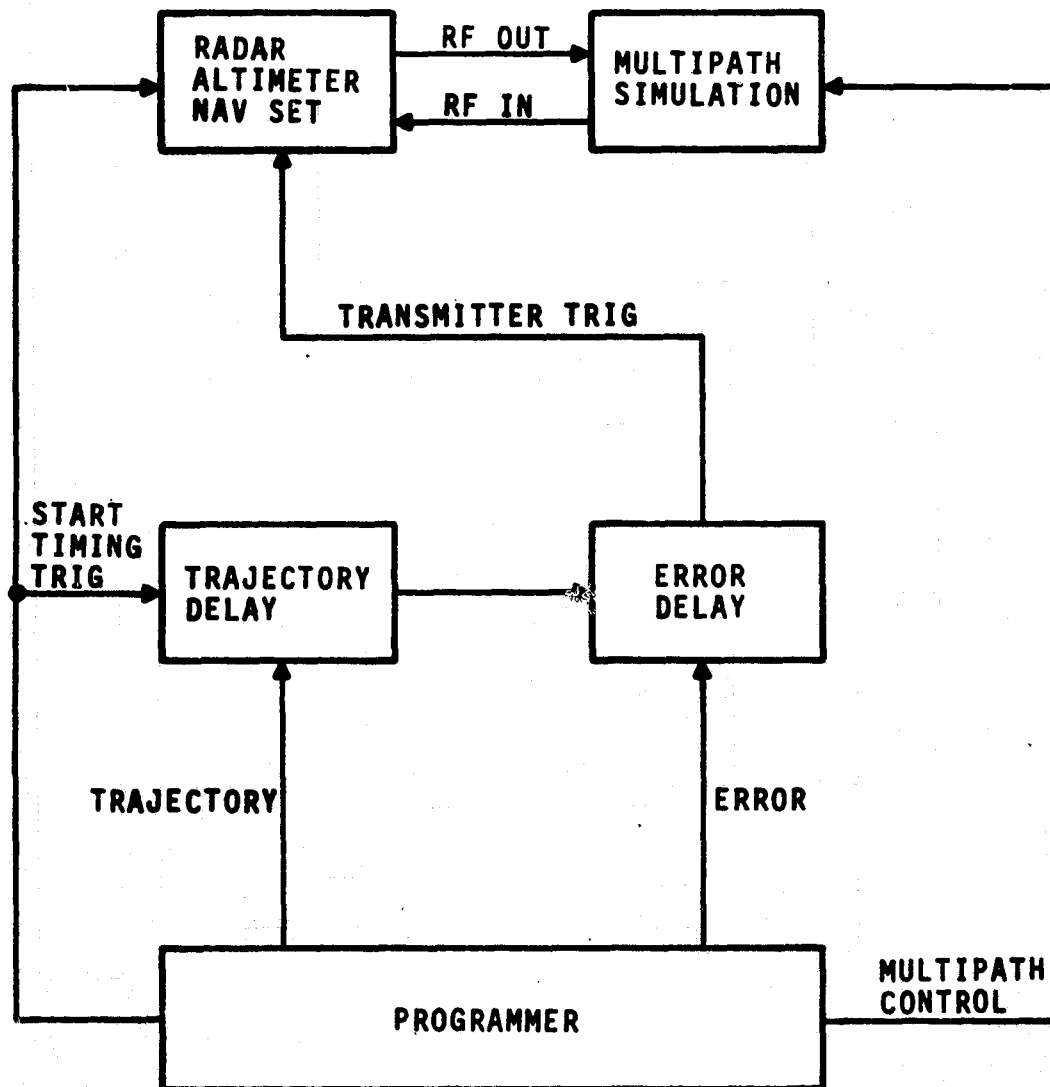


FIGURE 19 RADAR ALTIMETER BVE SETUP .

The time delay corresponding to height is taken with a scale factor of 492 feet per microsecond. In fact, the height (wheel height) is expressed as a function of elapsed time on trajectory.

From 200 feet to 60 feet the expression for height is

$$h = (x - 13,500) \tan 3^\circ - 18.61 \text{ feet, } x > 15,000, \text{ where the}$$

ground range, x , is defined as in the MSBLS trajectory;

$$x = \frac{7.197t^2}{2} - 489t + 23,290$$

time t being referenced at start of pullup (see figure 8).

The final flare to touchdown, starting with 60 feet wheel height over threshold, will be an exponential decay of height and sink rate, with touchdown established by zero wheel height at a sink rate of 2 fps.

The expression in this region becomes

$$h = 67.435 \exp[(19.853 - t)/3.718] - 7.435 \text{ feet}$$

$$x < 15,000$$

Simulation of height must take into account any delay inherent in the altimeters tracking loop. This requires a high resolution on the height function and height programming on a pulse by pulse basis.

The height simulation can be done as in the simulation of MSBLS range by programming of sink rate rather than height directly. Height can be decremented at 1/2 radar foot steps at the preprogrammed rate.

If the instantaneous value of the height trajectory is compared to radar altimeter readout at the same point in time, any lag due to the time constant of the altimeters tracking loop will show up in the data.

B. RADAR ALTIMETER ERROR FUNCTIONS

1. ANTENNA SPACING FOR ALTIMETER

It is assumed that the altimeter will be calibrated to read zero wheel height while the vehicle is on the ground, with zero roll and pitch, and with the altimeter antennas 4 feet apart and 4 feet above the ground. (Rockwell spec on the radar altimeter). A height error due to antenna spacing therefore increases with height, and this error will be expressed as a function of elapsed time through the trajectory function. The antenna spacing error will be incorporated as a time delay function in combination with the trajectory time delay generator. For antennas with 4 foot spacing zero calibrated four feet above ground, the antenna spacing error is almost 0.5 feet at 200 feet, and zero at touchdown.

2. ROLL AND PITCH

The altimeter error due to roll will not be incorporated, because the roll angles expected below 200 feet will not significantly change the altimeter readout, taking into account the beam width of the radiation (45°) and the probable

symmetry of the altimeter antennas each side of the roll axis.

On the other hand, the altimeter error due to pitch will be incorporated as a BVE function. The error due to pitch becomes very significant, since the pitch can become about +10 degrees relative to the pitch obtained for calibrated zero height, assuming that the wheels are much closer to the axis of pitch rotation than the altimeter antennas are. (If subsequently the vehicle computer makes a correction for pitch, this portion of the BVE can be deleted).

The height error due to pitch will be calculated using tentative assumptions that (1) the antenna moment of pitch rotation is say 40 feet greater than the wheel moment of rotation, and (2) the pitch angle changes from -3 to +10 degrees pitch, linearly with time, between 200 feet wheel height and touchdown. Using 40 feet moment arm and +10 degrees, the error becomes 7 feet. The height error due to pitch will be found from a pitch program as a function of elapsed time, and will be incorporated as another time delay function in combination with the trajectory time delay generator.

In addition to the pitch bias, the vehicles pitch is expected to servo about the nominal value introducing a time correlated random noise component into the altimeter reading. If a 1 degree RMS pitch fluctuations is assumed, the 1 sigma height noise becomes .7 feet. This error will, therefore, be simulated by summing into the time delay a random delay selected from a Gauss Markoff process with standard deviation of .7 feet and time constant of 1 second.

3. TERRAIN HEIGHT AND SLOPE

The altimeter readout is interpreted as height above touchdown, and so the height above the terrain is in error by the height of the terrain, even if the terrain measure is perfect. A terrain height fluctuations will be modeled as a gaussian distributed function with a 1σ dispersion of 2 feet. This error will be incorporated as still another time delay function in combination with the antenna spacing time delay generator.

The effect of the terrain as a reflected region over the illuminated sector of the antenna pattern will be treated as a separate BVE function in a later section, particularly with respect to the multipath effect of reflecting surface at distances greater than minimum distance vertically from the antenna.

Since the altimeter is designed to operate from 2500 feet and will be used for BVE only below 200 feet, it is assumed that the signal return is generally at the amplitude of receiver saturation, with sufficient margin to negate the need to consider changes in reflection amplitude from the illuminated terrain below 200 feet height. It is estimated that a program to change the amplitude of the BVE signal is not worth the effort.

4. SUMMARY OF TIME DELAYS

The radar altimeter BVE time delay generator will incorporate programmable height and height error functions of elapsed time for (a) trajectory, (b) antenna spacing, (c) pitch, (d) terrain, and (e) a fixed bias of .5 feet (1σ) selected prior to each simulation run. The fixed bias is included because it is probably realistic for typical altimeter installation.

5. MULTIPATH ON ALTIMETER BEAM

The pointing angle of the beam and its beam shape have no effect on the altimeter measurement, as long as the signal is received straight down. No signal can be received from less than vertical distance except by some vehicle structure reflection, which is not anticipated for any duration that would upset range tracking. The multipath encountered here is the result of reflections and scattered radiation from the approximate circle of terrain around the nadir, and the size of the circle depends primarily on the radiation pattern and the height and secondarily on the pitch.

The main effect to be anticipated from the terrain circle of reflected signals is to widen the pulse width of the received microwave pulse by flattening the leading edge and stretching its trailing edge.

for the beam width of 45 degrees and pitch less than 10 degrees the maximum angle off the nadir is taken as 30 degrees, and the maximum range is 1.15 times the altitude. This makes the pulse width the nominal 100 nanoseconds plus 15 percent of the height (in nanoseconds at the scale value of 492 feet per usec). At 200 feet (204 feet antenna height) the extra distance is 30.6 feet, and the extra delay slightly over 62 nanoseconds.

Widening of the altimeters trailing edge should not have an appreciable effect on the altimeters error because the altimeter is supposed to track the leading edge.

The first portion of the rising pulse edge should be fairly clean since it is received from straight down. Higher on the pulse risetime, energy scattered from the terrain circle starts combining with the straight down signal resulting in a distorted pulse envelope. The exact shape of the pulse leading edge depends on the conditions of the reflected surface and cannot be predicted. Since the conditions of the reflected surface are changing with the motion of the craft, the exact shape of the return leading edge will fluctuate with time. The fluctuations add a random noise component to the position of the altimeters track gate.

It does not appear to be feasible to effect the leading edge distortion and pulse stretching by changing the pulse width in the modulator of the set. However, it does appear feasible to modify the pulse shape after it has been transmitted by branching through coaxial cables of various lengths of transmission delay and recombining the signals from all the cables to receive a combined (and distorted) rf pulse.

In order to implement a fluctuating pulse envelope, energy passing through the coaxial cables can be

controlled by RF switches so that only selected lengths of delay can be recombined to form the return signal. Decision as to which switches are to be on, can be made on a random basis at a given time interval.

VI TACAN BVE REQUIREMENTS

Requirements for a TACAN BVE which can accurately determine the error model of a representative TACAN navigation aid can best be accomplished by utilizing a commercially available programmable TACAN Beacon Simulator set.

An external programmer can be utilized to generate the trajectory for bearing and range which is judged "representative" of the space shuttle application.

The programmer can also generate the bias and random noise which is associated with the TACAN ground station and with propagation of the RF energy.

The proposed BVE setup would resemble the block diagram of Figure 20. The TACAN Beacon Simulator and the TACAN Navigation set are commercially available. The programmer and an interface for conversion of error variables into phase and delay fluctuations of the TACAN RF signal would have to be built. TACAN derived data is compared to instantaneous values at sample trajectory points and the deviations are taped.

A. TACAN BVE TRAJECTORY

TACAN trajectory proposed for the BVE exercise deviates somewhat from the shuttle's typical operation, but it is designed for range and bearing rates which will expose the TACAN navigation sets errors thoroughly.

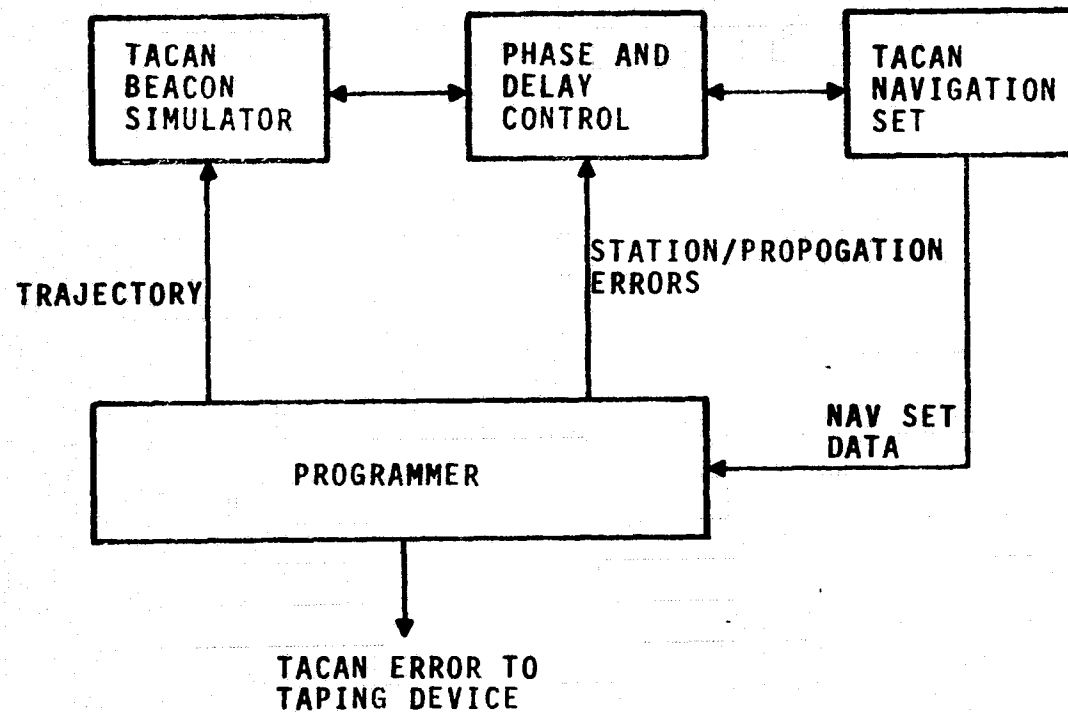


FIGURE 20 TACAN BVE SETUP

For DME (R in nautical miles) and bearing θ (in degrees) the trajectory programs are expressed for $R=399$ and $\theta = 90^\circ$ at $t = 0$; they are arranged to make the bearing value and the bearing rate both zero at $t = 300$ seconds, $R = 12$ nm. For t greater than 300 seconds θ remains zero (centerline coinciding with MSBLS) and R decreases at 0.08 nm/sec (288 knots) as the MSBLS.

The equations used for figure 21 are:

$$(1) \quad R = 399 - 2.5 t + 1.21 \frac{t^2}{300} \quad \text{from } t = 0 \text{ to } 300 \text{ seconds}$$

$$\text{and } (2) \quad \theta = 10^\circ \left(3 - \frac{t}{100}\right)^2 \quad \text{from } t = 0 \text{ to } 300 \text{ seconds}$$

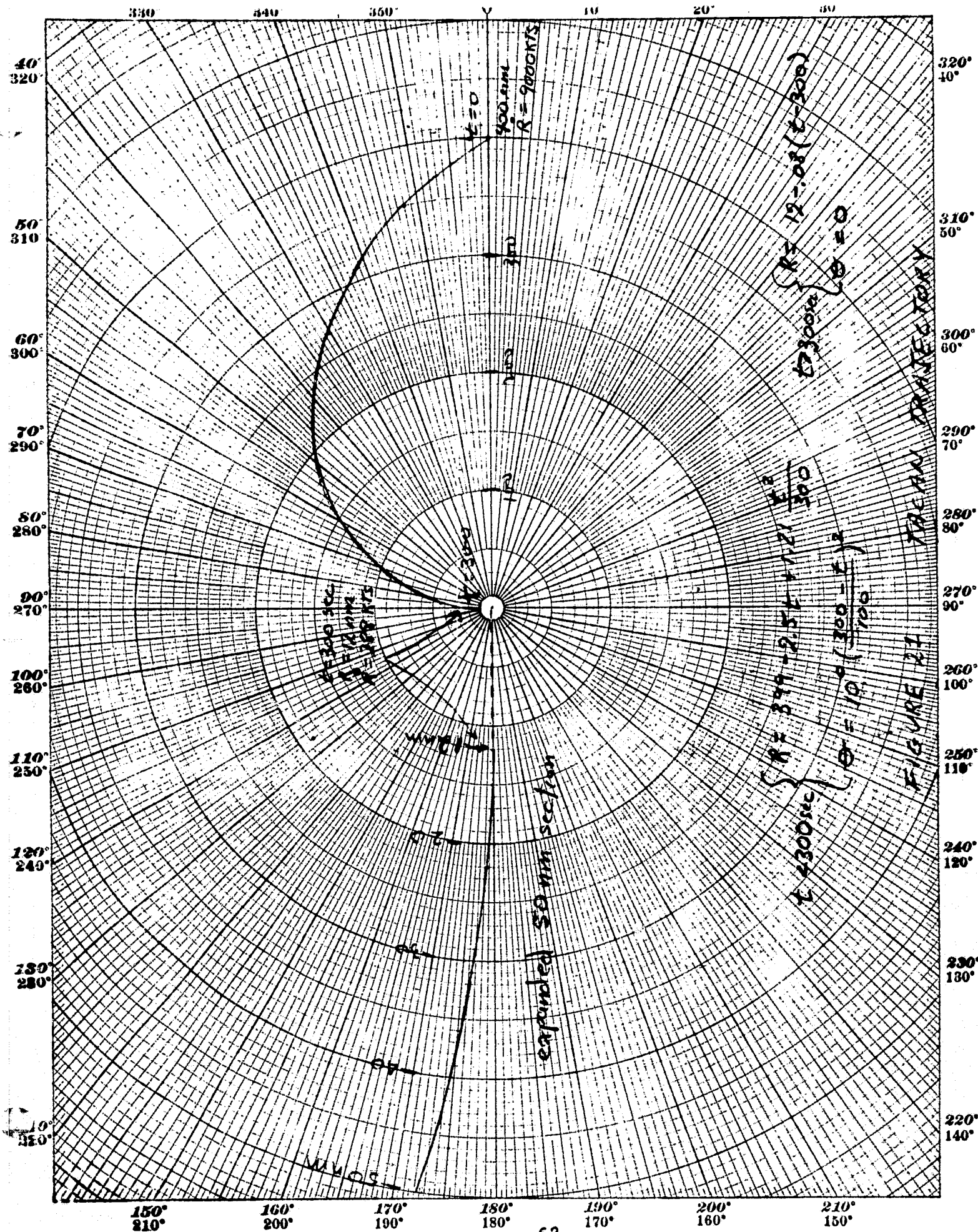
$$(3) \quad \text{After } t = 300, \theta = 0 \text{ and } R = 12 - .08 (t - 300)$$

$$\text{From equation (1)} \quad \dot{R} = -2.5 \text{ nm/sec} = 9000 \text{ kts at } t = 0$$

$$\dot{R} = 0.08 \text{ nm/sec} = 288 \text{ kts at } t = 300$$

$$\text{And from equation (2)} \quad \dot{\theta} = -0.2 \left(3 - \frac{t}{100}\right) \text{ degrees per second.}$$

The bearing rate decreases from 0.6 degrees per second between $t = 0$ and 300 seconds.



B. BVE TACAN ERROR MODEL

TACAN signal at the input of TACAN navigation set is to resemble a signal encountered during the shuttle's operation. This signal must be corrupted by an error which is expected to arise from the ground station and from effect of signal propagation.

BEARING ERROR

Reference 1 gives the bearing error for a typically "good" system as .5 degrees of which .25 degrees is related to the airborne decoder. This leaves an RSS difference of .433 degrees as due to ground station and propagation effects.

The bearing error is assumed equally divided between bias and random noise. This yields a 1 sigma bias of .306 degrees. The bias component for a given BVE simulation should be chosen from a gaussian distributed function prior to the simulation and held constant through that simulation.

The bias error will be introduced by advancing or retarding the 135 Hz modulation of the bearing signal generator relative to the reference pulses at 135 Hz.

Random bearing error is primarily due to multipath distortion of the omnidirectional TACAN signal. One sigma value of this error component is given as .306 degrees. The error value fluctuates with bearing, and thus with flight time. The time constant is given as 10 seconds for 600 knots, and will be taken in the BVE as a time constant equal to $6000/V$ (in knots); this changes the time constant from .7 seconds at start of the

trajectory to 20 seconds at 12 K feet altitude over the trajectory program.

The random phase shift will be changed at intervals of 1 second, making the changes increasingly time-correlated as the flight progresses down to 14 K feet altitude. According to the time constant and the one-sigma value associated with a calculated gaussian distribution, each new value will be a remnant of the previous sample value combined with a random value, the relative proportions depending on range rate in the trajectory.

RANGE ERROR

A reasonable error model for DME due to ground station and propagation effects is taken from reference 1 and 3.

The random error is given as a one sigma value of 90 feet (and a time constant of one second) and a bias value that is range-dependent, taking into account the changing signal level affecting the DME transponder bias. The one sigma DME bias is given as 555 feet for a range greater than 200 nmi linearly running down to 211 feet for a range less than 200 miles with a time constant of 300 seconds.

The random error will be changed at 1/4 second intervals with a time constant of one second, the bias error (range dependent one-sigma value) will be changed at intervals of 30 seconds, using a time constant of 300 seconds.

DME errors will be introduced by inserting a bias and random component into the simulation of range delay.

A summary of the bearing and range errors to be included in the BVE simulation is as follows:

Bearing

Bias - .306 degrees (1 sigma)

Noise - .306 degrees, time const = $6000/V$ sec

DME

Bias = 555 feet (1 sigma); Range > 200 nmi
= $211 + \frac{344R}{200}$ (1 sigma); Range < 200 nmi } Time Const = 300 sec

Noise - 91 feet (1 sigma) ; Time Const = 1 sec

The computing processor for generating the statistical distributions for TACAN bearing and DME errors (both bias and random) will be identical with the processor used for MSBLS BVE, except for programming the operational exercise.

VII ONE WAY DOPPLER BVE REQUIREMENTS

A review has been made of the potential sources of error in a one-way measurement of the doppler received at an orbiting space shuttle from a ground station. The error sources originally considered were:

1. Tropospheric refraction
2. Ionospheric refraction
3. Frequency stability of the ground station transmitter
4. Multipath
5. Location of the ground station
6. Communication modulations on the signal to be measured
7. Amplitude modulation on the signal to be measured by pointing inaccuracies of the tracking signal
8. Phase noise on the transmitted signal
9. Polarization uncertainty in the transmitted signal

In discussing these items with Bruce Williamson at JSFC, citing previous Apollo work in two-way doppler, he assured me that only the first two items were of any significance; frequency stability is well taken care of by two Cesium clocks for long term stability, and a crystal oscillator to obtain short term stability (although one-way doppler may not be as elegant); multipath a few degrees above the horizon is not significant because of the directive antenna; the location of the ground station is known to within about 30 feet; communication modulations are well outside the ± 55 kHz band of the doppler signals; pointing accuracy of the antenna

directing system is well within a beamwidth and it does not hunt appreciably; phase noise on the transmitter was well below other noises; no polarization effects were noted and this is thought to be due to the existence of circular polarization at both transmission and reception (Williamson was not sure).

An exponential model of the atmosphere in an equation given by W.M. Lear (Reference 8) was used for obtaining the tropospheric refraction. For the ionosphere, an empirical equation developed by Cubic Corporation (Reference 13) was used for ionospheric refraction.

Since the calculated effects of these refractions will be accounted for in the orbital tracking equipment, one is left merely with the residual, unpredictable variations that the model or equation doesn't account for. In the case of the tropospheric model, this is variations in the actual troposphere from the true exponential distribution. For the ionosphere, this is variations in the height and density of the electron clouds from the assumed values. Estimates of these variations indicate that 95% of the tropospheric errors can be removed if the index of refraction (n_s) at the ground station is known and used in the calculations. Only 80% of the ionospheric errors can be removed, but they are already very small compared to the tropospheric errors, so this is of no consequence. Figure 22 shows the envelope of uncorrectable refraction errors that are expected to remain after all factors are considered. A circular orbit 100 nautical miles above the earth was assumed and a carrier frequency of 2 GHz was also assumed. The

errors are plotted as a function of time from the moment of closest approach (overhead). The two points where the elevation angle is 5 degrees are indicated --- it is seen that the residual errors are about 18 Hz at the 5° elevation angles dropping to zero at times near zero. (The curves may not be valid below 3° elevation angle). Within 50 seconds of zero time, the residual error is less than 3Hz. Williamson mentioned that during the Apollo program, the doppler introduced by a rotation of the space craft at a rate of 2 revolutions per hour (0.0005Hz) was detectable. I didn't check as to whether this was a regular capability or if it occurred only once. In any case, this suggests that the correlation time of the residual errors is very long, and in addition, the atmosphere must have been very much like the model atmosphere. From this, we probably can assume that a specific value of residual error exists for each pass.

The data for Figure 22 was arrived at in the following way: Orbital Frequency (Hz) = R101 = $360 / (84.4 \times 60 (R105/R102^{3/2}))$

where R102 = earth radius

R105 = orbital radius (earth rad. + altitude)

Tangential velocity (ft./sec.) = R106 = $2 \times R105 \times 6076.1 \times R101/360$

Tangential doppler (Hz) = R107 = $R106 \times \text{frequency (MHz)} / 984$

Received doppler = $R107 \cos (R120)$

where R120 = angle between the tangential velocity vector and a line to the ground station.

For a circular polar orbit with the ground station at a pole;

$$\text{Elevation angle of the vehicle} = R110 \arctan \frac{(R105 \sin (R101 \times t) - R102)}{(R105 \cos (R101 \times t))}$$

$$\text{Range to vehicle} = R111 = \sqrt{(R105)^2 - 2 \times R102 \times R105 \sin(R101 \times t) + (R102)^2}$$

The various values of elevation angle and range are put into the Lear and Cubic tropospheric and ionospheric models and the refraction errors derived. The tropospheric errors in range and angle are plotted in Figure 23 for a nominal value of the index of refraction (1.000313). The ionospheric error in range is plotted in Figure 24 --- it is seen that these range errors are about 1/10th of the tropospheric range errors. The angular error due to the ionosphere is even less noticable and is not plotted.

The way in which these range and angle errors manifest themselves in terms of doppler error is as follows:

- a. An elevation angle error adds or subtracts from the angle R120, amounting to about 10% of the overall doppler error. This error is shown in Figure 25.
- b. The rate of change of elevation angle error modifies the apparent tangential velocity of the vehicle. It is the major error contributor and amounts to about 90% of the overall error. This error is shown alone in Figure 26.
- c. The range error produces no error in the doppler so long as it is constant.

- d. The rate of change of range error (whether due to tropospheric or ionospheric effects) gives a small apparent change in angle $R120$. This contributes less than 1% of the overall error. This error for the troposphere and ionosphere are shown in Figure 27. It is seen that the ionosphere introduces less than .04 Hz of error.

In summary, a simulator of the one-way doppler errors should select a random value from an assumed Gaussian distribution with a mean of zero and a one sigma value of 18 Hz; then, vary the frequency in a manner that simulates the shape of one of the curves shown in Figure 22.

AS 0811-60
5 X 5 TO THE HALF INCH
SQUARE
DOPPLER UNCERTAINTY IN HERTZ

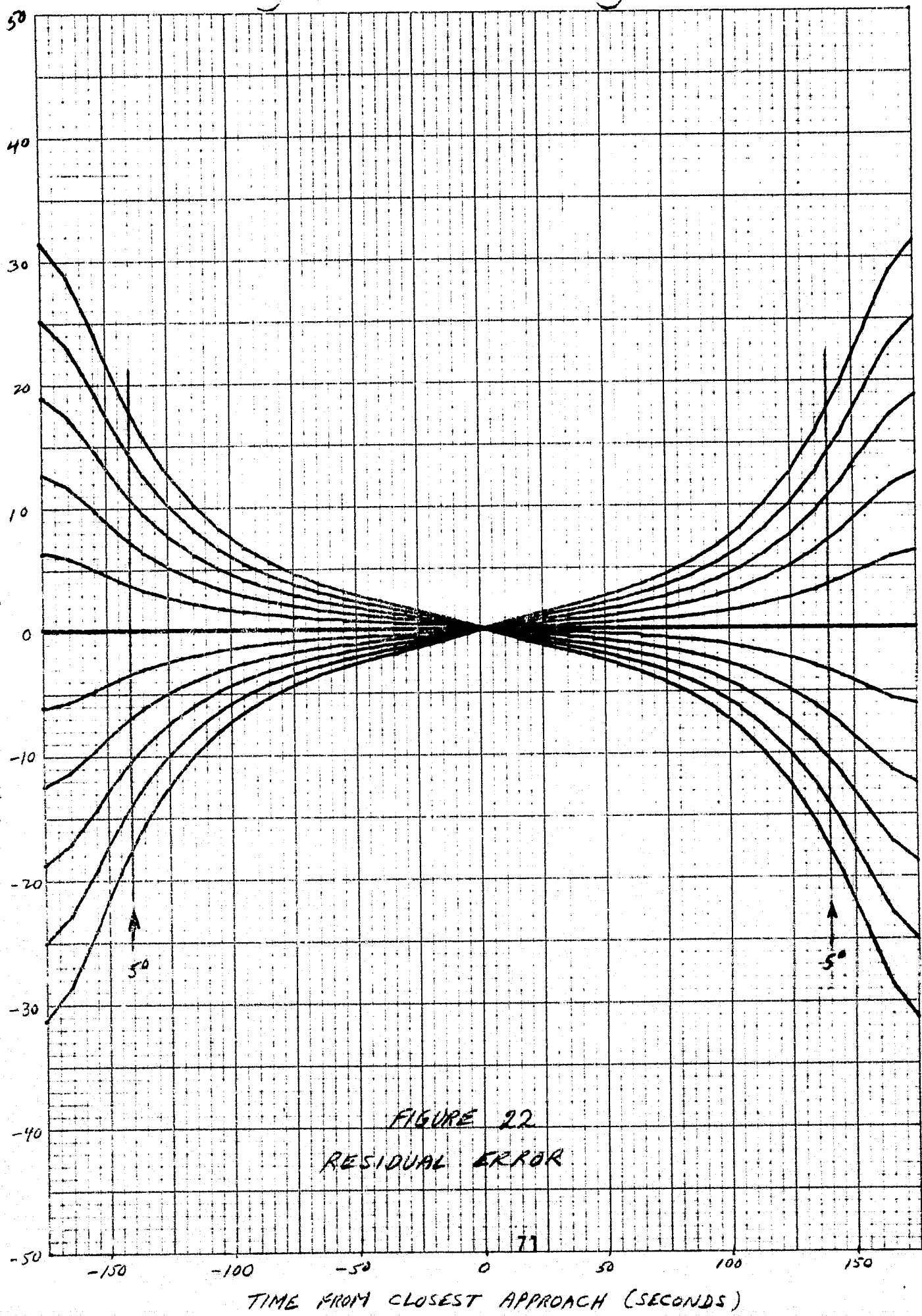
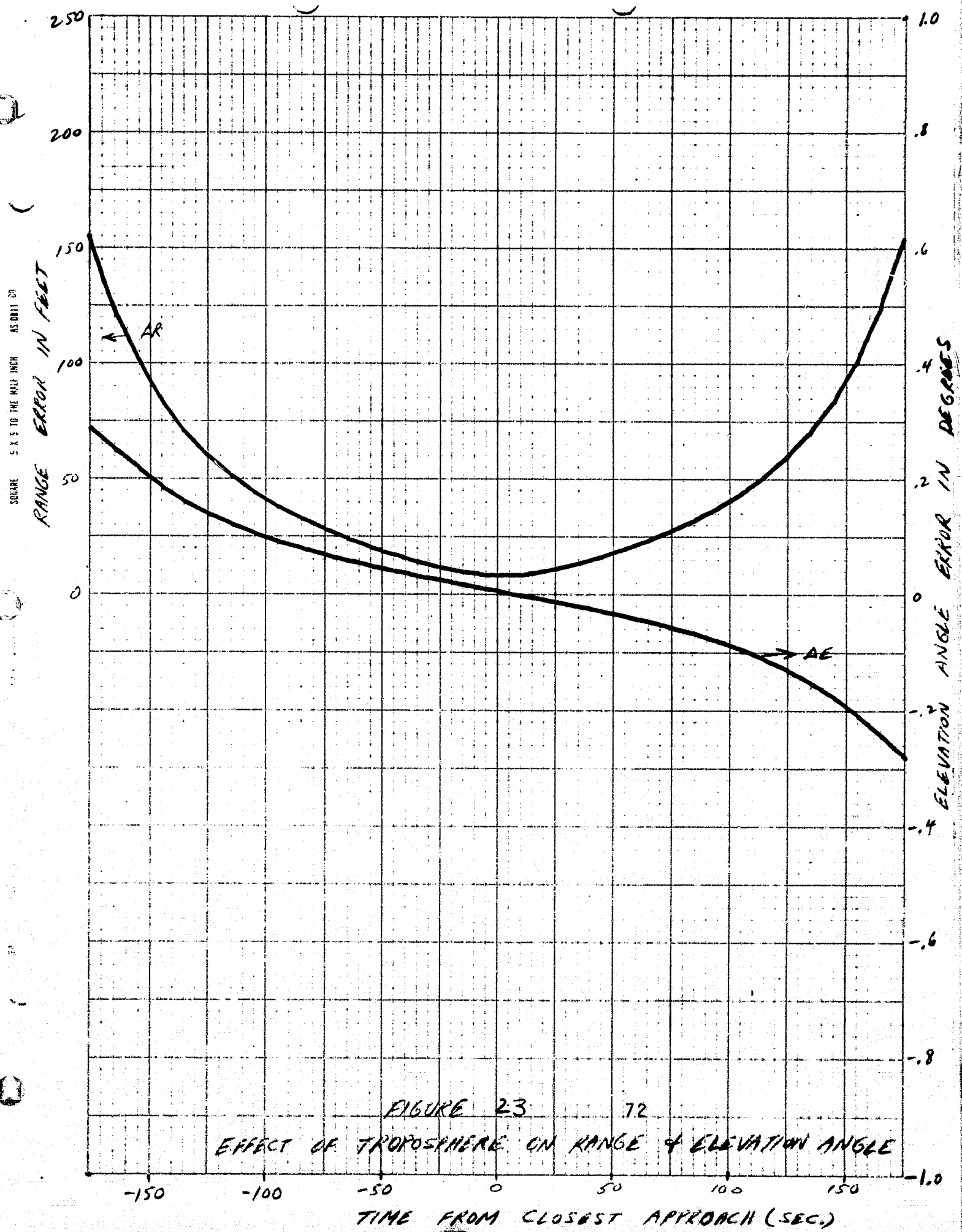


FIGURE 22
RESIDUAL ERROR



SQUARE 5 X 5 TO THE HALF INCH AS DET. -25

RANGE ERROR IN FEET

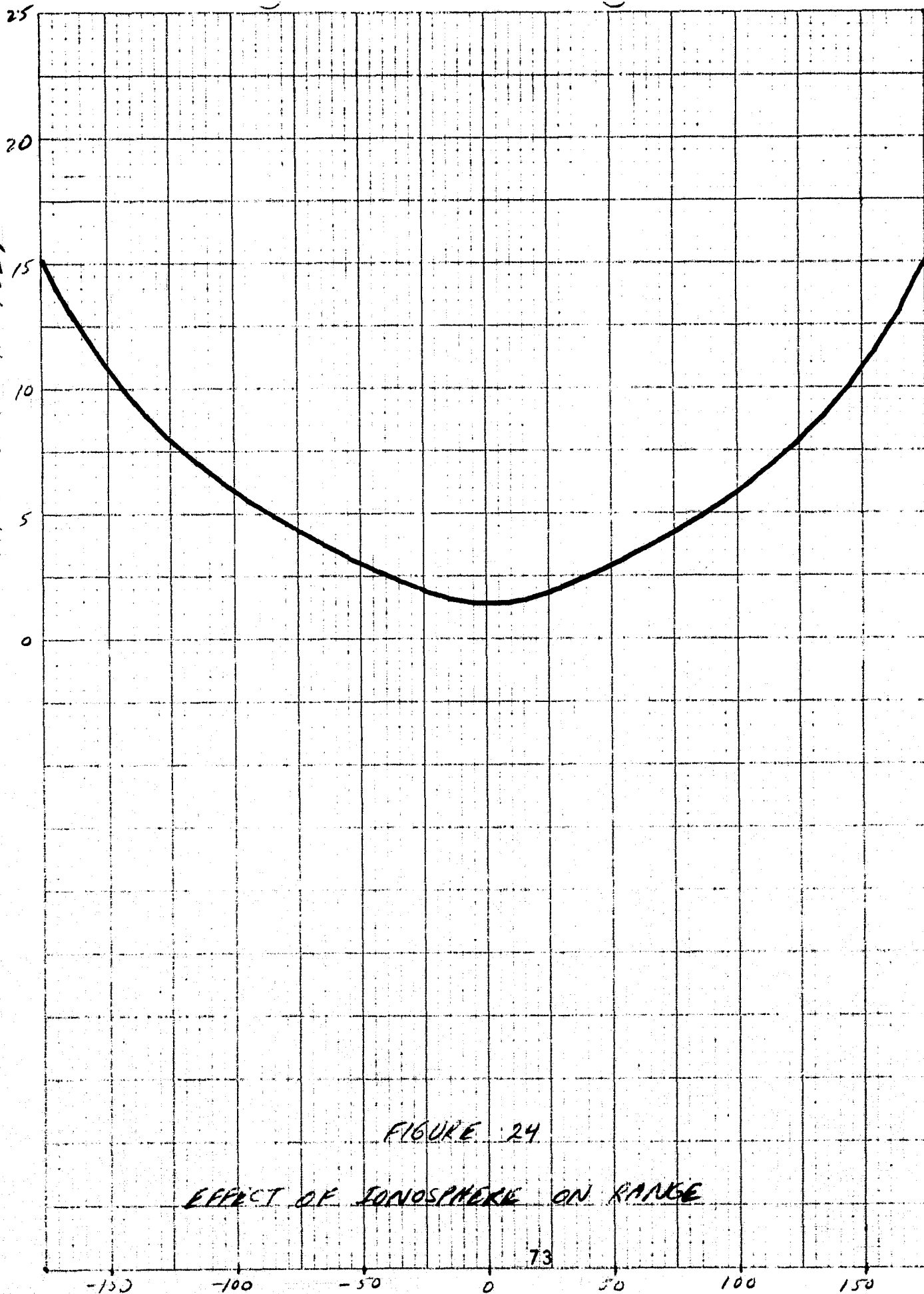


FIGURE 24

EFFECT OF IONOSPHERE ON RANGE

TIME FROM CLOSEST APPROACH (SEC.)

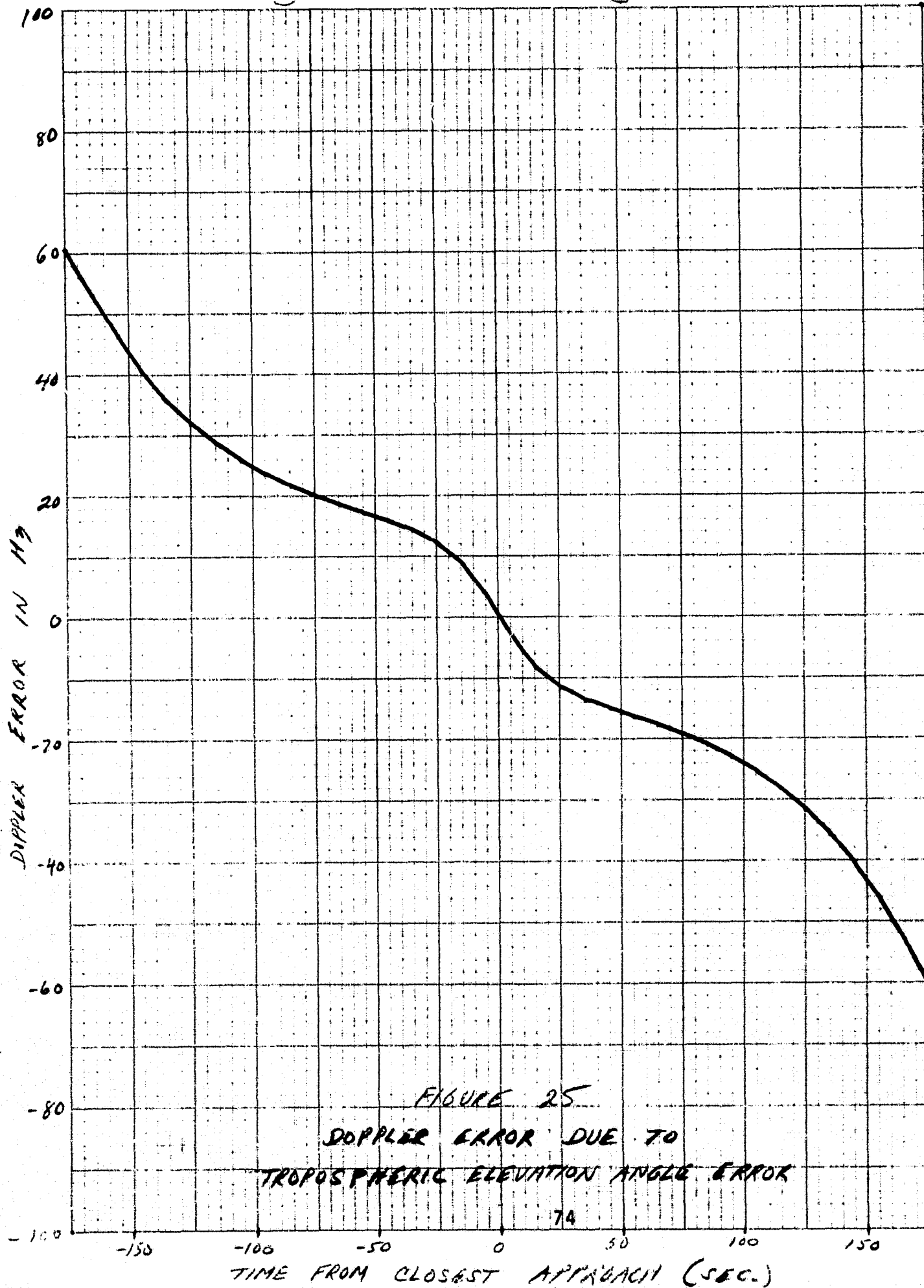


FIGURE 25
DOPPLER ERROR DUE TO
TROPOSPHERIC ELEVATION ANGLE ERROR

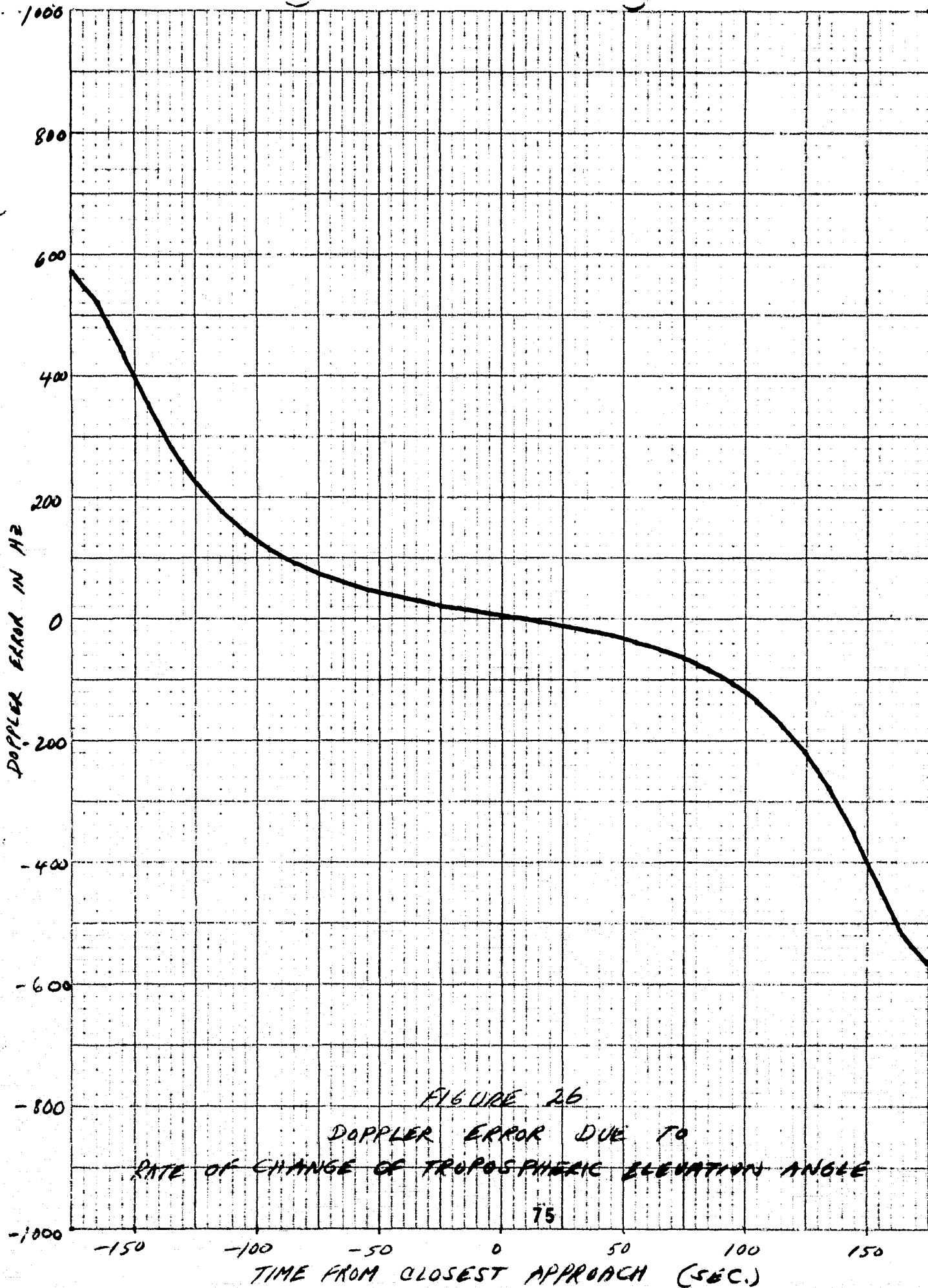


FIGURE 26
DOPPLER ERROR DUE TO
RATE OF CHANGE OF TROPOSPHERIC ELEVATION ANGLE

SOURCE 5 X 5 TO THE HALF INCH AS ORBIT 30

DOPPLER ERROR IN MHz

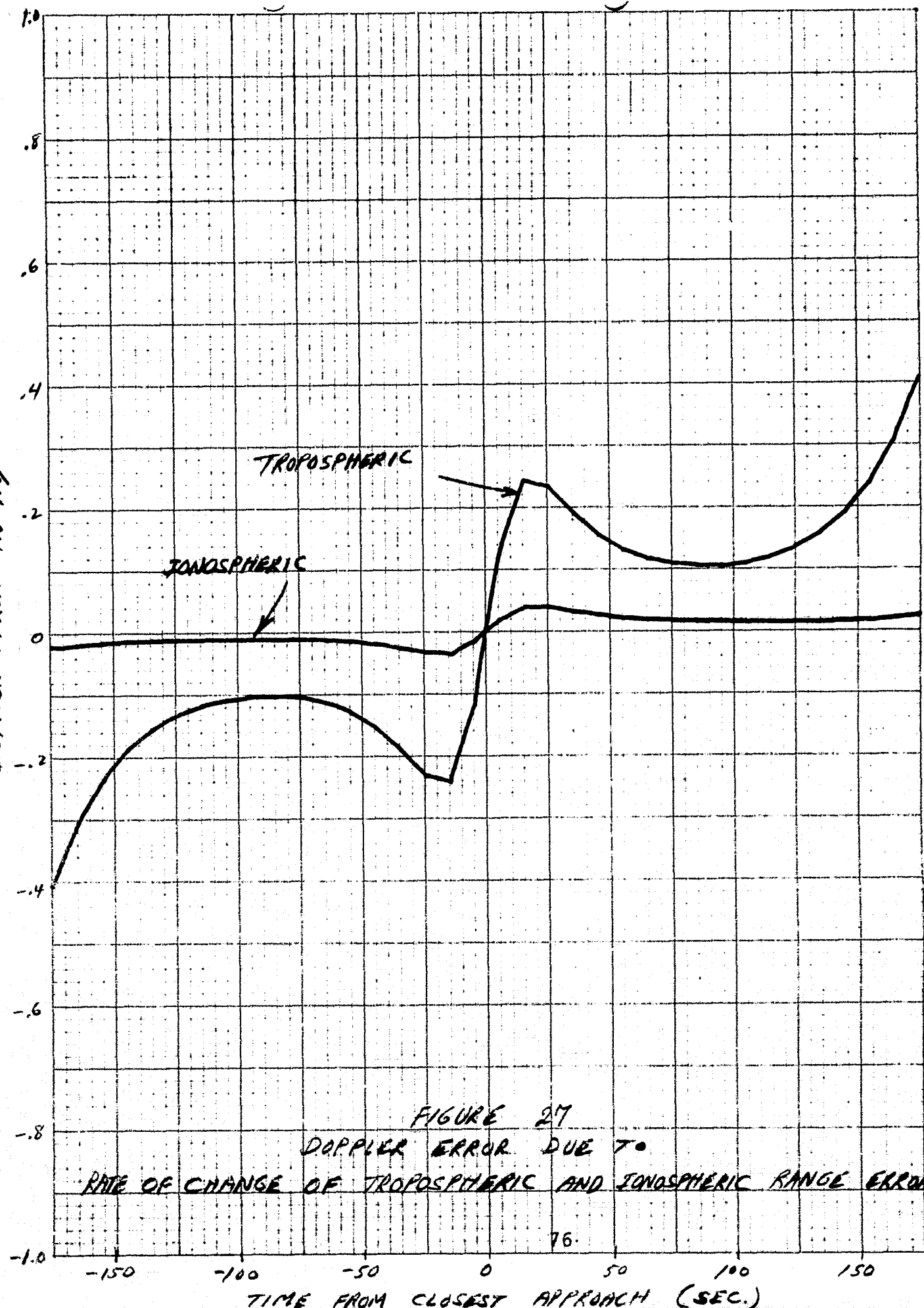


FIGURE 27
DOPPLER ERROR DUE TO
RATE OF CHANGE OF TROPOSPHERIC AND IONOSPHERIC RANGE ERROR

VIII. RENDEZVOUS RADAR BVE REQUIREMENTS

This section describes a concept for the BVE equipment to exercise the angle and range tracking capability of a candidate Rendezvous Radar. The aim of the BVE is to assess by actual measurement, the validity of error models that have been used during optimization of the radar system design. The situation wherein the radar is required to provide tracking data on large, uncooperative targets at short range is given particular emphasis in the BVE concept. These targets may be over 10 meters in length and must be tracked to within 100 feet of the radar. Although such a target subtends an angle up to several degrees, and amplitude fluctuations in the return signal may exceed 20 dB, the radar must continue to provide accurate angle rate and range rate information and at least determine target position in range and angle to within the target dimensions.

The BVE must be a practical, controllable simulation for the expected variations in target size, geometry, and motion. Furthermore, the radar environment of the BVE installation should minimize the sources and/or effects of external influences (such as multipath and clutter) that will not be a part of the radar environment in space.

A. ERROR SOURCES

The sources of error in the tracking data may be broadly separated into

- a) sources within the radar system and
- b) external sources

The internal error sources are generally well known and are usually controllable by component design and manufacture. Examples of these error sources are thermal noise, data granularity, servo drift and offset, mechanical flexures, servo noise, etc. These error sources were not a direct consideration in the BVE concept.

The external error sources arise from target noise and the nominal dynamic motion of the target relative to the radar.

Control of the effects of these external error sources is largely the problem of system optimization. The system designer proceeds to establish an error model which will form the basis for the system design. The BVE is required to simulate the sources of error on which the design was based and to permit suitable variation of the error sources to establish performance margins in the radar system.

Target noise appears as a modulation of the return signal in amplitude, angle of arrival polarization, doppler shift, and target range.

1. ANGLE NOISE

Angle noise coupled with amplitude fluctuation are the most serious as regards their contribution to radar angle tracking errors. Dynamic lag error in the angle tracking loop results in an increase in angle scintillation noise power and places a constraint on the degrees of freedom available to the system designer.

The error model in this case is an estimation of the angle noise spectrum and the amplitude noise spectrum, and

is further determined by the available observation time.

The primary variables that are available to the system designer for the purpose of minimizing the effects of target angle noise are (a) angle servo bandwidth, (b) AGC bandwidth, (c) choice of tracker type i.e. monopulse vs lobing (d) choice of signal processing technique (e.g. frequency agility). The manner in which these variables are controlled and combined requires careful consideration of all of the system performance requirements. The major trade-off however, will involve choice of servo bandwidth that is satisfactory for operation with the given target noise model and for the specified dynamic tracking requirements. These factors drive the choice of servo bandwidth in opposite directions. The BVE must provide the capability to allow optimization of servo bandwidth by a process of measuring the performance of a tentative design in the presence of a simulated error model.

2. RANGE NOISE

Range noise is similar to angle noise in terms of its spectral energy distributions. The rms value of range noise can be approximated by 0.1 to 0.3 times the target span along the range coordinate and is a function of the target shape and complexity. The design problem for the range tracker reduces primarily to an optimum choice of servo bandwidth to satisfy the opposing requirements of a given target noise environment and a specified target dynamics situation. The BVE must provide a simulation of target noise and dynamics.

3. DOPPLER NOISE

The major source of doppler noise for the class of targets involved in the shuttle missions is closely related to the rate of change of angle noise. In the doppler coordinate this appears as a continuous (but noisy) spreading of the average doppler spectrum, rather than introduction of discrete spectral lines (such as might result from propeller noise in an aircraft target). Simulation of the angle noise characteristics will result in a suitable simulation of the doppler noise spectrum.

4. POLARIZATION MODULATION

Polarization rotation from a complex target appears in the radar as amplitude noise. The BVE should provide simulation of amplitude noise with a suitable range of variation of spectral density but is not required to provide polarization rotation directly.

B. BVE CONCEPT FORMULATION

For the purposes of definitizing the requirements for a BVE, the rendezvous radar is assumed to have the following general characteristics:

Operating frequency	- Ku-band
Type	- Low PRF, pulse
Frequency Agility	- 200 MHz peak-to-peak deviation at a 200 Hz rate
AGC response	- more than 10 Hz bandwidth
Angle tracker type	- Amplitude monopulse

Range tracker type

- Split-gate, "center of gravity" tracker

Antenna

- 50 cm diam. parabola

Antenna Near Field

- $(2 \frac{D^2}{\lambda}) \sim 28$ meters

The required radar performance for close range tracking of an uncooperative target is:

Typical target

- Right circular cylinder, 3 meters in diameter and 18 meters long; could be stabilized or tumbling in any axis at a few RPM.

Minimum range

- 30 meters

Angular rate

- 0 to 5 degrees/sec.

Range rate

- 0 to 100 m/sec.

Maximum errors (3σ)

- .5 degrees angle

.008 degrees/sec angle rate

10 meters range

1 meter per second range rate

The effect of target scintillation on radar angle tracking performance has been extensively analyzed in the literature (see references 14 and 16). Although most of the available data relate to aircraft type targets, the following general conclusions are still valid for the short-range tracking of an extended object in space.

1. A wide-bandwidth, short time-constant AGC is essential to remove as much of the amplitude scintillation as possible from the tracking loop.

2. There is no clear-cut advantage to a monopulse system over a conical scan or lobing system unless a spread frequency

technique is used in the transmitter to reduce angle noise. However, monopulse would be preferable for targets tumbling in space at a rate high enough to introduce amplitude spectral energy at a frequency in the vicinity of the scan rate.

3. Pulse-to-pulse frequency agility can substantially reduce the angular tracking jitter in a monopulse system as a result of target glint. The frequency excursions between pulses must be great enough to decorrelate the glint.

Two conditions must exist for improvement from frequency agility:

1. The pulse-to-pulse deviation must exceed a critical frequency difference, Δf_c , that depends on the extent of the target. This critical frequency difference has been shown to be

$$\Delta f_c = \frac{c}{2D} \quad (1)$$

where c is the velocity of light, D is the target extent. For a target 18 meters long this difference must, therefore, be approximately 8 MHz.

2. The radar PRF must exceed the glint bandwidth. This bandwidth is a function of target width, tangential velocity, and rate of rotation.

The glint bandwidth F_g is approximated for design purposes by:

$$F_g = \frac{1}{\lambda} \left(2 \frac{VD}{R^2} + \omega \right) \quad (2)$$

where

L is the target length,

V the linear velocity of the target with respect to the radar platform,

R is the target range,

D is the projected target miss-distance, and

ω is the target rate of rotation.

For example, an 18 meter target at 100 meters, traveling with respect to the radar at 10 meters per second such that the miss-distance is 30 meters, and rotating at only 1 RPM will have a glint bandwidth of 28 Hz. Thus the radar PRF must be several times 28 Hz for frequency agility to improve tracking accuracy.

A significant input to the BVE concept formulation is the need for frequency agility in the radar to mitigate the effects of target noise at close range and to enhance target detection at long range.

Validation of the improvement in tracking accuracy due to frequency agility requires a physical simulation of the target noise with physical dimensions approaching the actual target dimensions.

An alternate method of simulating a target noise environment would be to generate an electrical analogue of the noise model and sum it into the servo loop prior to bandwidth reduction. This method provides no basis for determination of system behavior with frequency agility and is therefore not considered further.

Ideally, the BVE set-up including the radar under test, should be in a clean electromagnetic environment so as to eliminate introduction of error sources that are not a part

of the space environment. Clutter and multipath are examples of such error sources. An anechoic chamber is an ideal environment for the BVE set-up. An outdoor range or roof-top range is suitable provided electromagnetic absorber material is provided to eliminate clutter and multipath effects.

C. BVE HARDWARE DESCRIPTION

The proposed BVE hardware and radar test set-up are illustrated in Figure 28. The BVE target simulator utilizes a slotted waveguide array with each slot shunted by a diode. The energy radiated from the slots can be controlled individually or in any desired combination so as to produce controlled positioning of the effective center of radiation. The waveguide array is mounted on a turntable and this combination is positioned 30 meters away from the radar. Thirty meters is the minimum specified tracking range of the radar and is just beyond the near field of the assumed antenna.

The source of energy for radiation from the waveguide array is a sample of the radar transmitted signal. The connection between radar and BVE is made by a waveguide run which includes a programmable attenuator. An attenuation range of 20 db is provided. Since the radar receives a re-radiated sample of its own transmitted signal it is possible to maintain frequency tracking for use with frequency agile mode of operation. A means is thus provided for evaluation of improvement of tracking accuracy with frequency agility.

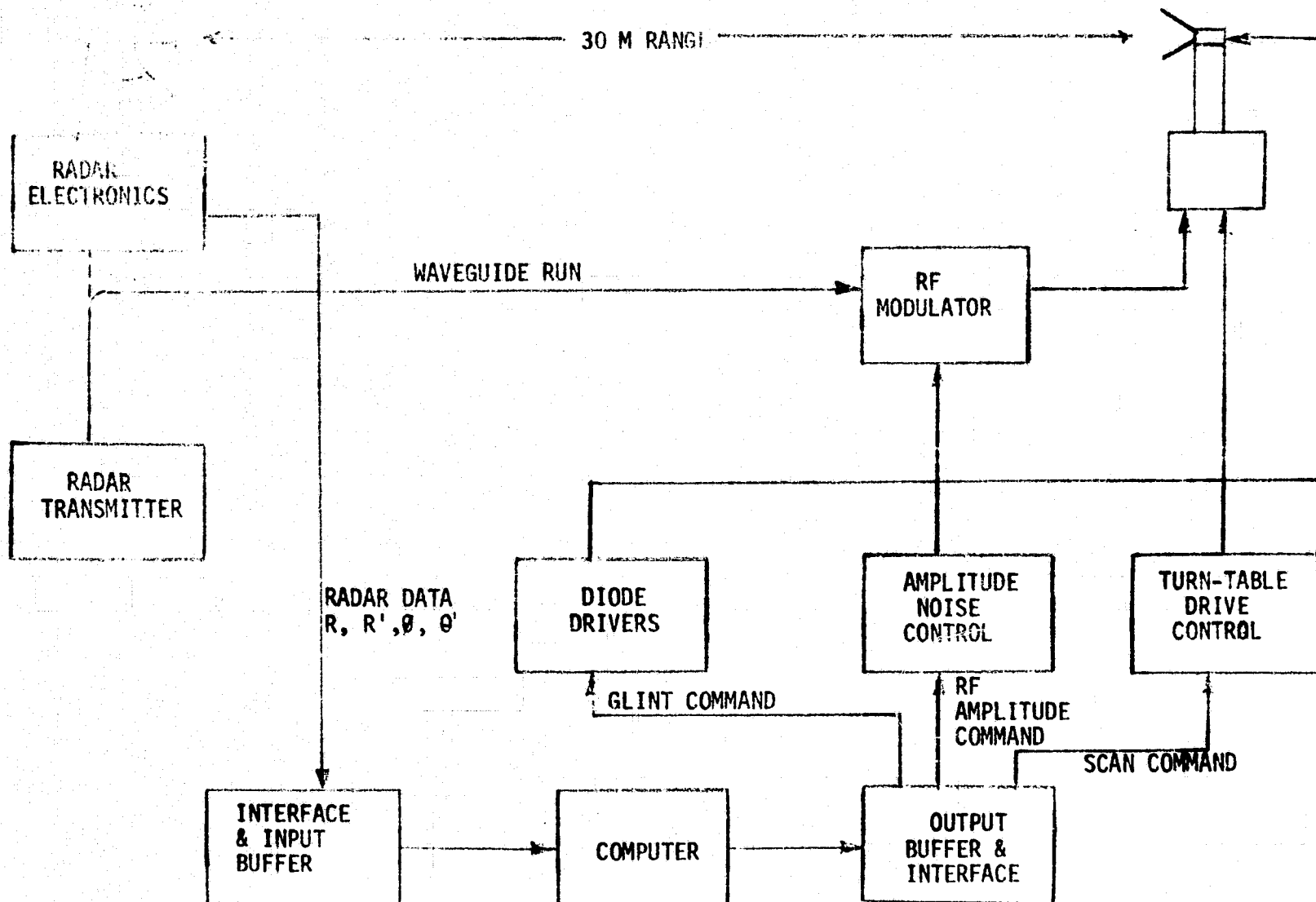


FIGURE 28. TEST SET-UP FOR THE RENDEZVOUS RADAR - PERFORMANCE AGAINST SCINTILLATING TARGET

A computer and data recording system provides the output signals required to simulate angle noise, amplitude noise, range noise and doppler noise. The data recording system records angle and range data from wideband and narrow band points in the radar.

The wideband data sampled in the angle and range error detectors prior to bandwidth reduction is processed to verify the spectral density of the simulated target noise. The narrow band data (recorded from the radar data outputs to the G&N computer) is processed to evaluate its accuracy and suitability to accomplish the RR mission.

The computer provides the flexibility to generate the noise sources individually or in combination and to vary their spectral densities over the range of values expected for RR targets.

Amplitude noise is controlled by the RF modulator in the waveguide run between the radar transmitter and the BVE slotted array. This device is capable of providing greater than 20 db attenuation in 3 db steps.

Angle noise is simulated by controlling the on-off state of the diodes in the slotted array. The diodes can be driven individually or in suitable combinations to synthesize any desired glint spectrum. A brass-board model was constructed and tested during the course of this investigation to establish the on-off ratio achievable by a single diode across a slot.

The appendix gives test results and shows that a 20 db on-off ratio is readily achieved.

It is presently anticipated that an array of 10 meters in length with 20 slots will provide adequate simulation of a suitable range of angle noise distributions.

Doppler noise is simulated by scanning the waveguide array through a small angle by driving the turntable on which it is mounted. A maximum doppler shift of 1 Hz requires an angular velocity of about 0.1 degree/second. The turntable drive signal is generated by the computer in accordance with the required distribution of the doppler noise components.

Scanning of the waveguide array also produces the range noise simulation. Computer Generation of the control signal inputs to the BVE will require more detailed knowledge of expected target geometries.

For purposes of calculating detection probabilities at long range, the targets are presently classified as Swerling type I. These targets generally conform to chi-square distributions with degrees of freedom between 0.6 and 4, and it is often possible to approximate actual density functions by using other chi-square models.

APPENDIX

To demonstrate that radiation from slots in waveguide can be controlled by a shunt diode placed across the center of the slot, a breadboard model was constructed. The model consisted of a single slot in the broad wall. Mounted over the slot was a microstrip circuit containing the microwave diode (Alpha DSG6474C) and a filtered bias circuit.

The slot was then tested in an anechoic chamber. The radiation pattern was measured with the diode open (not biased), and repeated with a bias of approximately 50 ma. Approximately 20 db of isolation was readily achieved from the biased to the unbiased condition.

IX. SELECTION OF NAVAIDS FOR BVE SIMULATION

Selection of the MSBLS navaid to verify its error model was quite natural since AIL is the contractor for the MSBLS system and has had extensive experience in the microwave lading field. Availability of scanning beam hardware such as ground simulators and airborne receivers were also a factor,

The Radar Altimeter navaid was also chosen for the BVE simulation. This choice was based on the similarity in the simulation of radar altimeter height and DME range.

Tacan navaid would be the next likely candidate for the BVE simulation. Commercial Tacan receivers and simulation hardware are available. We did not choose Tacan this time around because of the added hardware and software complexity which would be required.

Rendezvous Radar and One Way Doppler (OWD) navaids are still in the planning stages and, therefore, have not been chosen for the BVE simulation.

The OWD would fit more closely to the BVE concept as a benchtop laboratory setup.

The Rendezvous Radar preferably would require a larger setup in an anechoic chamber.

X. SYSTEM DESCRIPTION OF ERROR VERIFICATION TECHNIQUE

The MSBLS and Radar Altimeter error verification procedure is based on the generation of a signal at the navaid input which resembles as closely as possible the signal which will be encountered by the shuttle during flight. The verification technique simulates a typical shuttle trajectory for each navaid and generates error sources due to ground equipment and propagation effects.

A. GENERATION OF PSEUDORANDOM NUMBER SEQUENCES

Simulation of noise sources is based on pseudorandom number generation techniques. The BVE is capable of generating pseudorandom numbers of the uniform, rayleigh and gaussian distributions. The pseudorandom numbers are then converted to analog form and used to corrupt the signal to the navaid.

1. UNIFORMLY DISTRIBUTED PSEUDORANDOM NUMBER SEQUENCE

A microprocessor within the BVE is programmed to generate a uniformly distributed pseudorandom number sequence by utilizing the so called congruential method.

The basic algorithm of this method used on digital machines is taken from reference 19.

$$u_i = aU_{i-1} + C \text{ (mod } m)$$

where

U_i = i^{th} random number

a = multiplicative constant

c = additive constant

m = largest number of the computers word

We used the multiplicative congruential method ($C=0$). This method has been found to behave well statistically if restrictions are placed on the modulus m , multiplier a and the starting number U_0 .

Application of this method on a binary computer is given in reference 19 as:

1. $m = 2^b$, where b = number of bits in the computers word
2. starting number U_0 is chosen as a positive odd interger
3. multiplier a is chosen = $8t + 3$, where t = positive interger yielding a value of a near $2^{b/2}$.

For our purposes, the number of bits in the computers word was 16. The multiplier a was set to $253_{(10)}$.

Using the above procedure, we were able to generate a well behaved number sequence. Histograms generated by this procedure showed a very close resemblance to the ideal uniform distribution.

2. OTHER DISTRIBUTIONS

Algorithms for generating distributions other than uniform were taken from reference 1.

A Rayleigh distributed sequence was generated by forming the expression

$$R_i = \sqrt{-2 \ln U_i}$$

where

R_i = Rayleigh distributed number

U_i = uniformly distributed number between 0 and 1

A table lookup was used to generate the Rayleigh variable.

The Rayleigh distributed sequence was used in the simulation of MSBLS multipath.

The gaussian distributed sequenced was formed in the following manner

$$W_i = R_i \cos(2\pi U_{i-1}) \quad \text{where } R_i = \text{Rayleigh distributed variable} \\ U_{i-1} = \text{Uniformly distributed variable.}$$

The cosine function was generated by a table lookup.

The gaussian variable was used in the simulation of MSBLS and Radar Altimeter bias errors.

Another pseudorandom sequence utilized by the BVE is the Gauss markoff Process. This is a time correlated (bandlimited) gaussian sequence. i.e. the value of the i th variable is a function of the value of the $(i-1)$ th variable.

This process is formed by

$$X_i = \alpha X_{i-1} + \sqrt{1-\alpha^2} \sigma_x \omega_x$$

where

- X_i = Gauss Markoff number
- σ_x = standard deviation of the process
- ω_x = gaussian number
- α = correlation coefficient
= $e^{-\Delta T/\tau}$

where ΔT = sampling interval
 τ = time constant

If a waveform is generated using this process, the amplitude of this waveform fluctuates randomly with an RMS value equal to the standard deviation of the process. The periodicity of this waveform depends on the time constant. Once cycle of the waveform is approximately 4 time constants.

The Gauss Markoff sequence can be used to simulate slowly changing random processes. We used it to simulate MSBLS signal strength fluctuations due to airborne antenna pattern scallop, and radar altimeter height fluctuations due to terrain fluctuations and vehicles pitch angle fluctuations.

B. MSBLS SIMULATION

1. SIMULATION OF ANGLE TRAJECTORY

The azimuth and elevation trajectory of Figure 6 and 9 is stored as a series of points in a read only memory. The data points are spaced 2 seconds apart. Each data point consists of the angle value to a resolution of $1/128$ deg and an increment per MSBLS update (to a resolution of $1/2048$ deg). During each 2 second interval, the programmed MSBLS angle starts at the table value and is linearly updated with the increment value each .2 seconds forming a smooth angle rate.

Block diagram of the angle trajectory simulation is shown in Figure 30. The angle register is updated with an angle (azimuth or elevation) every .2 seconds. The angle counter is used to count timing signals of the simulated scanning antenna. These timing signals are resolved to $1/128$ degree of antenna rotation and are also used to generate the MSBLS angle code.

A digital comparator determines that the trajectory angle value in the angle register is reached by the angle counter (to a resolution of $1/128$ th degree) and a START BEAM signal is generated.

The START BEAM signal sets off the beam counter which sequentially addresses a read only memory containing a sin X/X type of antenna pattern. The pattern converted to an analog signal

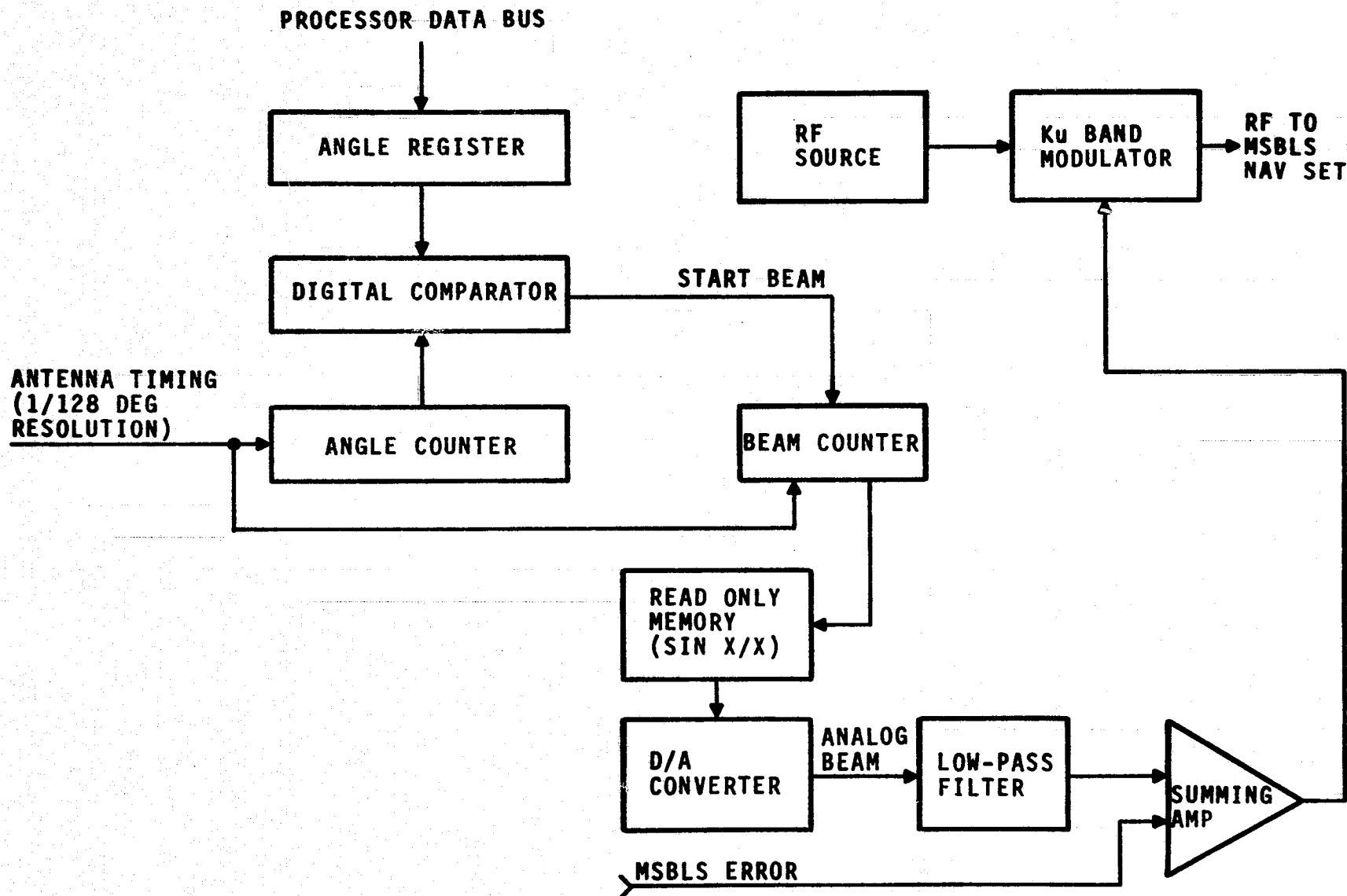


FIGURE 30 MSBLS ANGLE TRAJECTORY SIMULATION

simulates the envelope of the MSBLS angle beam. A summing amplifier is used to add noise to the beam envelope. The composite signal modulates a Kuband RF source to the MSBLS Navset.

The MSBLS angle code is generated according to the antenna timing signal. The pulsed code also modulates the Kuband source. The RF signal to the Nav set then is made up of a pulsed beam with a sin X/X type of envelope corrupted by noise which is postulated as "typical" for the shuttle operation.

Angle error is calculated by the processor by subtracting the measured angle value from the programmed angle value. If the Navset fails to update, (due to a temporary signal loss for example) then the error is calculated as programmed value minus the last valid Navset update (stale data).

2. SIMULATION OF DME TRAJECTORY

Simulation of DME range is done at video utilizing a high resolution, high accuracy digitally programmable time delay generator. An interrogation from the MSBLS navset (see figure 31) is detected via a circulator and provides an input to the digital time delay generator. The digital delay generator is preceded by a fixed 80 usec delay which corresponds to zero range in the MSBLS system. Some adjustment of the fixed delay is provided in order to calibrate the system. Output of the delay generator delayed by the appropriate range keys an RF source to generate a reply to the Navsets interrogation.

Programming of the digital delay generator is done by a hardware software combination. The processor initializes the trajectory counter to a value of range delay at the start of the MSBLS trajectory. The processor also initializes the range rate register. The number in this register determines the period of an output pulse train from the range rate counter. The range rate counter output pulse train decrements the trajectory counter and hence the digital word to the delay generator in 1 nanosecond (1/2 ft) steps. The range rate register is updated with a new value every 2 seconds. The net result of this simulation is a range delay smoothly decrementing in 1/2 foot steps with a range rate update every 2 seconds.

DME biases (installation, refraction and pulse threshold) are summed by the processor and loaded into the error register. Programmed delay to the digital

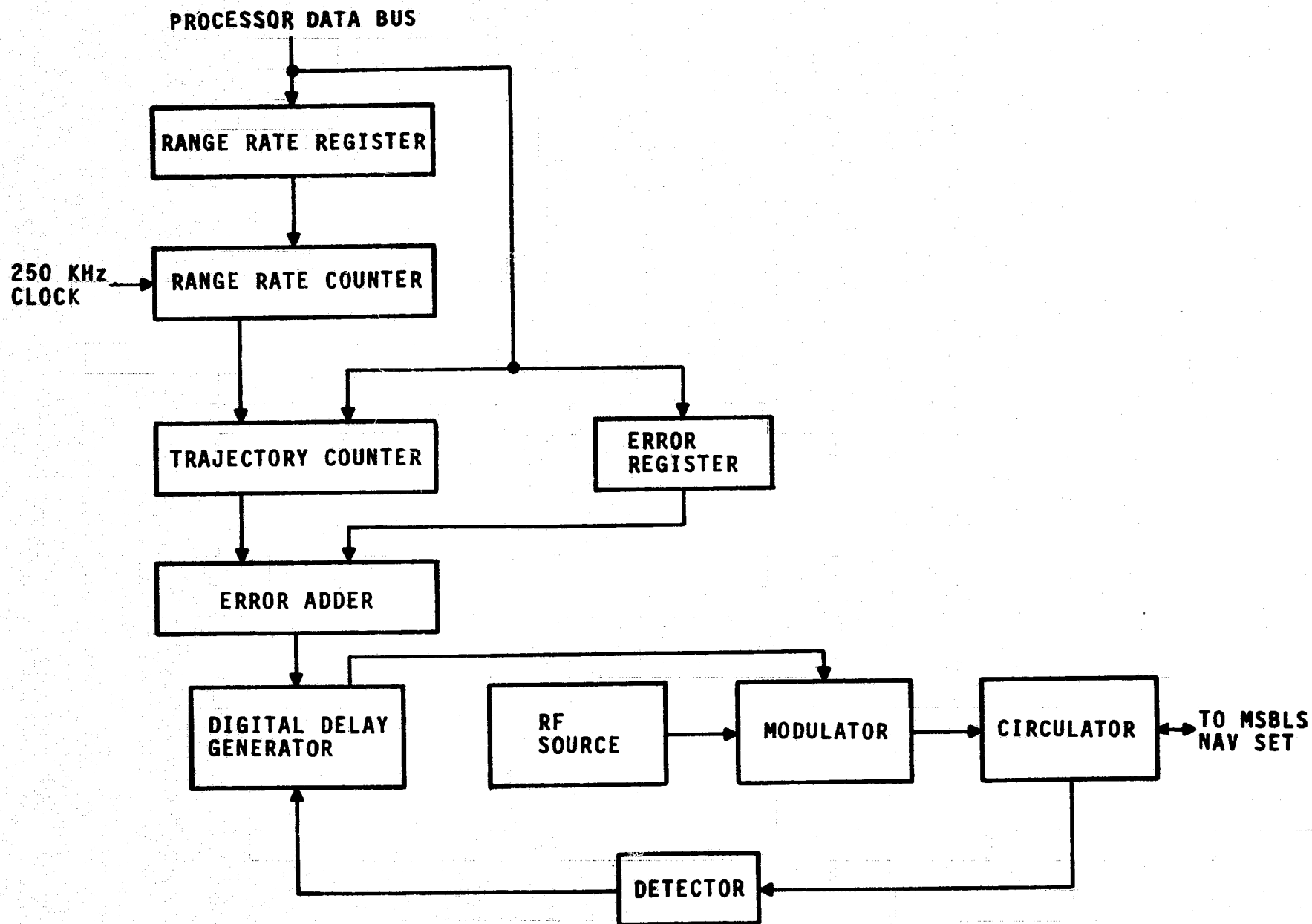


FIGURE 31 MSBLS RANGE SIMULATION

delay generator consists of the sum of the trajectory and the biases.

DME error is calculated as soon as range data from the Navset becomes available to the processor. At this point in time, the processor reads the instantaneous trajectory value (from the trajectory counter) and calculates the error as programmed range in feet minus measured range in feet.

If the MSBLS Navset misses a DME cycle (due to a temporary signal loss) then the error is calculated as the instantaneous trajectory value minus the last valid Navset derived sample (stale data).

3. SIMULATION OF MSBLS ERRORS

MSBLS errors are calculated by the processor and must be converted to analog form in order to be summed with the MSBLS video beams (see figure 32). Each error source is loaded into a register, converted to an analog signal and summed with other error sources and with the MSBLS beams.

Simulation of multipath is done by generating rayleigh distributed pseudorandom numbers whose standard deviation corresponds to the simulated multipath level. During the time a simulated azimuth elevation or DME beam is seen by the Navset, the processor loads the multipath register with a new pseudorandom number for each pulse within the MSBLS beam. The multipath noise in analog form is summed with the video beam and modulates the RF to the Navset. RF pulses are therefore corrupted with a random amplitude disturbance.

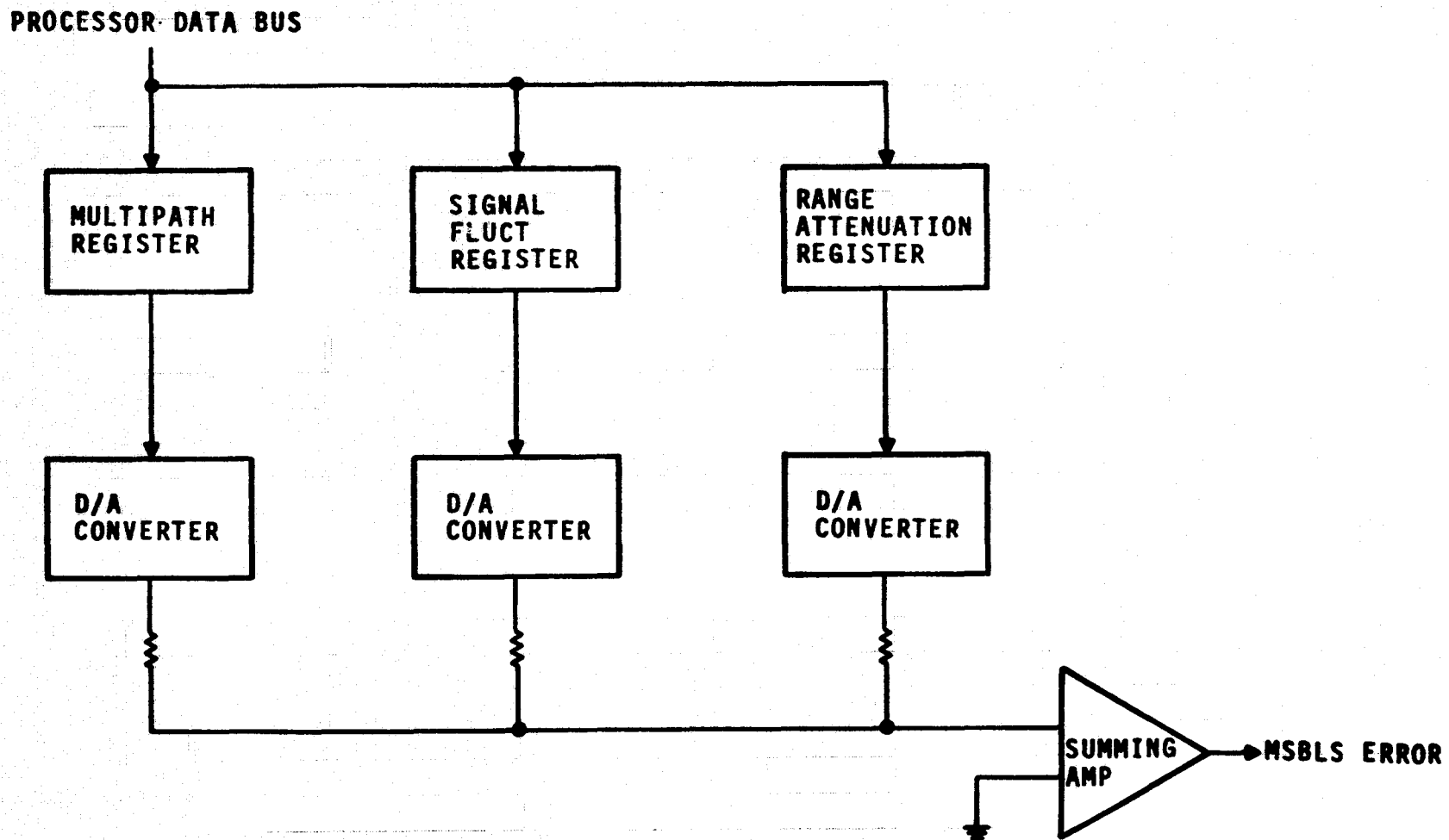


FIGURE 32 MSBLS ERROR SIMULATION

Slowly changing signal fluctuations (due to airborne antenna pattern scallop) are simulated by generating a time correlated Gauss-Markoff process. Standard deviation of the process corresponds to a value programmed in via the front panel. Time constant of the process is also programmed via the front panel. The time constant determines the update rate of the Signal Fluct register and hence the spectral density of the analog signal.

Range attenuation is derived from the trajectory table. An attenuation value and an attenuation increment is taken from the table every 2 seconds. The attenuation value is loaded into the attenuation register at the start of the 2 second cycle and is linearly decremented by the attenuation increment after each MSBLS update. Different attenuation tables are used for the azimuth elevation and DME functions. The tables follow the signal streanth patterns of figure 11, 15, and 16.

DME BIASES

Simulation of DME biases is done by directly summing the error components and loading into the error register of figure 31. DME bias consists of an installation bias, refraction bias and threshold bias. The installation bias is calculated by the processor prior to each simulation run, by choosing a value from a gaussian distributed function with a standard deviation of 10 feet. The standard deviation is a programmable parameter and may be changed

via front panel control. Refraction bias and threshold bias are fixed functions of trajectory. These functions are stored as a series of points, one for each 2 seconds of the MSBLS trajectory.

ANGLE BIAS

Azimuth bias consists of an installation offset. Elevation bias consists of an installation offset plus a trajectory dependent term due to refraction.

The installation offset is calculated by the processor by choosing a value from a gaussian distributed function with a standard deviation of $.02^\circ$ prior to each simulation run. Elevation refraction is taken from a table once every 2 seconds during the simulation.

Block diagram of the angle bias hardware is shown in figure 33. The ADP (angle data pickoff) generator generates antenna timing signals. The reference ADP signal depicts $1/8$ degree of antenna movement and is used to generate the angle beam. The bias delay generator accepts timing signals of $1/1024$ degree resolution and generates an ADP signal which is out of phase with the reference ADP by an amount dependent on the bias value from the processor. This signal is used to pulse code the MSBLS angle data so that an offset between the angle beam and the MSBLS code develops.

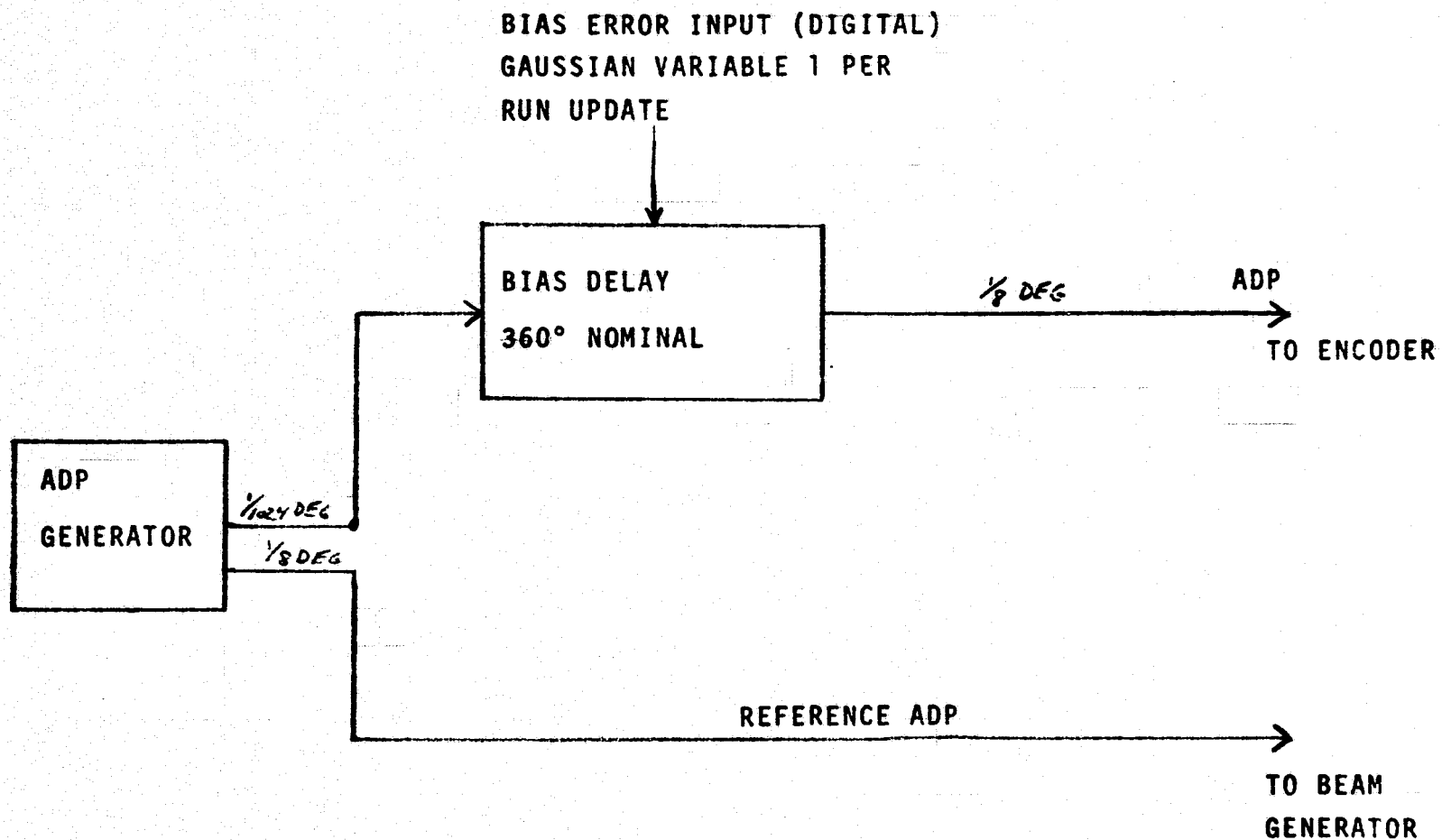


FIGURE 33.

BIAS ERROR INTERFACE (ANGLE FUNCTION)

4. TAPING MSBLS DATA

Azimuth, Elevation and DME errors (Programmed value minus measured) can be taped in real time. In addition, one parameter can be selected for taping via the front panel. This allows the taped error to be correlated with time, elevation angle, azimuth angle, range, signal streanth or any of the other parameters.

C. RADAR ALTIMETER SIMULATION

1. TRAJECTORY SIMULATION

Radar altimeter trajectory is simulated using an internal PRF generator (see figure 34). A pulse output starts the timing circuits of the radar altimeter navaid. Height delay is simulated by delaying this pulse by the appropriate height delay. At the end of the delay cycle, the navaid's transmitter is fired. The RF signal goes through attenuators and delays for multipath simulation and returns to the navaid's receive input.

Control of the digital delay generator is identical to the MSBLS DME simulation. The processor initializes the height and sink rate and the start of the simulation. The height is decremented in 1/2 foot steps at the programmed sink rate. Sink rate is updated at a 1 per second interval in accordance with the trajectory of figure 8. Error is computed by subtracting the navaid derived height from the instantaneous value of the programmed height.

2. RADAR ALTIMETER ERRORS

All radar altimeter error sources, except multipath, are summed and loaded into the error register.

The random noise sources, vehicle pitch fluctuation and terrain irregularities, are simulated by choosing pseudorandom numbers from a gauss markoff process for each error source. Standard deviation and time constant of each is

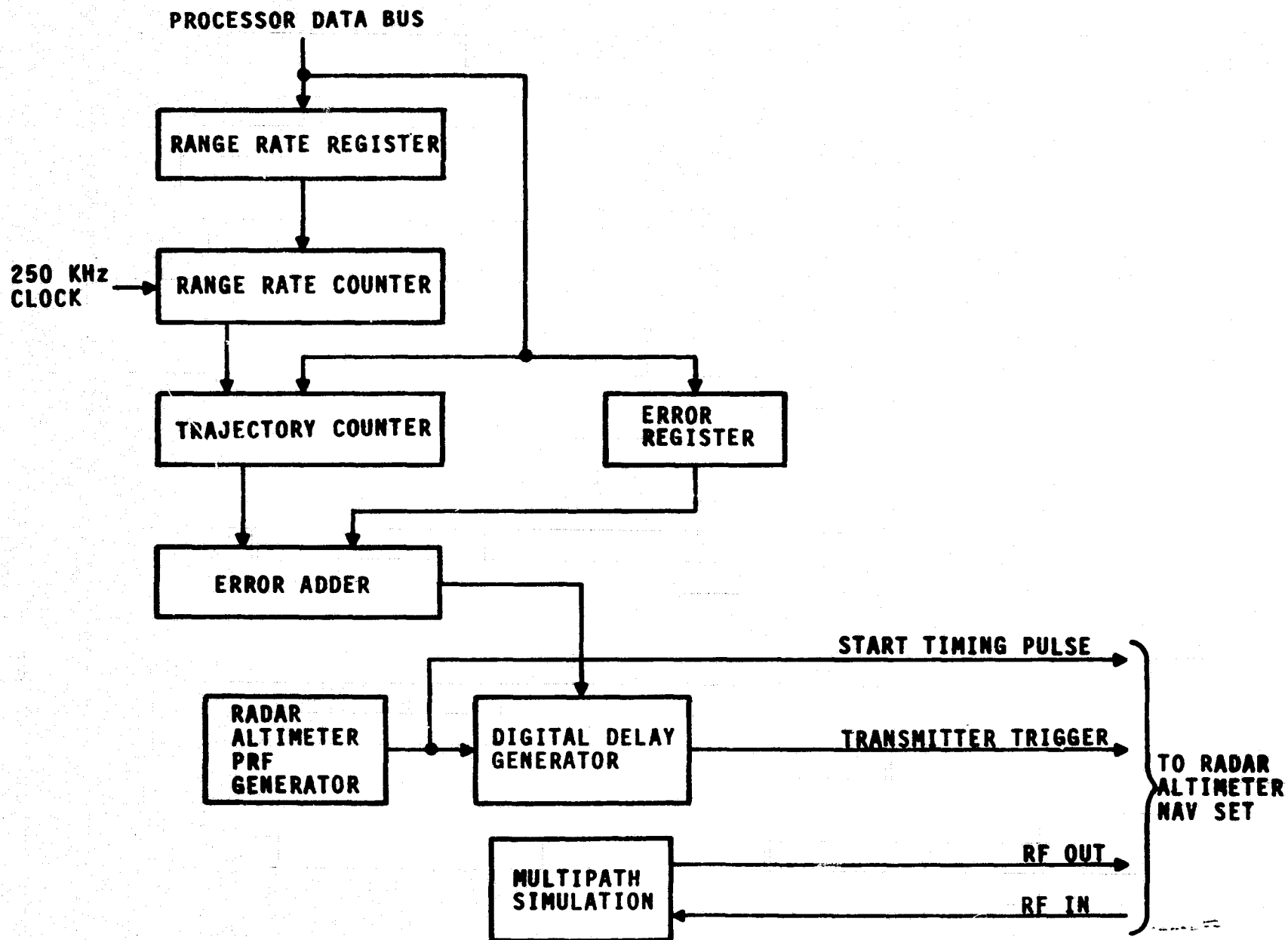


FIGURE 34 RADAR ALTIMETER RANGE SIMULATION

programmable via the front panel. Default values of .7 feet and 1 second for pitch fluctuation and 2 feet and .2 seconds for terrain irregularities are used in the absence of programmed inputs.

Installation bias is generated by choosing a value from a gaussian distribution prior to each simulation run. The standard deviation is again programmable. A default value of .5 feet is used in the absence of programmed input.

Two other bias errors, one due to the vehicles pitch and one due to the separation of the transmit and receive antenna are also used in the error summation. These biases are derived from a table as a function of time. They can be disabled via front panel.

Simulation of multipath is done at RF (see block diagram of figure 35). The RF output of the radar altimeter is split into 8 lines. Each line goes through delays (ranging from 5 nsec to 100 nsec) and attenuators. Four of the eight lines pass through RF switches before recombining to a single RF output. The RF switches are controlled by the processor which turns them on and off on a random basis at a predetermined time interval.

The net result of this simulation is an RF pulse whose shape is continually and randomly changing being fed into the radar altimeters receive input. This pulse should closely resemble an actual ground return. The time interval at which the pulse shape is changing is closely coupled to the vehicles velocity

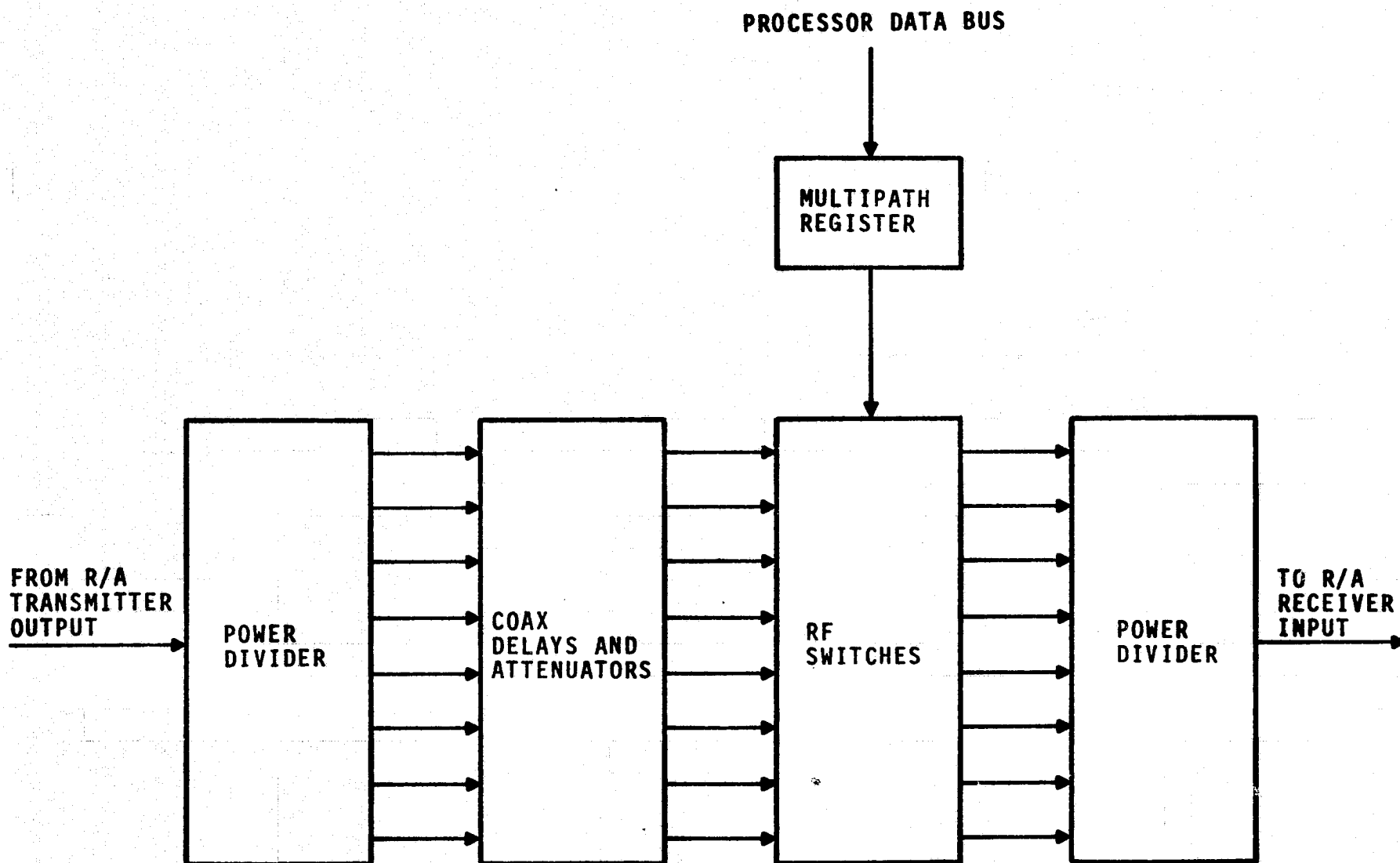


FIGURE 35 RADAR ALTIMETER MULTIPATH SIMULATION

and to the conditions of the reflecting surface. This parameter was therefore left programmable. A default value of .3 seconds is utilized in the absence of a program input.

3. TAPING RADAR ALTIMETER DATA

The navaid error (programmed height minus measured height) is taped at .1 second intervals throughout the simulation run. A parameter which can be selected via the front panel can also be taped. This provides the capability of taping height error as a function of time, programmed height, pitch bias or any of the other parameters.

XI. VERIFICATION OF NAVAID ERROR MODEL

A. MSBLS

MSBLS BVE simulation runs were performed using "default" parameters, i.e. noise amplitudes and spectral densities were set to values which were postulated as "typical" of the space shuttle terminal environment. Data was averaged over 30 consecutive error samples to determine the bias and standard deviation for each (AZ/EL and DME) function. The data was taken at acquisition about 10 nm in range.

1. AZIMUTH FUNCTION

Azimuth parameters for the simulation run were as follows:

- | | |
|------------------------|-------------|
| a. beamwidth | 2 degrees |
| b. multipath level | -28 db |
| c. bias | .02 degrees |
| d. signal fluctuations | 1 db |
| e. time constant | 1 second |

Navaid derived azimuth error is given in Table I A. Bias error for this run was $-.0029$ degrees and random noise (1 sigma) was $.039$ degrees. Analytically derived azimuth error model for this set of conditions is given in Table II. The random noise (1 sigma) is predicted to be $.04$ degrees. The difference between the analytic model and the navaid derived model is $.001$ degrees. This difference is small when one considers that the navaid derived standard deviation is in

itself a random variable from one computation to another and a mean value and 1 sigma dispersion can be assigned to it.

For 30 sample averaging, reference 1 gives the computed standard deviation as within 35 percent of the actual standard deviation (if an infinite number of samples were used) with an 80 percent confidence level. In other words, if many computations were performed, each one using 30 sample averaging, then in 80 percent of the cases the computed standard deviation would be within 35 percent (.014 degrees) of the actual value.

The computed bias of $-.0029$ degrees is within the analytically derived 1 sigma level of $.023$ degrees.

2. ELEVATION FUNCTION

Elevation parameters for the BVE simulation run were as follows:

- | | | |
|----|---------------------|-------------|
| a. | beamwidth | 1.5 degrees |
| b. | multipath level | - 23 db |
| c. | bias | .02 degrees |
| d. | signal fluctuations | 1 db |
| | time constant | 1 second |
| e. | refraction bias | ON |

Navaid derived elevation error model (Table I B) at acquisition, averaging 30 samples, shows a bias of $-.018$ degrees and a random noise error (1 sigma) of $.033$ degrees. This result compares favorably with the analytically derived error model (Table 3). Random noise component of the analytic model is $.044$ degrees, a 25 percent difference from the navaid

data.

Computed bias of $-.018$ degrees is within the analytically derived 1 sigma level of $.023$ degrees.

3. DME FUNCTION

DME parameters for the BVE simulation were as follows:

- a. multipath level -20 db
- b. bias 10 ft.
- c. signal fluctuations 1 db
- time constant 1 second
- d. refraction bias ON
- e. DME threshold bias ON

Navaid derived bias (Table I C) is 59.7 ft. and standard deviation is 18.3 ft. Analytically derived error model (Table 4) yields a bias of 31.6 ft. and a random noise error of 16.92 ft. BVE derived error model correlates favorably with the analytic model.

A. AZIMUTH

B. ELEVATION

C. DME

.00586	-.04883	-56.75000
.05273	-.04688	-48.87500
.00781	-.04883	-54.75000
.02148	-.01953	-67.75000
.00195	-.05078	-4.75000
.11035	-.03809	-58.00000
.02930	-.01660	-43.00000
-.05176	.00488	-43.00000
.05566	-.02441	-52.25000
-.04395	-.02246	-58.12500
-.02051	-.02246	-67.25000
-.01855	.01660	-2.50000
-.00195	-.07715	-55.62500
-.05273	.03125	-54.00000
-.02344	-.05566	-67.00000
-.06250	-.03223	-63.12500
-.03613	.00684	-65.25000
-.08008	.00684	-63.00000
-.01660	-.02051	-72.25000
-.00586	-.00098	-68.62500
.01367	.02734	-77.87500
-.01074	-.03418	-62.37500
.01660	.04785	-76.12500
.02930	-.02832	-66.37500
-.00488	-.02441	-87.00000
-.02441	.00586	-64.37500
.02539	-.00496	-64.12500
-.03809	.01953	-62.00000
.04883	.00586	-79.25000
-.01465	-.06641	-84.87500
BIAS	BIAS	BIAS
-.00293	-.01839	-59.67500
ST DEV	ST DEV	ST DEV
.03942	.03300	18.28930

TABLE 1. BVE DERIVED MSBLS ERROR DATA

ORIGINAL PAGE IS
OF POOR QUALITY

TABLE II

PULSED KU-BAND SCANNING BEAM SYSTEM ERROR BUDGET

AZIMUTH ANGLE DATA AT:
 7 DEG AZIMUTH
 17 DEG ELEVATION
 10.4 NMI DISTANCE

NOTE: BEAM RECEIVED IN CLEAR
 --NO MAIN-LOBE MULTIPATH.

RAINFALL RATE = 0 MM/HR

SYSTEM CHARACTERISTICS:

BEAM WIDTH AT -3 DB = 2 DEG
 DECODER THRESHOLD AT MINUS 3 DB
 ANTENNA GAINS MINUS LINE LOSSES = 19 DB
 TRANSMITTER PEAK POWER = 2.2 KW
 SCAN MOTION: FULL MECHANICAL CYCLES/SEC = 2.5 HZ
 1-WAY MECH. TRAVEL PER FULL CYCLE = 88 DEG
 OFFSET OF DATA AND MECH. ZERO ANGLES = 0 DEG
 ANGULAR RATE = 682.3 DEG/SEC (INVERSE = 1.4655 MSEC/DEG)
 BEAM DWELL (AT-3 DB) = 2.9 MSEC
 PRP CODING: ZERO DEG = 60 USEC
 SCALE FACTOR = 2 USEC/DEG
 CODE HITS: PER DEGREE = 19.8
 PER BEAM DWELL = 39.3
 RECEIVER NOISE FIGURE = 12 DB
 RECEIVER IF BANDWIDTH = 15 MHZ IF SNR = 30.2 DB
 ANGLE OUTPUT RESPONSE (UPDATE/SCAN) = 100 PCT

ERROR CONTRIBU-
TION IN DEGREES

BIASES:

1. ROLL AXIS LEVEL ERROR = 0.01 DEG	0.003
2. PITCH AXIS LEVEL ERROR = 0.01 DEG	0.0004
3. YAW BORESIGHT ERROR = 0.01 DEG	0.01
4. ANGLE PICKOFF BIAS = 0.02 DEG	0.02
5. ENCODER XTAL OSC ERROR = 0.003 PCT	0.0011
6. DECODER XTAL OSC ERROR = 0.005 PCT	0.0019
7. DECODER CIRCUIT BIAS = 0 DEG	0

BENDS (CYCLIC AT <1 HZ):

8. SIDELobe SIG AFTER REFLEC. = -28 DB	0.0377
--	--------

SCAN-TO-SCAN UNCORRELATED NOISE:

9. RCVR NOISE BEAMSHAPE ERROR	0.0081
10. RCVR NOISE ANGLE DATA ERROR	0.0001
11. BEAM-PULSE RESOLUTION ERROR	0.0103
12. ANGLE PICKOFF INCREMENT = 0.125 DEG	0.0009
13. ANGLE PICKOFF JITTER = 0.025 DEG	0.0002
14. ENCODER CLOCK RESOLUTION = 250 NSEC	0.0009
15. PULSE TRANSMISSION JITTER = 15 NSEC	0.0003
16. DECODER CLOCK RESOLUTION = 125 NSEC	0
17. DECODER PULSE-TIMING JITTER = 20 NSEC	0.0004
18. AIRBORNE OUTPUT INCREMENT = 0.004 DEG	0.0012

SYSTEM RESULTANTS (1-SIGMA):

RSS OF BIASES	= 0.0227
RSS OF BENDS	= 0.0377
RSS OF NOISE	= 0.0132
RSS OF BENDS + NOISE	= 0.04
RSS OF ALL ERRORS	= 0.0459

ORIGINAL PAGE IS
 OF POOR QUALITY

TABLE III

PULSED KU-BAND SCANNING BEAM SYSTEM ERROR BUDGET

ELEVATION ANGLE DATA AT:
 7 DEG AZIMUTH
 17 DEG ELEVATION
 10.4 NMI DISTANCE

NOTE: BEAM RECEIVED IN CLEAR
 --NO MAIN-LOBE MULTIPATH.

RAINFALL RATE = 0 MM/HR

SYSTEM CHARACTERISTICS:

BEAM WIDTH AT -3 DB = 1.3 DEG
 DECODER THRESHOLD AT MINUS 3 DB
 ANTENNA GAINS MINUS LINE LOSSES = 19 DB
 TRANSMITTER PEAK POWER = 2.2 KW
 SCAN MOTION: FULL MECHANICAL CYCLES/SEC = 2.5 HZ
 1-WAY MECH. TRAVEL PER FULL CYCLE = 44 DEG
 OFFSET OF DATA AND MECH. ZERO ANGLES = 15 DEG
 ANGULAR RATE = 344.1 DEG/SEC (INVERSE = 2.9058 MSEC/DEG)
 BEAM DWELL (AT-3 DB) = 3.7 MSEC
 PRP CODING: ZERO DEG = 60 USEC
 SCALE FACTOR = 2 USEC/DEG
 CODE HITS: PER DEGREE = 30.9
 PER BEAM DWELL = 39.9
 RECEIVER NOISE FIGURE = 12 DB
 RECEIVER IF BANDWIDTH = 15 MHZ IF SNR = 30.2 DB
 ANGLE OUTPUT RESPONSE (UPDATE/SCAN) = 100 PCT

ERROR CONTRIBU-
TION IN DEGREES

BIASES:

1. ROLL AXIS LEVEL ERROR = 0.01 DEG	0.0011
2. PITCH AXIS LEVEL ERROR = 0.01 DEG	0.01
3. YAW BORESIGHT ERROR = 0.01 DEG	0.0003
4. ANGLE PICKOFF BIAS = 0.02 DEG	0.02
5. ENCODER XTAL OSC ERROR = 0.003 PCT	0.0014
6. DECODER XTAL OSC ERROR = 0.005 PCT	0.0023
7. DECODER CIRCUIT BIAS = 0 DEG	0

BENDS (CYCLIC AT <1 HZ):

8. SIDELobe SIG AFTER REFLEC. = -23 DB	0.0436
--	--------

SCAN-TO-SCAN UNCORRELATED NOISE:

9. RCVR NOISE BEAMSHAPE ERROR	0.0052
10. RCVR NOISE ANGLE DATA ERROR	0.0001
11. BEAM-PULSE RESOLUTION ERROR	0.0066
12. ANGLE PICKOFF INCREMENT = 0.125 DEG	0.0009
13. ANGLE PICKOFF JITTER = 0.025 DEG	0.0006
14. ENCODER CLOCK RESOLUTION = 250 NSEC	0.0009
15. PULSE TRANSMISSION JITTER = 15 NSEC	0.0003
16. DECODER CLOCK RESOLUTION = 125 NSEC	0
17. DECODER PULSE-TIMING JITTER = 20 NSEC	0.0004
18. AIRBORNE OUTPUT INCREMENT = 0.004 DEG	0.0012

SYSTEM RESULTANTS (1-SIGMA):

RSS OF BIASES	= 0.0226
RSS OF BENDS	= 0.0436
RSS OF NOISE	= 0.0086
RSS OF BENDS + NOISE	= 0.0444
RSS OF ALL ERRORS	= 0.0498

TABLE 4

DME ERROR BUDGET

BIAS:

Additive	{ Ground, pulse, level shift	15 ft.
	{ Refraction bias	15 ft.
	Ground delay	10 ft.
		<hr/> 31.6 FT.

NOISE:

Multipath	13.49 ft.
Ground delay jitter	4.9 ft.
Ground clock increment	8.9 ft.
Ground thermal	<hr/> .83 ft.
	16.92 FT.

B. RADAR ALTIMETER

Radar altimeter BVE simulation was performed utilizing the following parameters:

- | | | |
|----|-----------------------------|---------|
| a. | bias | .5 ft. |
| b. | random terrain fluctuations | 2 ft. |
| | time constant | .2 sec. |
| c. | random pitch fluctuations | .7 ft. |
| | time constant | 1 sec. |
| d. | multipath time constant | .3 sec |
| e. | antenna spacing bias | ON |
| f. | pitch angle bias | ON |

Bias and standard deviation were computed using 30 consecutive error samples. A bias of 12.3 feet and a standard deviation of 3.54 feet were computed at the start of the radar altimeter trajectory (see Table 5A). Reference 1 gives an analytic error mode as .73 ft. or .013 h (1 sigma) and .19 ft. or .003 h (1 sigma) noise. At 400 ft. this yields a bias value of 5.2 feet and a random noise error of 1.2 ft.

The discrepancy between the analytic and the BVE derived standard deviation can be bridged by adding to the analytic model the 2 ft. terrain fluctuations and the .7 ft. pitch fluctuations which were simulated in the BVE but were not accounted for in the analytic model. Adding these two errors to the analytically derived standard deviation yields a value of 2.44 ft. (1 sigma). The deviations are within 31 percent of each other. For 30 sample averaging this is within the 80 percent confidence level.

The analytically derived bias does not account for the vehicles pitch or for the altimeter's antenna spacing error. At 400 ft. altitude pitch bias is 2.1 ft. and antenna spacing bias is .86 ft. Subtracting this from the computed bias yields 9.34 ft. which is within 1.73 sigma of the analytically derived 1 sigma bias value.

Table 5 B gives the computed bias and standard deviation near touchdown ($h \approx 20$ ft.). Computed bias is -2.99 ft. and standard deviation is 1.98 ft. The analytic error model yields a bias of .73 ft. and a standard deviation of .19 ft.

Bias calculation must take into account the vehicles pitch angle and the altimeters antenna spacing error. At 20 ft. altitude pitch bias is -3.7 ft. and antenna spacing bias is .74 ft. An offset of 2.96 ft. added to the computed bias yields .03 ft. bias which is within the analytically derived 1 sigma bias.

Terrain fluctuations and random pitch fluctuations must again be added to the analytic standard deviation. The RSS summation yields 2.12 ft. (1 sigma) which is within the 80 percent confidence bound of the computed 1.98 ft.

A. 400 FT. ALTITUDE

B. 20 FT. ALTITUDE

12.62500	-.37500
13.12500	.62500
13.87500	-3.37500
14.37500	-2.37500
14.12500	-.37500
17.62500	1.12500
16.87500	-6.87500
16.37500	-5.87500
17.12500	-3.37500
15.12500	-1.37500
13.87500	-1.87500
9.37500	-3.87500
7.87500	-6.37500
9.12500	-3.87500
11.62500	-3.62500
13.37500	-1.12500
11.87500	-3.62500
13.37500	-3.62500
13.12500	-5.12500
14.12500	-3.62500
14.87500	-6.12500
12.87500	-2.62500
13.37500	-1.12500
13.12500	-5.62500
12.62500	-3.12500
10.12500	-3.62500
7.87500	-2.12500
7.37500	-2.62500
6.12500	-2.12500
1.12500	-1.62500

BIAS

12.28333

ST DEV

3.54112

BIAS

-2.99167

ST DEV

1.98823

ORIGINAL PAGE IS
OF POOR QUALITY

TABLE 5. BVE DERIVED RADAR ALTIMETER ERROR DATA

XII. REFERENCES

1. Navigation Systems Characteristics
Revision 1, July 10, 1973
MPAD, LBJ Space Center, Houston, Texas
2. Avionics Navigation Systems
Myron Kayton and Fried
3. Proceedings of Space Shuttle Integrated Electronics
Conference, NASA TM X-58063, Volume 1,
May 11-13, 1971
4. Space Shuttle Program - Orbiter Avionics Description,
Orbiter Vehicle 101, Preliminary Design Review, Volume 2,
SD 74-SH-0171-2, May 1974
Space Division, Rockwell International
5. Radio Altimeter, ARINC Characteristic No. 552A
March 15, 1972, Aeronautical Radio, Inc.
6. Scolnik - Radar Systems
7. An Evaluation of the Microwave Landing System and
Other Terminal Nav aids for Use by the Space Shuttle,
NASA Internal Note MSC-EG-72-46, November 1, 1972
8. One Way Doppler Deviation, Discussion and
Application to Space Shuttle, W. M. Lear, MCS-07703,
February 13, 1973
9. Shuttle Communication and Tracking, USAF
Interface Control Document, ICD-2-OD034
10. Shuttle Orbiter/GSFC Communication and Tracking
Interface Control Document, ICD-2-OD044, January 1974
11. Feasibility/Trade-Off Analysis For A One Way Doppler
Extractor, Nossen and Starner, RCA Communication
Systems Division, Contract #NAS-9-13517, December 14, 1973
12. Preliminary Plans for Testing One-Way Doppler Assembly,
Job Order 16-609 Harton, Lockheed Electronics Co.
Contract NAS-9-12200, April 1974
13. Final Report CR-100 Implementation Study for Space
Shuttle, FTR/16-1, June 1971

14. J. H. Dums, D.D. Howard and A. M. King, "Phenomena of Scintillation Noise in Radar-Tracking Systems," Proc. IRE, May 1959
15. W. P. Birkmeir and N. D. Wallace, "Radar Tracking Accuracy Improvement by Means of Pulse-to-Pulse Frequency Modulation," IEEE Trans. Communications and Electronics, January 1963.
16. R. H. Delano. "A Theory of Target Glint or Angular Scintillation in Radar Tracking," Proc. IRE, December 1953
17. G. Lind, "Reduction of Radar Tracking Errors with Frequency Agility," IEEE Transaction on Aerospace and Electronic Systems, May 1968
18. J. L. Unger and K. J. Hammerle, "Target Resolution Improvement from Frequency Agility," Boeing Company Document No. D2-90248, March 1963
19. Barr, Gangaas & Schaeffer, "Wind Models For Flight Simulator Certification Of Landing And Approach Guidance And Control Systems", Report No. FAA-RD-74-206, December 1974.